Time-Delay Estimation Based Wireless-Networked Temperature Control System

Chhavi Suryendu

Department of Electrical Engineering
National Institute of Technology Rourkela
Rourkela-769008, Odisha, India
Aug 2015

Time-Delay Estimation Based Wireless-Networked Temperature Control System

A thesis submitted in partial fulfillment of the
requirements for the award of the degree of

Master of Technology by Research

in

Electrical Engineering

by

Chhavi Suryendu
Roll No. 612EE1002

Under the Guidance of

Prof. Sandip Ghosh

and

Prof. Bidyadhar Subudhi

Department of Electrical Engineering
National Institute of Technology Rourkela
2012-2015

Department of Electrical Engineering
National Institute of Technology Rourkela

C E R T I F I C A T E

This is to certify that the thesis entitled ***"Time-Delay Estimation Based Wireless-Networked Temperature Control System"*** *by* ***Ms. Chhavi Suryendu****, submitted to the National Institute of Technology, Rourkela (Deemed University) for the award of Master of Technology by Research in Electrical Engineering, is a record of bonafide research work carried out by her in the Department of Electrical Engineering, under our supervision. We believe that this thesis fulfills part of the requirements for the award of degree of Master of Technology by Research. The results embodied in the thesis have not been submitted for the award of any other degree elsewhere.*

Prof. Sandip Ghosh ***Prof. Bidyadhar Subudhi***

Place:Rourkela
Date:

To My Family and Friends.

Acknowledgements

I would like to express my deepest gratitude to my institute National Institute of Technology Rourkela for giving me the opportunity to be a part of it and providing me with all the required facilities.

I am truly indebted to my supervisors Prof. Sandip Ghosh and Prof. Bidyadhar Subudhi for their immeasurable support, encouragement and confidence in me throughout my work. They made me grow not just as a researcher but as a person and I will always look up to them. I would also like to thank our lab staff Mr. Sahadev Swain and Mr. Budhu Oram for their unconditional support.

I would like to thank my members of Masters Scrutiny Committee Prof. S. Das, Prof. S. Maity and Prof. D. R. K. Parhi for their valuable suggestions and advice. I would also like to thank Head of Department, Electrical Engineering.

Most importantly I am grateful to my family my grandparents, Maa, Pa, Di, Jiju, Bhaiya, Yogesh and Ghanshyam uncle and and my beloved friends for always being there.

Declaration

I certify that

- The work contained in this thesis is original and has been done by me under the general supervision of my supervisors.
- The work has not been submitted to any other Institute for any degree or diploma.
- I have followed the guidelines provided by the Institute in writing the thesis.
- I have conformed to the norms and guidelines given in the Ethical Code of Conduct of the Institute.
- Whenever I have used materials (data, theoretical analysis, figures, and text) from other sources, I have given due credit to them in the text of the thesis and giving their details in the references.
- Whenever I have quoted written materials from other sources, I have put them under quotation marks and given due credit to the sources by citing them and giving required details in the references.

CHHAVI SURYENDU

Abstract

The temperature control is one of the prominently used control in many process industries. Moreover, localized control of this system might be a problem, specifically for high temperature situations. A communication network can be used that replaces the localized control by remote control. Thus, a temperature control system with a wireless network in the feedback loop is studied to investigate its various issues. The network is introduced for sending temperature sensor signals to the controller. The advantages of using wireless network over erstwhile technologies are it eliminates the unnecessary wiring and hence simplifies the system. However, with these advantages, drawbacks like packet losses, time-delays, data packet disorder, etc. also follows which degrades the system performance. The major applications of this technology include industrial automation, building automation, intelligent vehicles, remote surgery.

This thesis focuses on development of both direct output feedback and observer based output feedback control algorithms for control of the above temperature control systems with network. A variable gain-type controller is used to improve performance of the system in uncertain delay situation. In a variable gain controller, the gain varies in accordance with delay values at that particular sampling interval. To estimate these delay values, time-delay estimators based on error-comparison and gradient descent methods are designed. Using the knowledge of estimated delay values, the gain of the controller is chosen. Simulation studies were pursued using MATLAB to verify the efficacy of the proposed controllers and estimators by considering appropriate model of the temperature control plant. The experimental studies using LabVIEW are also performed to validate the performance of the plant with the developed controllers and estimators.

Contents

List of Abbreviations

Abbreviation	Description
NCS	Networked Control System
MPC	Model Predictive Control
TTP	Time-Triggered Protocol
ARX	Autoregressive with Exogenous input
WSN	Wireless Sensor Network
LCD	Liquid Crystal display
NI	National Instruments
SCB	Shielded I/O Connector Box
DAQ	Data Acquisition
LMI	Linear Matrix Inequality
LTI	Linear Time-Invariant
PI	Proportional Integral
RHS	Right Hand Side
LHS	Left Hand Side
LMS	Least Mean Square
MAX	Measurement and Automation Explorer

List of Figures

List of Tables

Chapter 1

Introduction

1.1 Overview

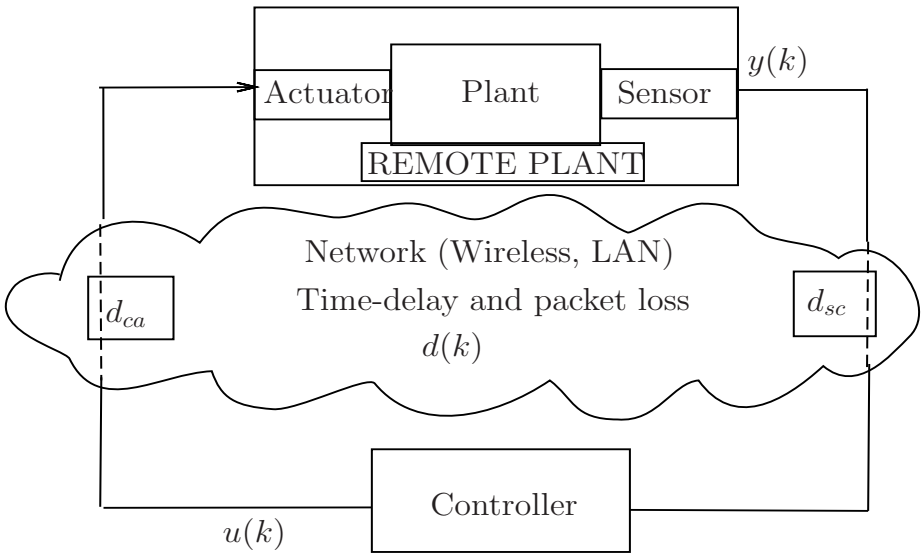

Figure 1.1: Networked Control System

A temperature control system is one of the most widely available control system in an industry. Blast furnace, different pipelines, boilers, etc. are various systems found in an industry that require precise temperature control. While controlling systems that deal with such high temperatures, the controllers need to be installed remotely from the plant area and the communication between plant and the controller is carried out via networks. This technique in which a communication network is used to complete the control loops is called as Networked Control Systems (NCS) as shown in Figure 1.1. Here, the output $y(k)$ of the remote plant and the input from the controller $u(k)$ is sent to the controller and the

actuator of the plant respectively via network. Both $y(k)$ and $u(k)$ during communication suffers time delay and packet loss d_{sc} and d_{ca} respectively.

This technique has been considered as a potential area of research in recent years due to increase in its applications in different fields. For example, Figure 1.2 shows automation of a building so as to control its room temperature from some remote locations. This can be achieved using networks as communication medium. The output of the temperature sensor is transmitted to the remote controller via wireless network and the controller output is sent to the air conditioner via another network. Similarly, in manufacturing plants the high temperatures of blast furnaces, pipelines etc can be controlled remotely by sending sensors output to the controller and control signals to the control valves through network. T_x and R_x denotes transmitter and receiver.

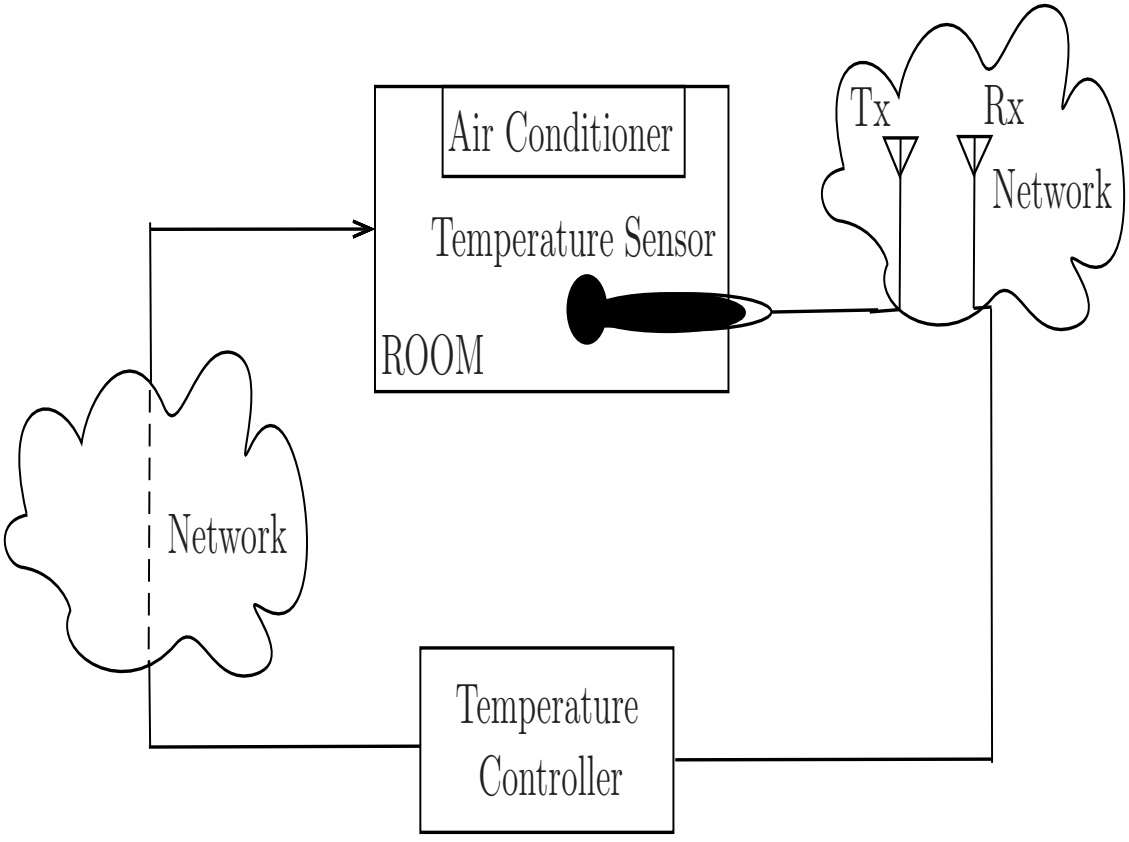

Figure 1.2: Building automation using networked control systems

This technique can also be used in designing and controlling of intelligent vehicles like Unmanned Aerial Vehicle (UAV), intelligent aircrafts etc. as shown in Figure 1.3. An unmanned aerial vehicle is an aircraft with no pilot on board. Hence, it can be used for surveillance of inaccessible areas, regions with harsh climatic conditions, for spying purposes, in defence applications etc.. Such intelligent vehicles require controlling from

some ground station. The figure shows the realization of controller which can be achieved by sending the sensor data (altitude, orientation, velocity etc.) of UAV to the controller and sending the control signals from the ground controller station to the UAV actuators via network.

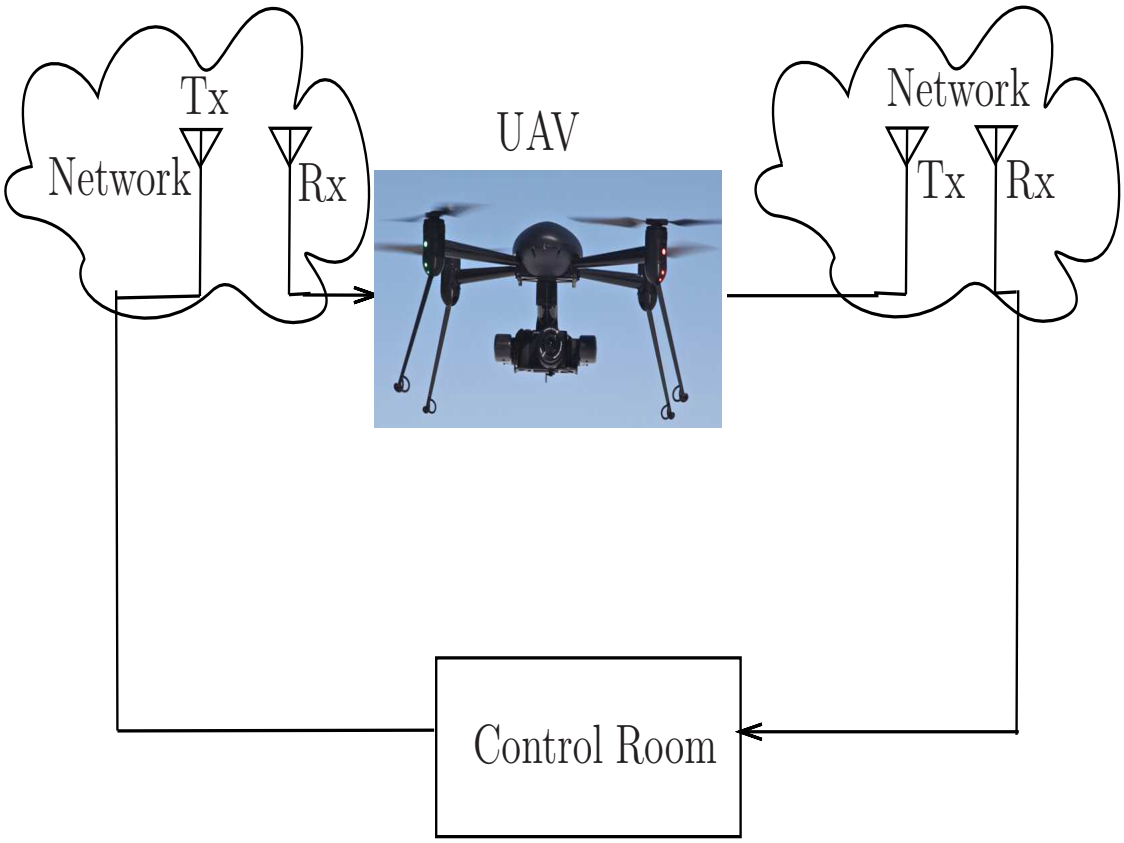

Figure 1.3: UAV control using networked control systems

This technique has simplified the installation of such systems by reducing wiring and hence enhancing the system maintenance and fault detection capability. Also, such simplification has made it easy to control them via remote and distributed control. These advantages of the technique have revolutionized its application sectors. NCS is a technique that helps in remote controlling of a plant via network. But the technique also comes with certain drawbacks like packet losses, time-delays etc. which may not seem harmful in case of simple applications but pose a threat to critical ones like temperature control of a chemical plant, control of UAV etc.. The communication through a network takes place by wrapping up the data to be sent in the form of packets. Time-delay is time required for travelling of these packets via the network from one point to another. Similarly, packet loss happens when these packets are lost due to high packet reception rate of routers than the sending rate. The packets are also considered to be lost if they arrive

after the packet that has been sent after them. Figure 1.4 shows round-trip delay suffered by signals. The actual plant output $y(kT)$ is sent at t_{sc} instant via network and received at t_{cs} instant, hence, a time delay d_{sc} is suffered by the plant output while arriving at the controller. This output is processed for computing the control input, thus, d_c is the controller computation time. d_{ca} is the delay suffered by the control signal $u(kT)$, sent at t_{ce} instant to the actuator. Hence, the total delay occurred is d. These impediments when introduced into the system, degrades the performance of the plant, and thus, paves the way for future research.

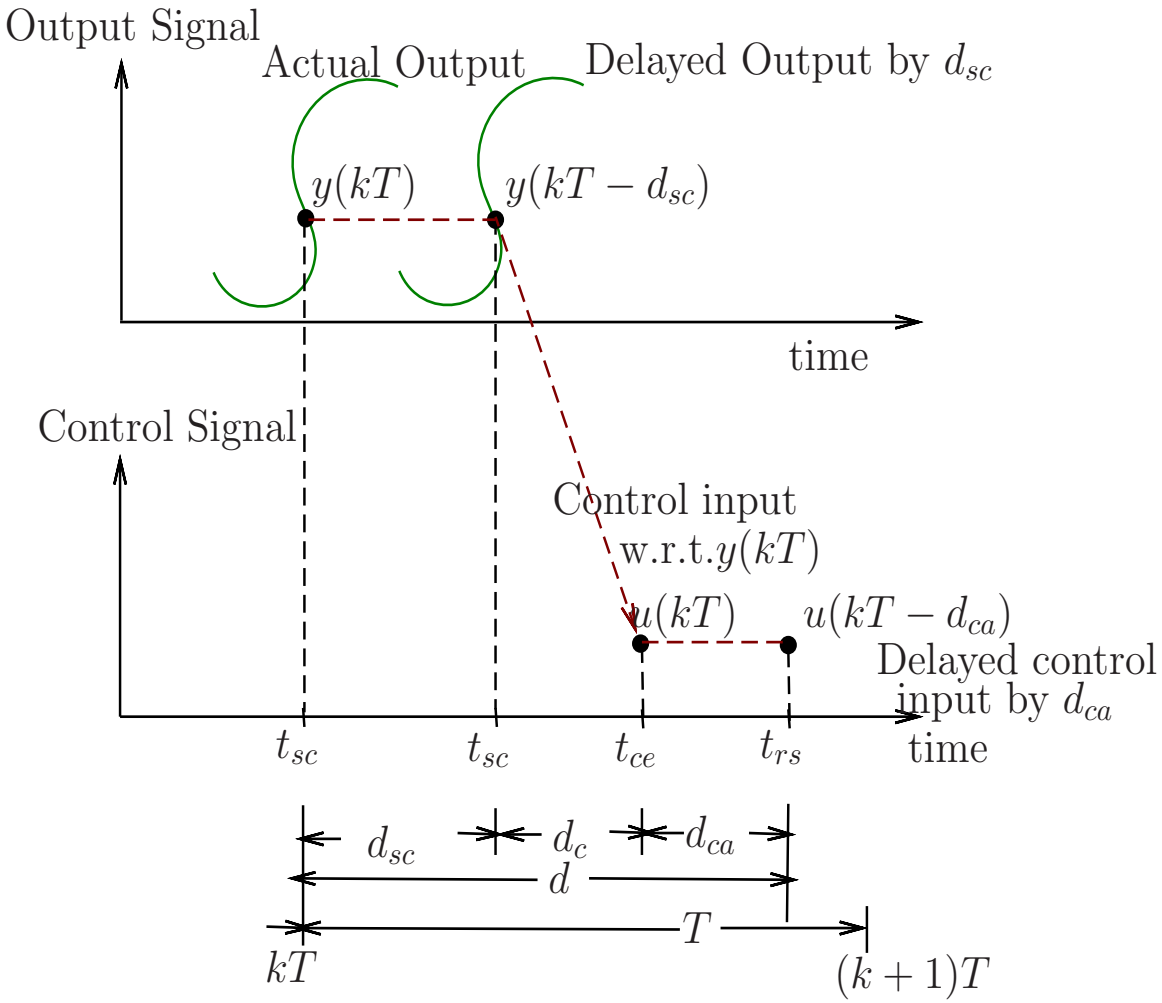

Figure 1.4: Timing diagram showing round-trip time-delay

1.2 A Brief Review on Networked Control System (NCS)

NCS has been extensively studied from the past few decades [1, 2, 3, 4]. Several survey papers have been published so far discussing different works and progresses in this inter-

discipline area. In [5], a survey on NCS is conducted discussing about architectures of NCSs, effects of packet losses and time-delays etc.. They also discussed various state estimation techniques like reduced computation estimation, estimation for multi-sensor plants, with local computation etc.. Here, stability of NCS and controller design to deal with packet losses and time-delays is also discussed. Various control methodologies for NCS are studied in [4]. They have also taken into account various NCS configuration for this study.

The available literature have used various techniques to compensate the effects of network in an NCS. In [6], a static, dynamic and observer based H_∞ controllers have been designed to control linear discrete time systems. An iterative LMI (Linear Matrix Inequality) approach is used in [7] to compute controller gains whereas [8] has used dynamic output feedback based event triggered controller. Same output feedback approach is used in [9] to deal with random delays modeled by Markov chain and in [10] modeled by discrete-time switched system. The stabilisation of NCS is also studied in [7, 8, 9, 10]. [11] and [12] used different PID (Proportional Integral Derivative)controllers whereas [13] used Smith predictor to stabilize systems with time-delays.

Besides the above non-predictive controller, predictive controller is widely used to counter the uncertain delay and packet losses. In [14], the delays in the feedback channel is handled by employing a networked predictive control system with an observer based output-feedback controller. In [15] the same technique is used to deal with time-delays in both the forward as well as feedback channels. In [16] and [17], both network induced delays and packet losses are dealt using predictive compensation and Model Predictive Control (MPC) respectively. Also if consecutive packet loss is bounded, the input to state stability for NCS is guaranteed in [18].

However, in these works, a constant gain is used to deal with time-varying delays. In [19], the above predictive control method is upgraded by considering variable gains in the controller for uncertain delays. An observer based output feedback approach is used to design controller gain. Variable gain controller signifies that the gains of the controller varies according to the delay values at that sampling interval. Similar variable gain approach is used in [20], but for a state feedback controller. Moreover, here the packet dropouts are considered to follow Markov process, thus transforming the closed loop system into a Markov system. This variable gain approach is also used in [21], to guarantee stability and robustness of the plant under random data loss situation. To enhance robustness, Particle Swarm Optimization (PSO) based technique is also used. However, to implement these controllers explicit online information on the delay values is required. In the above literature, time-triggered protocols are used for delay measurements which incorporates separate hardware interface devices. To eliminate these additional

hardware devices a delay estimator may be used.

In the following works, delay estimators for NCSs have been designed using various techniques. In [22] and [23], Smith predictor is used to estimate delays for continuous processes by making time-delay involved with the predictor track the plant time-delay. Here the delay values are estimated using gradient descent method. In [24], leaky bucket algorithm is used for off-line estimation of network delays. Adaptive Smith predictor and robust control are used in [25] to nullify the effects of time-delays and packet losses. In [26], analysis of the networked control system from both network and control point of view has been done. Here, both estimation and compensation of delay is carried out to improve the performance of the system. In [27], a non-probabilistic nature of the data and burstiness constraints applied on the data stream in the network is used for obtaining bounds on delay. Also for the parameters of a state space model with time-delay, an estimator is designed in [28]. These estimators though estimate the delay values, do not assure its convergence. Whereas, in [29] and [30], the convergence of estimated delay is achieved as well as the effect of delay is compensated using generalized predictive controller and multi-step regressive prediction respectively.

It may be noted that all the above works have considered different configurations [4] of NCS as per their own requirement and problem formulation. In these configurations, the plant output $y(k)$ is sent by the sensors to the remote controller and the control input $u(k)$ is sent to the actuator. Different networks like LAN (Local Area Network), wireless, etc. can be considered for communication between the control loops. On the basis of number of network channels the configurations can be divided into single channel or double channel NCS as shown in Figure 1.5 and Figure 1.6 respectively. In single channel configuration, the same channel forms the part of either feedback loop or forward loop or both feedback and forward loop. Thus, uniform network characteristics like time-delays, packet losses etc. are experienced. But in case of double channel network two different networks form the part of control loop. Hence, the network characteristic also varies. All these are general configurations of NCS which can be modified into hierarchical configuration in which in conjunction with the main controller, the plant also has a remote controller of its own as shown in Figure 1.7. The presence of remote controller with the plant ensures better system stability. In all the above mentioned configurations, the output is directly used as a feedback. But in some cases, when plant states are observable, an observer based output-feedback is used for controller design as shown in Figure 1.8a [19] and Figure 1.8b. The former estimates states $\hat{x}(k)$ using observer and send the states data to the controller via network whereas the latter sends the plant output via network and use this delayed output to estimate states $\hat{x}(k)$.

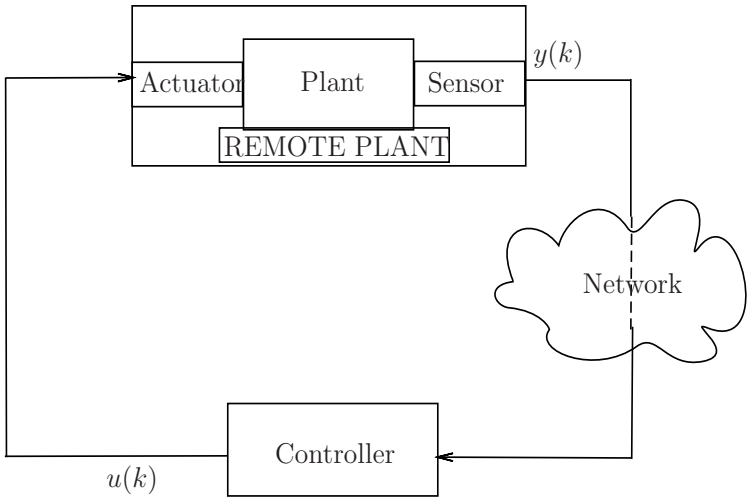

(a) Network in feedback loop

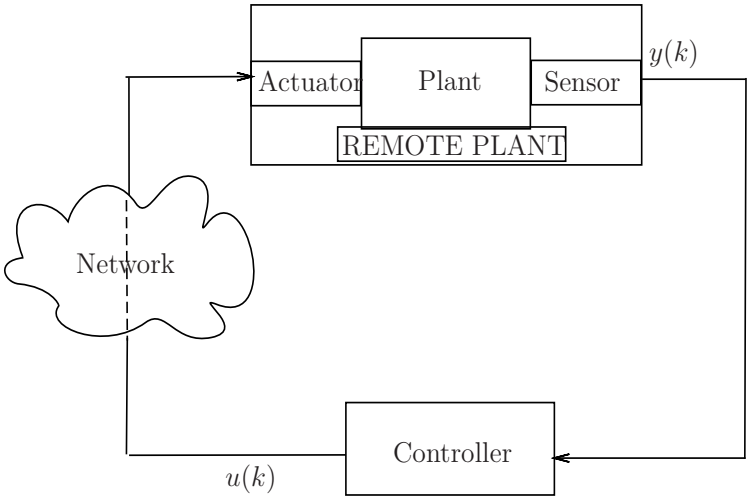

(b) Network in forward loop

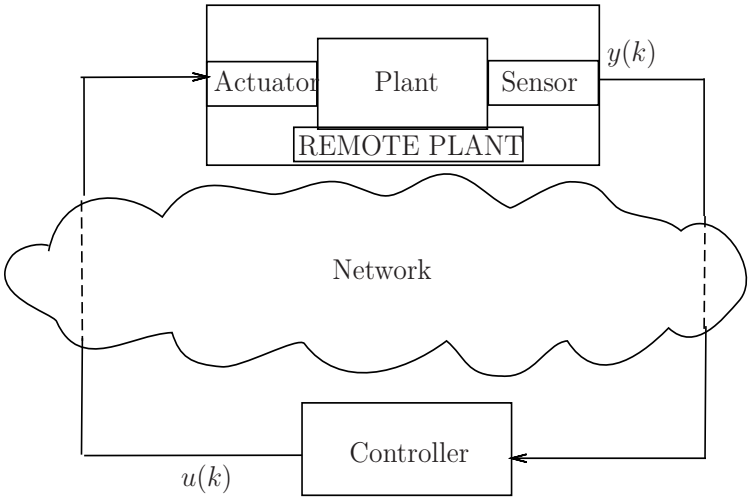

(c) Single network for both the loops

Figure 1.5: Single channel general NCS configuration

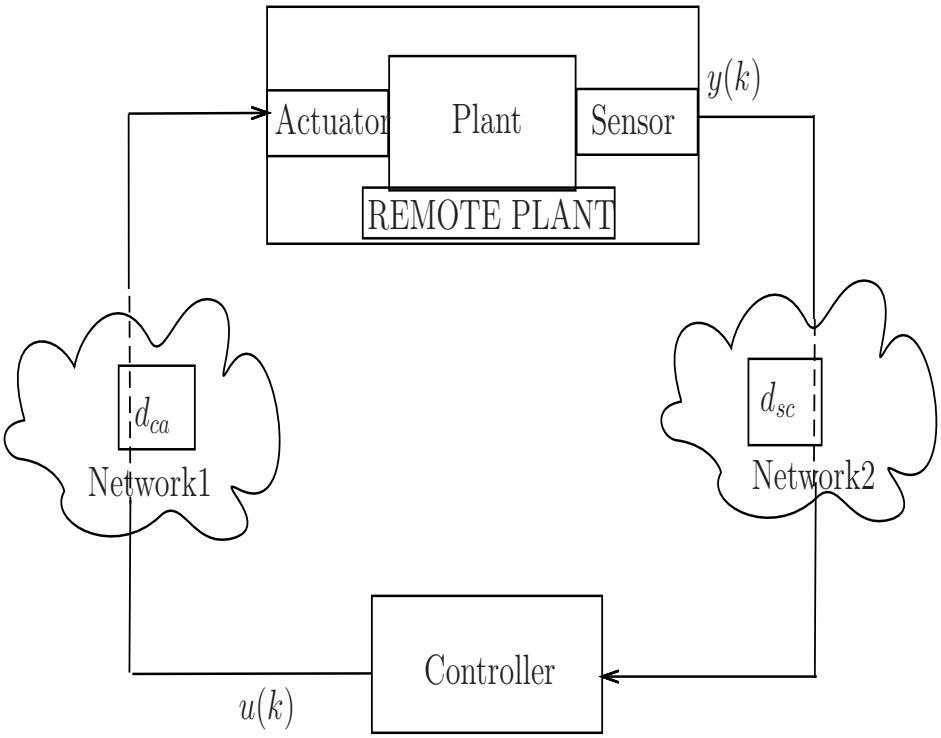

Figure 1.6: Double channel general NCS configuration

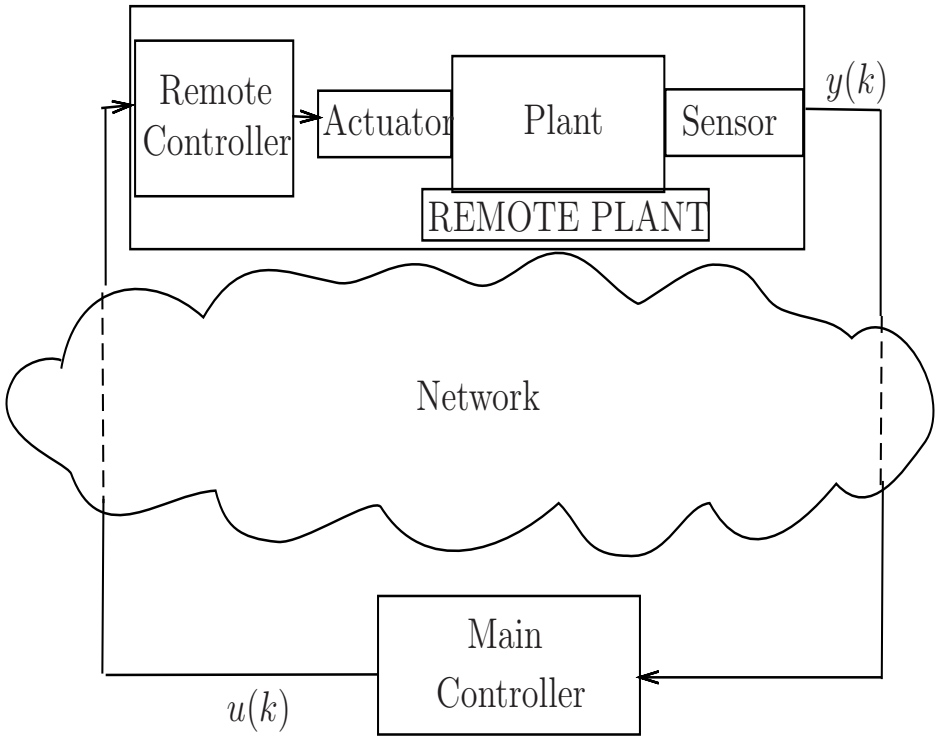

Figure 1.7: Hierarchical NCS configuration

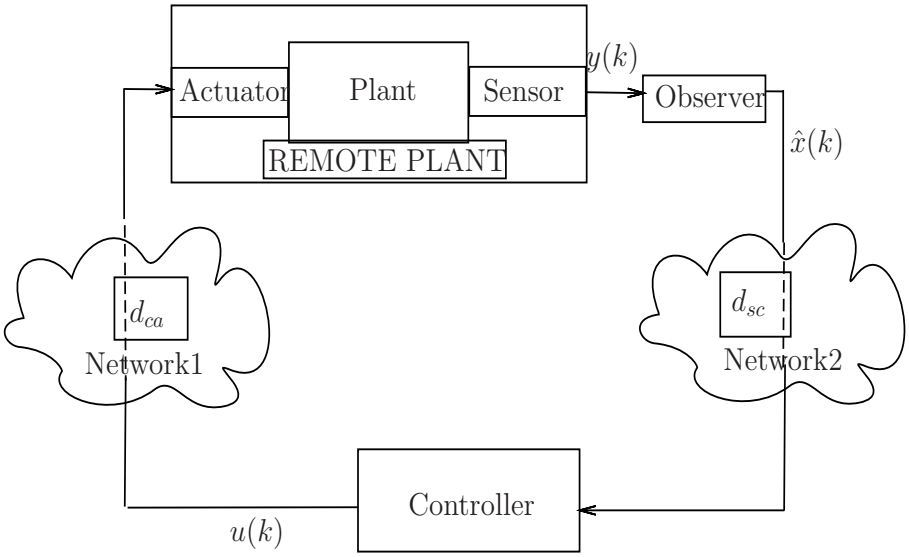

(a) Observer before the network

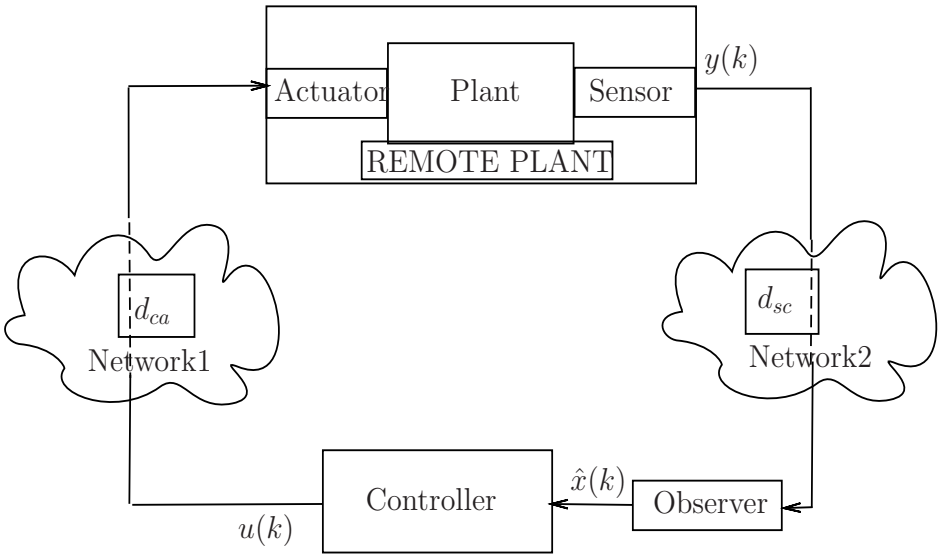

(b) Observer after the network

Figure 1.8: Observer based NCS configuration

1.3 Objectives of the Thesis

In literature, Time-Triggered Protocols (TTP), (TTP networks are often operated as separate networks with separate hardware interface devices and separate, but coordinated configurations) are used for delay measurements. If an estimator of delay and an adaptive control gain using the estimated delay information is designed, then employment of separate hardware interface devices can be avoided. Based on this motivation the objectives

of thesis were formed as:

- To develop a wireless network based temperature control system.
- To develop delay-estimation algorithms for avoiding the use of delay information and evaluating its performance.
- To study the performance of variable gain output-feedback controller using estimated delay information.
- To study the performance of fixed gain and variable gain state-feedback controller using estimated delay information.

1.4 Organisation of the Thesis

The thesis has been organised as follows:

- The present chapter (Chapter 1) gives an introduction of a Networked Control System (NCS) and the literature studied.
- Chapter 2 deals with development of experimental setup for a networked temperature control system. Here, network forms part of the feedback loop. The wireless sensor network modules constitute the network whose detrimental issues are studied and controlled via different controllers.
- Chapter 3 gives simulation and experimental study of the plant with output feedback controller. Here, the output feedback controller has variable gains which varies in accordance with delay values. These delay values are estimated using error-comparison and gradient descent method based estimators. The performance of these estimators with controller is studied.
- Chapter 4 studies the design of fixed and variable gain observer based output-feedback controller. A full state Luenberger observer is designed to estimate states of the plant which forms the control input. The performance of this controller with both the estimators is studied in this chapter. The performance of fixed and variable gain controller is also compared via both simulation and experimental studies.
- Chapter 5 describes contributions of the thesis and the future scope of the present work.

Chapter 2

Development of Networked Temperature Control System

2.1 Introduction

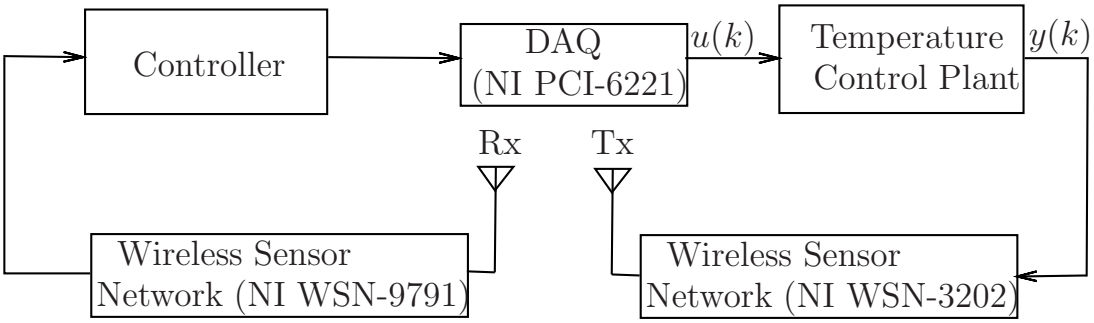

Figure 2.1: Block diagram of NCS setup

For development of NCS setup, the configuration shown in Figure 2.4 is used. In this configuration, computer (controller) sends control input to the plant via a Data Acquisition (DAQ) card. Here, network forms a part of the feedback loop which is used to transmit plant output to the controller i.e. the measured temperature output of the oven is sent to the Wireless Sensor Network (WSN) node 3202, which transmits it to WSN 9791 gateway. Thus, WSN node 3202 and WSN gateway 9791 forms the network. Further, WSN gateway 9791 returns the output to the same computer. A detailed description of all these components mentioned here is presented in the following sections.

2.2 The Temperature Control Plant

2.2.1 Description

The temperature control of blast furnace, boilers, etc is one of the most widely available control system in an industry. These systems are critical and require precise temperature control. The equipment used for experimental study of such systems is a laboratory based setup manufactured by Techno Instruments, shown in Figure 2.2. This setup forms the temperature control system of an electric oven plant [31]. The setup has a controller section providing simple PID controlling which can be connected to the oven via driver for temperature control. The temperature of the oven is converted into electrical signals via solid state temperature sensor with a sensitivity of $10mV/°C$. The setup also has a Liquid Crystal Display (LCD) for indicating the oven temperature in degree Celsius.

Figure 2.2: Temperature control plant laboratory setup

2.2.2 Modelling

The lumped model of this thermal system in terms of its thermal resistance and thermal capacitance, is based on the heat transfer from the heater coil to the oven and from the oven to the atmosphere. Since the transfer of heat from the oven to the atmosphere takes place not just from its thermal resistance but from every part of the oven, the

lumped model is just an approximation of this complex system. Also, the rise in oven's temperature is attributed to the energy input whereas falling of oven's temperature takes place only through heat loss. This also makes the system uncontrollable and unpredictable during cooling. For system that deals with small range of temperature, the heat transfer by radiation is neglected. Thus, for conductive and convective heat transfer

$$\Theta = \zeta \Delta Temp \tag{2.1}$$

where Θ is the rate of heat flow in Joule/sec, $\Delta Temp$ is the temperature difference in $^{\circ}C$, ζ is a constant. The thermal resistance analogous to its electrical counterpart may be defined as:

$$R = \frac{\Delta Temp}{\Theta} = \frac{1}{\zeta}. \tag{2.2}$$

Similarly, thermal capacitance is defined as:

$$C = \frac{\Theta}{d(\Delta Temp)/dt}. \tag{2.3}$$

From (2.2), considering zero initial condition, one can write

$$\Theta = C\frac{d(Temp)}{dt} + \frac{Temp}{R}. \tag{2.4}$$

Taking Laplace transform, the transfer function may be obtained as

$$\frac{Temp}{\Theta(s)} = \frac{R}{1 + sCR}. \tag{2.5}$$

Since, temperature rise in response to the energy input is not instantaneous, a transportation lag term $exp(-sT_1)$ is to be included into the transfer function. Also, taking $R = K_t$ and $RC = T_2$, with K_t being the gain and T_2 being the time-constant, one can write

$$\frac{Temp}{\Theta(s)} = \frac{K_t exp(-sT_1)}{1 + T_2 s}. \tag{2.6}$$

The transfer function (2.6) is a first order one of the temperature control plant. The parameters of this plant can be obtained using system identification toolbox of MATLAB [32].

System Identification toolbox for identifying oven parameters: The system identification toolbox is used to estimate and analyze both linear and non-linear plant models.

- The oven plant was made to run on an input signal of 0.5 V and the temperature changes are recorded every 15 seconds till the temperature gets constant i.e. the system reaches steady-state. This input and output data is recorded and stored in workspace of MATLAB.

- To launch system identification toolbox type "ident" on the command window.
- This toolbox provides the facility to import time-domain data from the workspace. Since, the samples were taken every 15 seconds, the sampling time was specified to be 15 seconds.
- Once the working data is imported, they can be used to estimate plant model after choosing a type from the list provided by the estimate pallet. Since, temperature control is a first order process, hence a process model with a single pole is selected for estimation.
- After the model is obtained, its validity can be checked using validation pallet. For example- when 'Model Output' is selected, it gives the graph of measured as well as simulated output with the best fit percentage.

The continuous-time model obtained after identification is

$$G(s) = \frac{Temp}{\Theta(s)} = \frac{0.5749 exp^{-2s}}{s + 0.003526} \tag{2.7}$$

Since, the controller design will be carried out in discrete-domain, the discrete-time counterpart of (2.7) for a sampling interval of 1 seconds is obtained as:

$$G(z) = \frac{0.5739}{z^3 - 0.9965z^2} \tag{2.8}$$

This discrete-time model can be represented in the observable canonical form as

$$x(k+1) = Ax(k) + Bu(k), \qquad y(k) = Cx(k), \tag{2.9}$$

where $A = \begin{bmatrix} 0 & 0 & 0 \\ 1 & 0 & 0 \\ 0 & 1 & 0.9965 \end{bmatrix}$, $B = \begin{bmatrix} 0.5739 \\ 0 \\ 0 \end{bmatrix}$, $C = \begin{bmatrix} 0 & 0 & 1 \end{bmatrix}$.

When a sampling time of 2 seconds is considered, the discrete time model may be derived as

$$G(z) = \frac{1.1458}{z^2 - 0.993z} \tag{2.10}$$

The corresponding observable canonical form representation is as:

$$x(k+1) = Ax(k) + Bu(k), \qquad y(k) = Cx(k), \tag{2.11}$$

where $A = \begin{bmatrix} 0 & 0 \\ 1 & 0.9930 \end{bmatrix}$, $B = \begin{bmatrix} 1.1458 \\ 0 \end{bmatrix}$, $C = \begin{bmatrix} 0 & 1 \end{bmatrix}$. Figure 2.3 shows the comparison of measured and simulated open loop response of the plant. The best fit percentage was found to be 93.43, which concludes that the plant model is quite appropriately identified.

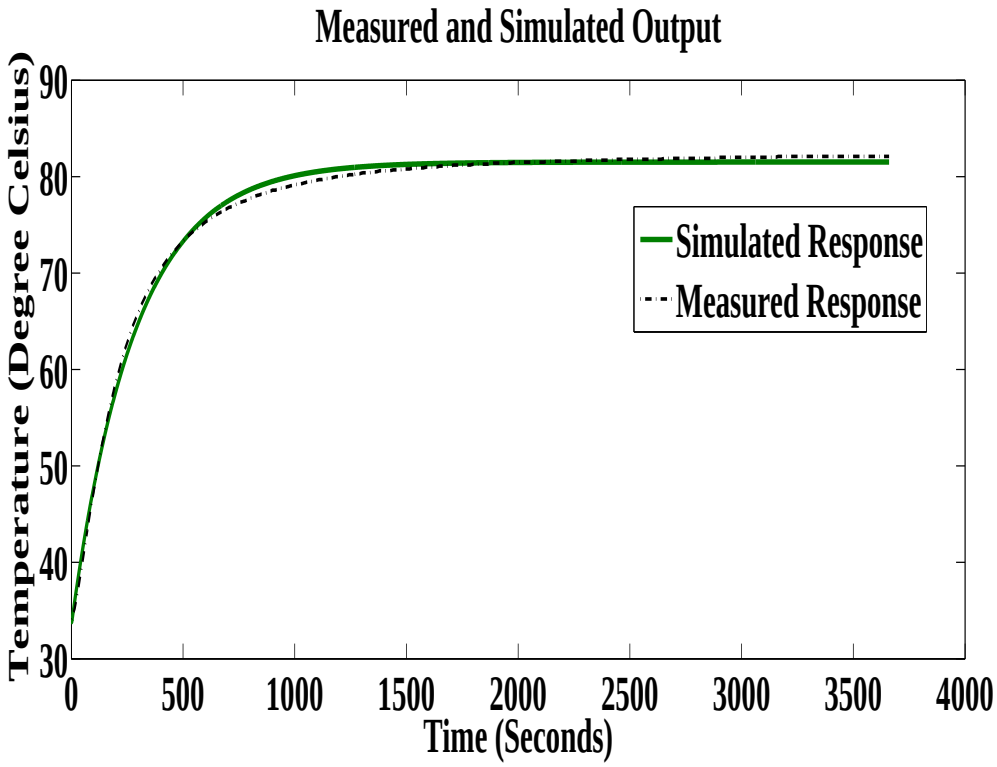

Figure 2.3: Open loop response of identified model of temperature control plant

ARX Model of Plant

An ARX model is identified by using interpolation technique to get temperature values every 2 seconds. The ARX111 model for 1 second sample delay and 2 seconds of sampling time is obtained as:

$$(1.118z^{-1})y(k) = (1 - 0.9932z^{-1})u(k) + e(k), \tag{2.12}$$

where $e(k)$ is the error signal. The figure 2.4 shows the discrete process model and ARX model responses alongwith experimental response. Responses of both the identified models satisfactorily match the experimental open-loop response of plant. However, we use the discretized model of the continuous-time identified model throughout the remianing of this work.

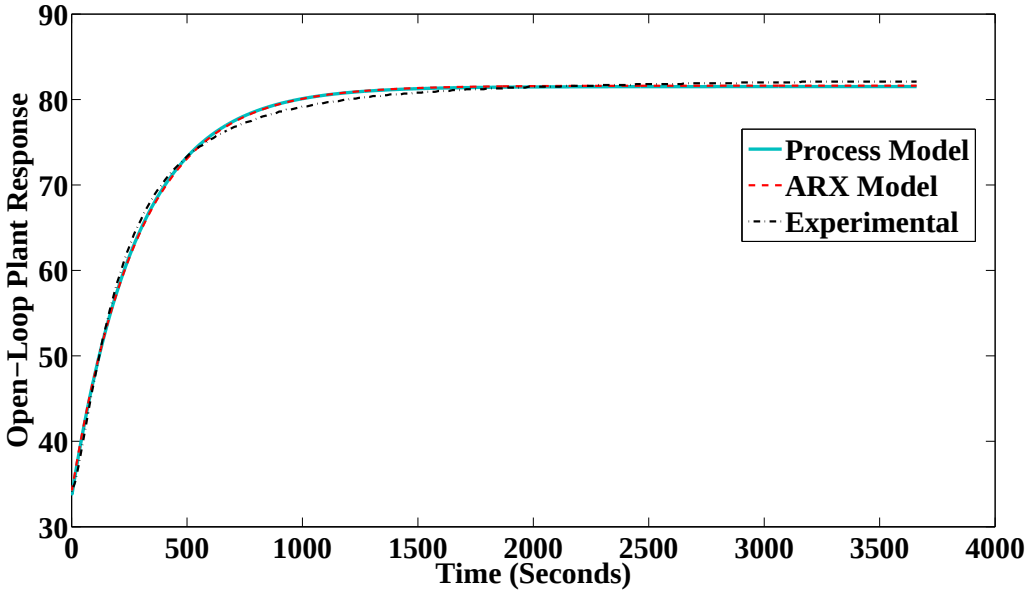

Figure 2.4: Open loop response of Process and ARX models

2.3 Development of NCS Experimental Setup

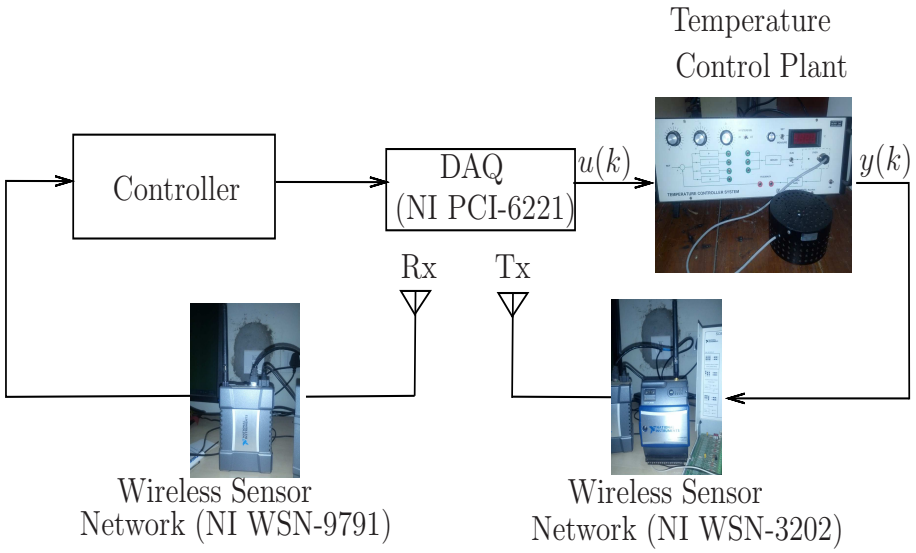

Figure 2.5: Schematic diagram of networked control systems

The network communication interface developed for experimental analysis is as shown in Figure 2.5. The various components used to form this NCS configuration are as follows:

- Data Acquisition card (DAQ) (See Figure 2.6): NI PCI 6221 [33] acts as an interface between external devices and computer. It provides both analog and digital input as well as output, counters/timers, frequency generator, phase-locked loop, external digital trigger channels. It has a maximum sampling rate of 740KS/s per channel. Both analog input and analog output have a resolution of 16 bits.

Figure 2.6: Data Acquisition card

- Shielded I/O Connector Block (NI SCB-68) (See Figure 2.7): The National Instruments (NI) make SCB-68 has a 68 screw terminal to connect to NI DAQ card which is connected to the computer. External signals are sent as well as received at the sockets present on SCB-68. It is a signal conditioning element that allows signal filtering or attenuation in case of signals that are noisy.

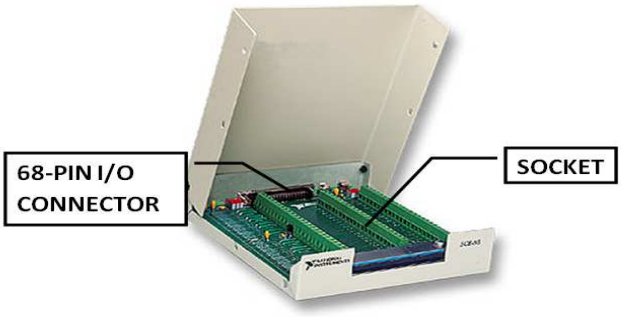

Figure 2.7: Shielded I/O Connector Block (NI SCB-68)

- Wireless Sensor Network Gateway 9791 (See Figure 2.8): The NI WSN system comprises of two kinds of devices: gateways and nodes. Gateways [34] act as network coordinator and takes care of message buffering, node authentication, and bridging between 802.15.4 wireless network and wired Ethernet network. In the

developed experimental setup, it acts as an interface between distributed WSN measurement nodes and controller. It communicates with the nodes through 2.4 GHz, IEEE 802.15.4 radio and has a 10/100 Mb/s Ethernet port for connection to the LabVIEW-based controller. The 802.15.4 radio of each NI WSN device aids communication of measurement data at low-power across a large network of devices. This wireless network has a data rate of 250 kbits/s and frequency bandwidth of 2400 MHz to 2483.5 MHz.

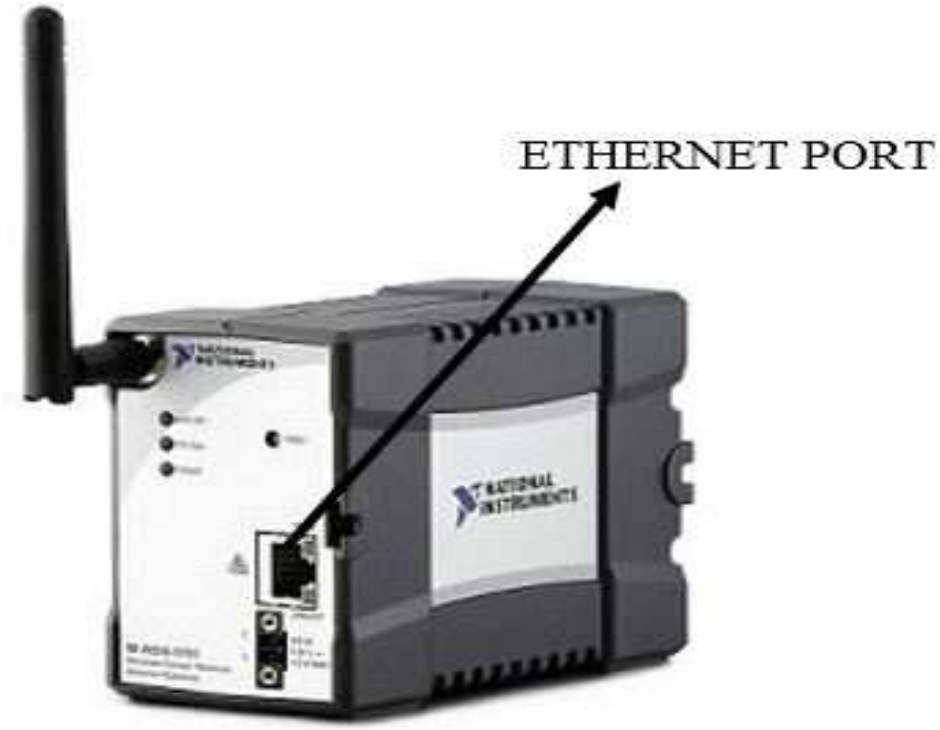

Figure 2.8: Wireless Sensor Network gateway 9791

- Wireless Sensor Network Node 3202 (See Figure 2.9): Nodes [35] mainly function as end nodes within the network which not only collect data and control DIO channels, but can also be programmed to act as routers that relays data from other nodes back to the gateway and Host PC. It also helps to acquire analog signals from external devices and sends them to WSN gateway 9791 wirelessly. It has 4 16-bit analog input channel to acquire input ranging from $\pm$0.5V to $\pm$10V and has an ADC resolution of 16 bits. The absolute accuracy of $\pm$0.5V channel is 7 μV and that of $\pm$10V is 137 μV. It also has 4 Digital I/O channels to handle 5-30V voltage range and a 12V, 20mA sensor power output. It has a minimum sampling interval of 1s.

Figure 2.9: Wireless Sensor Network node 3202

- LabVIEW: It [36] is the application software used to run the control in the NCS setup. It is a platform that provides facilities of generating, acquiring, processing signals so as to control a system. It has in-built blocks for various functions as well as supports program code generation. Every LabVIEW file has Block Diagram and Front Panel Window. The Block Diagram window is used for graphical programming whereas Front panel window is used to see the output. There are three type of terminals- constant and control are used for input whereas indicator serves as output. Before using LabVIEW to take measurements, the NI WSN devices must be configured using NI-MAX.

  Configuring and using NI-WSN:

  - Launch NI-MAX and expand Remote Systems to detect NI-WSN 9791 gateway connected to the computer.
  - Click NI-WSN 9791 and then click Add Nodes to add NI-WSN Node 3202.
  - Open a new project in LabVIEW and right click the project name to New>>Targets and Devices.
  - Select WSN Gateway from Existing target and device to add NI-WSN 9791 to the Project Explorer window.
  - Expand node 3202 of gateway 9791, to drag I/O variable as indicator to the block diagram window of any file to acquire or send signals.

  - **Control Design and Simulation Module**: This module in LabVIEW has blocks for various functions required to control any plant. The state observer, discrete and continuous state space models, delay blocks, gains are the various functions used in this work.

– **MathScript RT Module**: This module helps to use .m files of MATLAB in LabVIEW. It provides platform to develop program codes in MATLAB and running the same in LabVIEW.

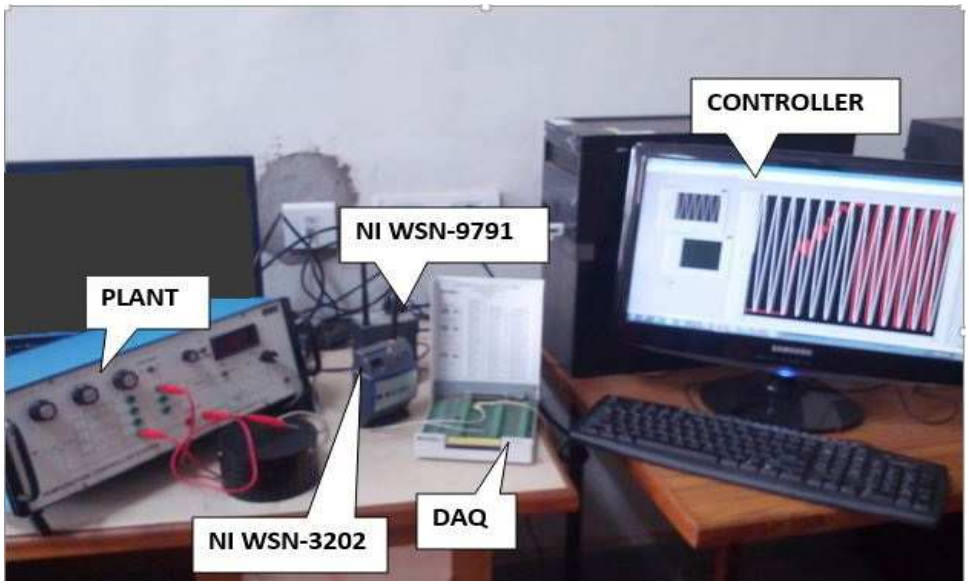

Figure 2.10: The temperature control setup with network in the feedback loop

- The setup: A picture of the complete experimental setup is shown in Figure 2.10. It shows that the input to the temperature control plant is sent via DAQ card whereas the output from the plant is sent to the controller via WSN modules.

2.4 Network Delay Measurement

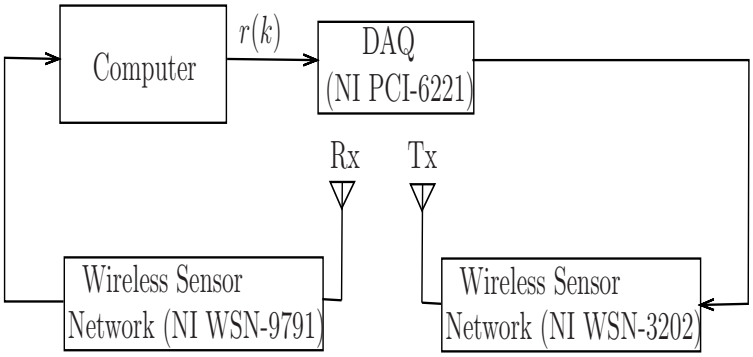

Figure 2.11: Block diagram for round-trip delay measurement

To estimate the maximum delay occurring in the network the setup shown in Figure 2.11 is used. A combination of sine waves of different frequencies $r(k)$, 90 degree apart

in phase is sent via DAQ card to the WSN node 3202, which after passing through the network is received at the same computer. Figure 2.12 shows the LabVIEW model in which a DAQ Assistant block is used to send combination of sinusoidal signal to DAQ card. The output of WSN gateway is received through AIO indicator.

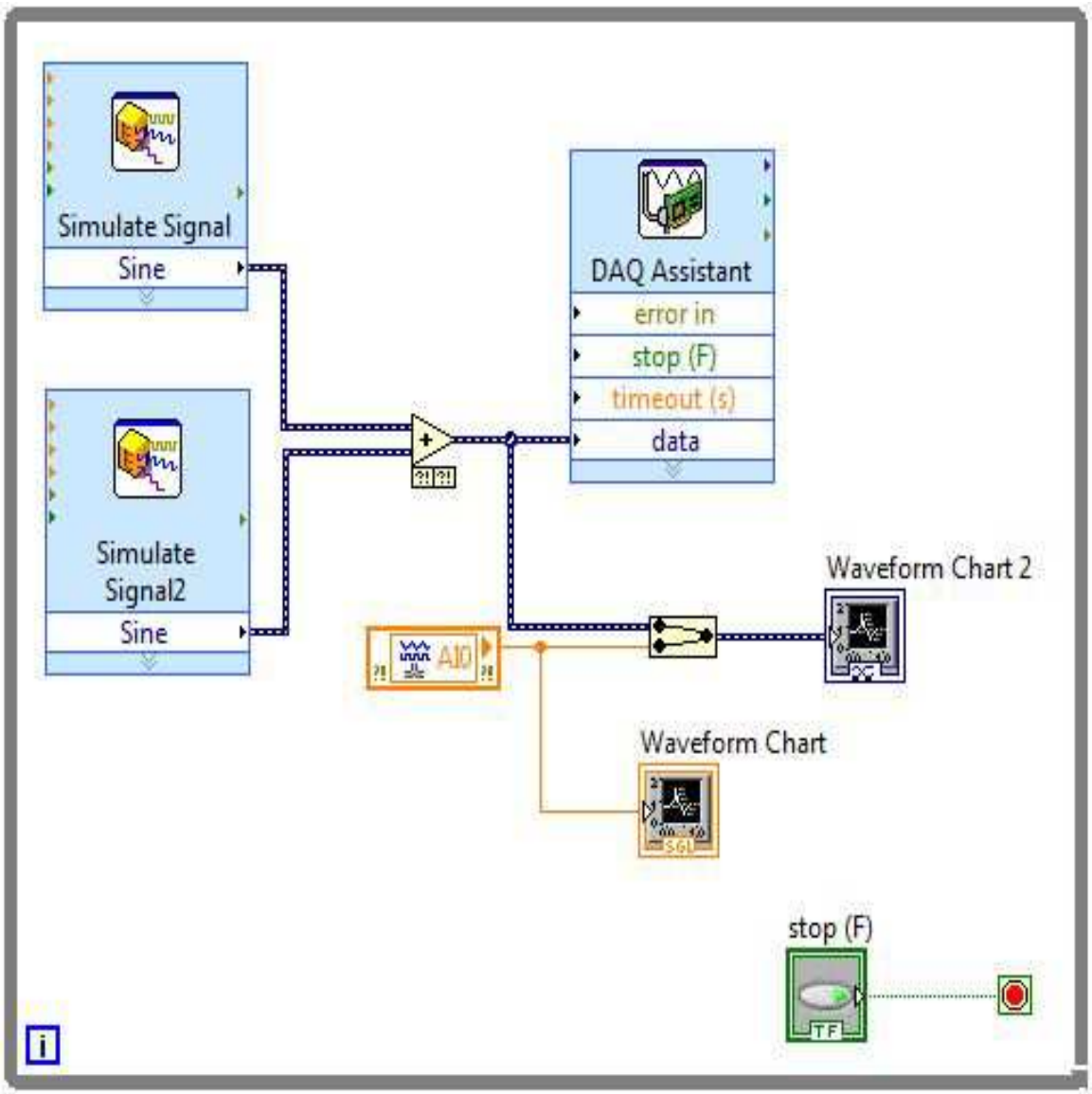

Figure 2.12: LabView Diagram for sending and receiving signals

When a sampling time of 1 second is considered, the maximum delay occurring in the network was found to be 6 seconds. The sent (Black) and received (Red) signals in this case is shown in Figure 2.13.

For the study of packet loss, the sent and the received signal for each sampling time of 1 second is retrieved as shown in the Table 2.1.The table includes sent and received data with small quantization error from Figure 2.13 within the range of 42^{nd} to 54^{th} seconds.

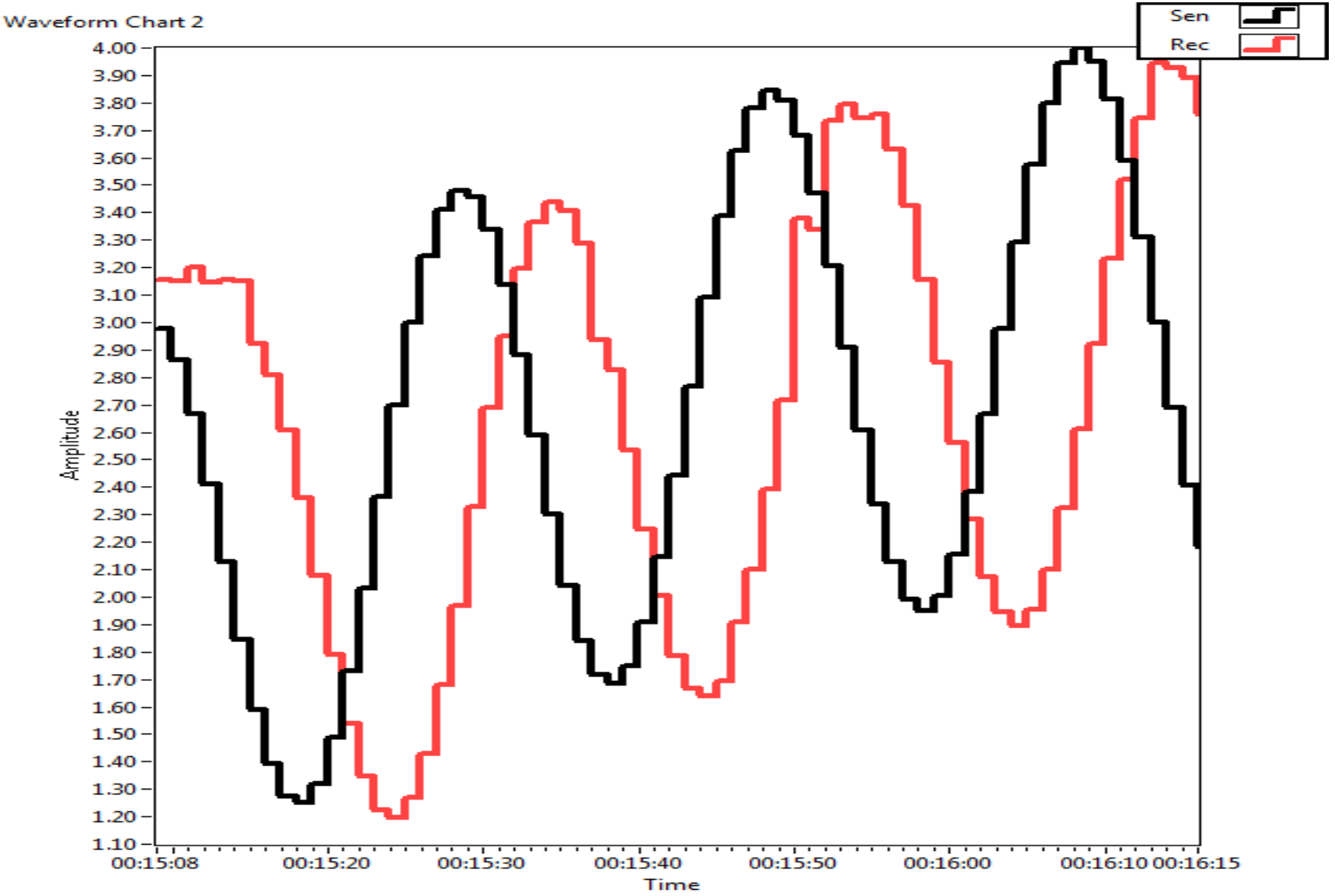

Figure 2.13: Time-delay between the sent and received signals (Sampling time=1s)

Taking the delay of 6 seconds into account we can say, that the data 3.09 sent at the 43^{rd} second should be received at the 49^{th} second. But the data value received at 49^{th} second is 3.38, which is far more than the sent value. Also from Figure 2.13 we can see that the data is not updated at the 49^{th} second. Hence, this sent packet of 43^{rd} second is lost. Similarly the data sent at 45^{th} second is lost. However, the number of such lost packets over minutes of running is found to be small. Such a low packet loss is due to the slow communication and might be higher if faster communication is sought.

Sent signal		Received signal	
Time-stamp	Signal value	Time-stamp	Signal value
00:15:42	2.77	00:15:42	1.67
00:15:43	3.09	00:15:43	1.64
00:15:44	3.39	00:15:44	1.69
00:15:45	3.62	00:15:45	1.91
00:15:46	3.78	00:15:46	2.1
00:15:47	3.84	00:15:47	2.39
00:15:48	3.81	00:15:48	2.72
00:15:49	3.68	00:15:49	3.38
00:15:50	3.47	00:15:50	3.34
00:15:51	3.21	00:15:51	3.74
00:15:52	2.91	00:15:52	3.8
00:15:53	2.61	00:15:53	3.75
00:15:54	2.34	00:15:54	3.76
00:15:55	2.13	00:15:55	3.63
00:15:56	1.99	00:15:56	3.43
00:15:57	1.95	00:15:57	3.16
00:15:58	2.01	00:15:58	2.85
00:15:59	2.15	00:15:59	2.56
00:15:60	2.38	00:15:60	2.28

Table 2.1: Observation of packet loss

The sent (black) and the received (red) signals are as shown in Figure 2.14. It is seen that the received signal is delayed by 13.195 seconds. Also the signal suffers packet loss as well as uncertain time-delays. The received signal in Figure 2.16 seems distorted at the edges when compared to the sent signal. This blue region shows the duration of packet loss. Moreover, in case of time-delay, as shown in Figure 2.15, the received signal is not updated for around 0.1 second. Since, occurrence of this delay is random, it is termed as uncertain time-delay. Thus, maximum delay occurring in the network is obtained as 14 seconds.

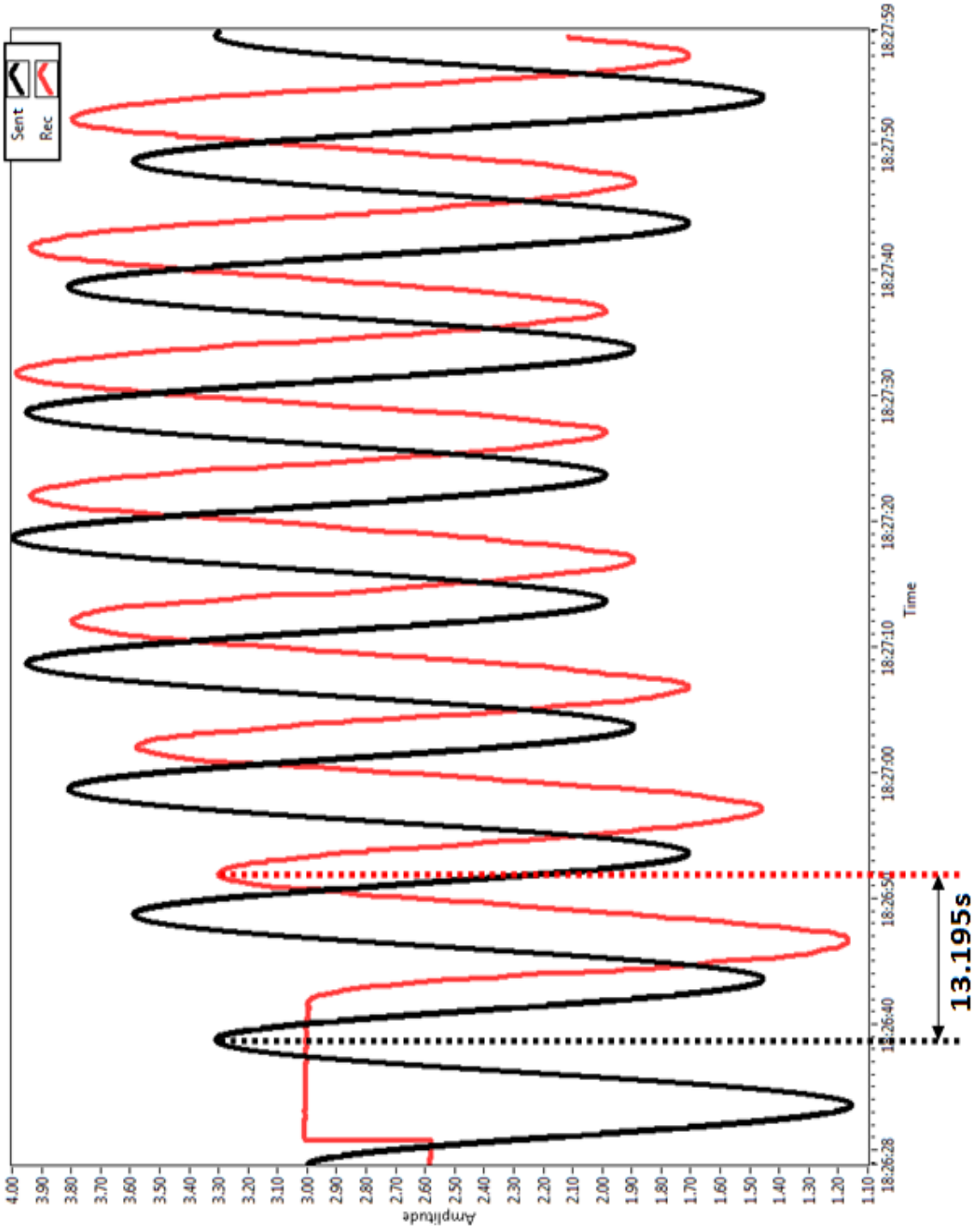

Figure 2.14: Time-delay in the network

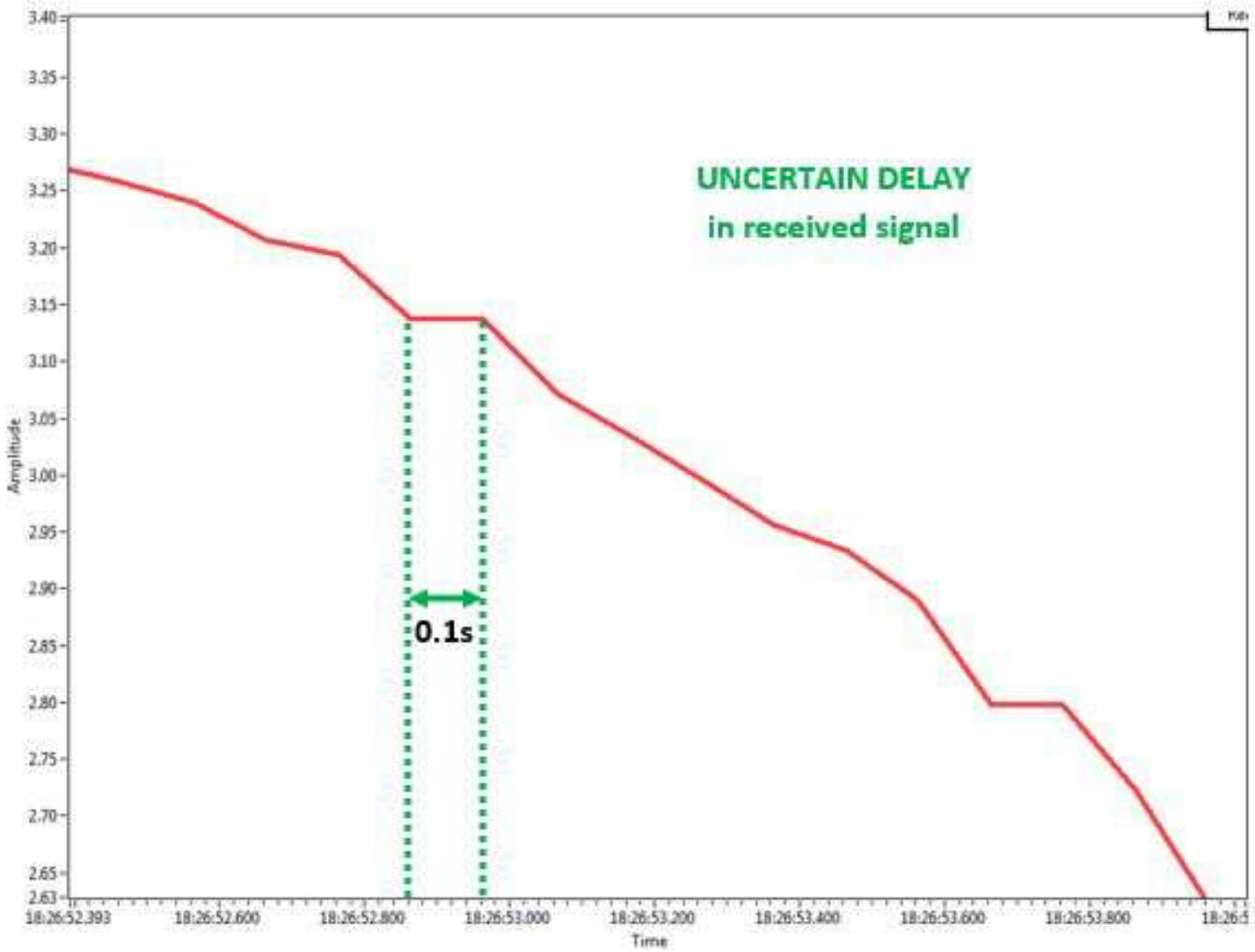

Figure 2.15: Uncertain Time-delay in the network

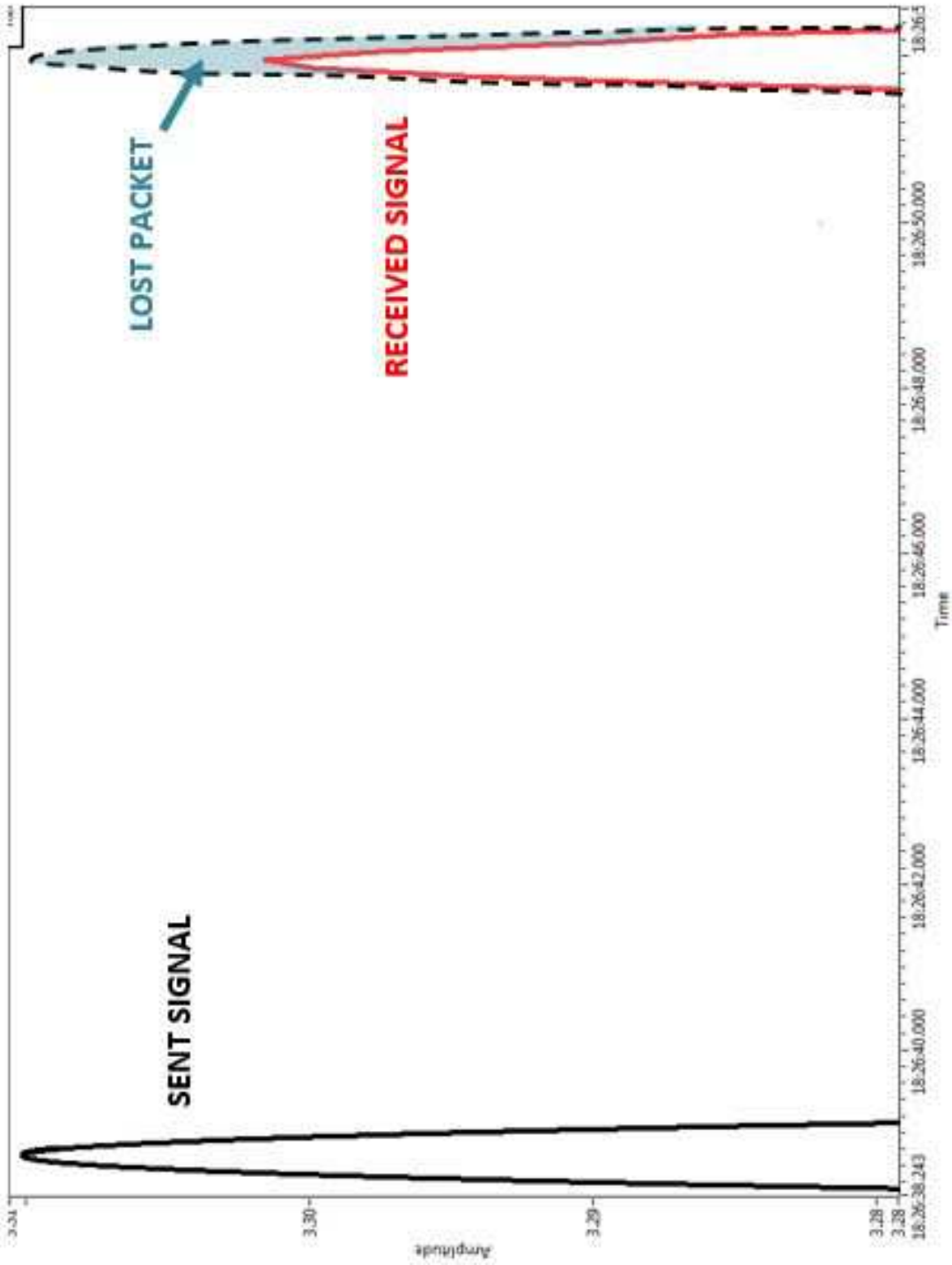

Figure 2.16: Packet loss in the network

2.5 Chapter Summary

This chapter focuses on detailed description of the temperature control plant, and the various other components required to form the NCS setup. The mathematical modeling of oven plant is also presented and the validity of the model is discussed based on the best fit percentage of measured and simulated output of the plant. In the last section, the procedure for measurement of the maximum delay in the network is presented in detail with all the relevant figures. The initial tests shows that the maximum delay of the network, which includes time-delay, packet loss and uncertain time-delay, is 7.

Chapter 3

Output Feedback Controller with Delay Estimator

3.1 Introduction

This chapter takes into account an output feedback controller for dealing with the network issues like packet losses and time-delays. As per the available literature, [37] presented some sufficient conditions to control a discrete-time LTI (Linear Time Invariant) system using a scaling LMI approach to static output feedback controller. Whereas, in [38], a robust output feedback controller is designed to deal with the time-varying uncertainties for both continuous and discrete time linear systems. In [39], the output feedback H_∞ controller is employed to compensate for network induced time-delays, packet losses, random packet losses, for a non-linear networked control systems whereas in [40] the same controller is use to deal with time-varying delays and obtain stochastic stability of Markovian jump systems. In [41] a predictive output feedback approach is used to deal with random network delays. Hence, in this chapter an output feedback approach is used for the controller design. Due to network in the feedback loop, a delayed plant output forms the control signal, which is required to achieve control of NCS. Moreover, the controller gains are chosen according to the delay occurring in the network. Hence, it is clearly evident that control signal is constituted using delay information $d(k)$. This information on delay can either be deduced using time-triggered protocols as in [19] or can be estimated. Estimating the delay values is more preferred over time-triggered protocols because the latter requires additional hardware interface devices. Hence, in this chapter an Error-Comparison and Gradient Descent method based estimator is also designed.

The chapter focuses on output feedback closed loop control of the oven plant. It also deals with designing of Error-Comparison and Gradient Descent method based estima-

tor whose performance is demonstrated by simulation as well as experimental results. The non-divergence of the latter is also discussed. The simulations are done using MATLAB/SIMULINK and the real time experimentation results are obtained using LabVIEW.

3.2 Output-Feedback Controller

3.2.1 System description

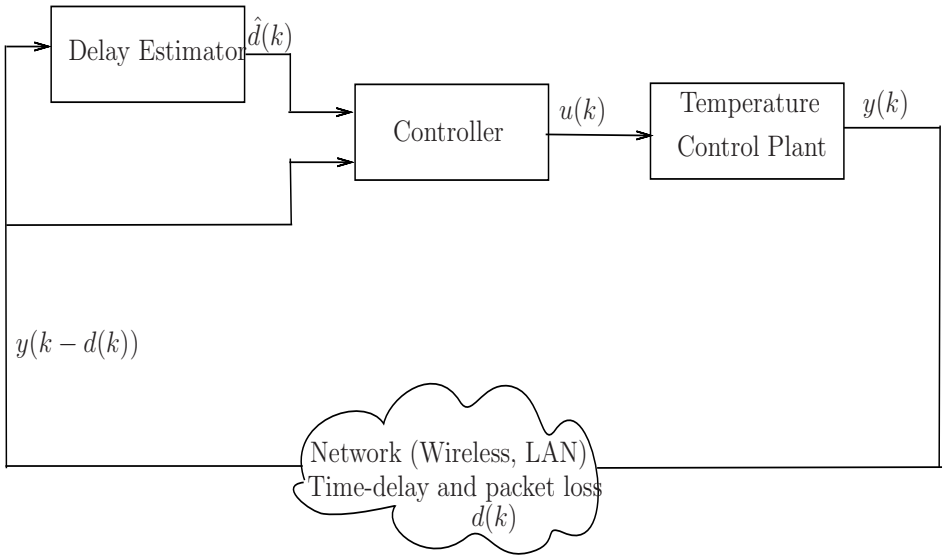

Figure 3.1: Schematic diagram of NCS for output feedback control

The NCS including the controller configuration is shown in Figure 3.1. In this, the output of the plant $y(k)$ is sent via network to the controller and the delay estimator. The delay estimator uses the delayed output to estimate the delay values $\hat{d}(k)$. These delay values are required to choose the controller gain. This controller gain and the delayed output is used by the controller to form the control input $u(k)$ of the plant. Since, the communication considers fixed sampling intervals of either 1 second or 2 seconds, time-driven controller is used throughout this work.

The discrete-time plant for this NCS configuration is chosen as:

$$x(k+1) = Ax(k) + Bu(k), \qquad y(k) = Cx(k), \tag{3.1}$$

where $x(k) \in R^n$ is the state vector; $u(k) \in R^m$ is the control input to the plant; $y(k) \in R^p$ is the plant output; A, B and C are constant matrices of suitable dimensions. $d(k)$, $0 \leq d(k) \leq N$, is the random time-delays induced by the network in the feedback channel, which possibly includes the packet losses. Due to the presence of network in the

feedback loop, a delayed output of the plant is available for designing the control gains. PI (Proportional Integral) controller is one of the most widely used controllers in industries. The reason being its simplicity of design and easy tuning ([11], [12]). Hence, the PI controller is considered in this work. For implementation, the digital PI velocity algorithm ([42]) is considered as:

$$\begin{aligned} u(k) &= \frac{K_o}{1-z^{-1}}\left[(1-z^1)+\frac{T}{2T_i}(1+z^{-1})\right]y(k-d(k)), \qquad (3.2)\\ &= u(k-1)+K_o(1+T_i)y(k-d(k))+K_o(1-T_i)y(k-d(k)-1),\\ &= u(k-1)+v(k), \qquad (3.3)\end{aligned}$$

where T_i is the integral time constant and

$$v(k) = K_{d(k)}\bar{y}(k). \qquad (3.4)$$

where $K_{d(k)} = \begin{bmatrix} K_o(1+T_i) & K_o(1-T_i)\end{bmatrix}$ and $\bar{y}(k) = \begin{bmatrix} y(k-d(k)) \\ y(k-d(k)-1)\end{bmatrix}$. This control input is used for the plant, that yields the closed loop dynamics as:

$$\bar{x}(k+1) = \bar{A}\bar{x}(k)+\bar{B}v(k), \qquad \bar{y}(k) = \bar{C}_{d(k)}\bar{x}(k), \qquad (3.5)$$

where $\bar{x}(k) = \begin{bmatrix} x^T(k) & \dots & x^T(k-d(k)-1) & u^T(k)\end{bmatrix}^T$, $\bar{A} = \begin{bmatrix} A & 0_{n\times(N+1)n} & B \\ I_{(N+1)n} & 0_{(N+1)n\times n} & 0_{(N+1)n\times m} \\ 0_{m\times(N+1)n} & 0_{m\times n} & I_{m\times m}\end{bmatrix}$, $\bar{B} = \begin{bmatrix} 0_{(N+2)n\times m} \\ I_{m\times m}\end{bmatrix}$, $\bar{C}_{d(k)} = \begin{bmatrix} 0_{p\times(d(k))n} & C & 0_{p\times((N+1-d(k))n)+1} \\ 0_{p\times(d(k)+1)n} & C & 0_{p\times((N-d(k))n)+1}\end{bmatrix}$. Here, matrix $\bar{C}_{d(k)}$ depends on the delay values. When the disturbance $w(k)$ is introduced in the noisy measurement in the output, the closed loop system of (3.5) can be rewritten as

$$\bar{x}(k+1) = \bar{A}\bar{x}(k)+\bar{B}v(k)+\bar{E}w(k), \qquad \bar{y}(k) = \bar{C}_{d(k)}\bar{x}(k)+\bar{H}w(k), \qquad (3.6)$$

where, $\bar{E} = \begin{bmatrix} E \\ 0_{(n(d(k)+1))+m\times v}\end{bmatrix}$, $\bar{H} = \begin{bmatrix} H \\ 0_{p\times v}\end{bmatrix}$, with E and H as system matrices of appropriate dimensions. The closed loop dynamics in (3.22), can be written in the augmented form as:

$$\begin{bmatrix}\bar{x}(k+1) \\ \bar{y}(k)\end{bmatrix} = (\hat{A}+\hat{B}\hat{K}\hat{C})\begin{bmatrix}\bar{x}(k) \\ w(k)\end{bmatrix}, \qquad (3.7)$$

where, $\hat{A} = \begin{bmatrix}\bar{A} & E \\ \bar{C} & F\end{bmatrix}$, $\hat{B} = \begin{bmatrix}\bar{B} \\ D\end{bmatrix}$, $\hat{C} = \begin{bmatrix}\bar{C} & H\end{bmatrix}$, $\hat{K} = K_{d(k)}$ with $D = 0$ is system matrix of appropriate dimension.

Now, the objective is to design the output feedback controller gain $K_{d(k)}$. The values of controller gain is chosen according to the delay values $d(k)$ and these delay values are estimated using proposed estimators.

3.2.2 Controller design

To design an output feedback controller (3.4) so as to meet H_∞ performance of the closed-loop system (3.7), the controller design in [6] is followed. For comprehensiveness, the result of [6] is detailed next.

An H_∞ controller interpreted in terms of induced l_2 norm as:

$$\frac{\sum_{k=0}^{+\infty} y(k)^T y(k)}{\sum_{k=0}^{+\infty} w(k)^T w(k)} < \gamma^2. \tag{3.8}$$

This implies that the system (3.7) satisfies an H_∞ performance of γ, if the following is satisfied.

$$-y(k)^T y(k) + \gamma^2 w(k)^T w(k) > 0, \tag{3.9}$$

Based on the above definition the following is the result of [6].

Theorem 3.2.1. [6] *For closed loop system (3.7) and $\gamma > 0$ with known μ and η, if there exist appropriate dimension matrix $\hat{P}$, G, V, U and J, such that*

$$\begin{bmatrix} \Xi_{11} & (G\hat{A} + \hat{B}V\hat{C})^T & (\hat{B}^T\hat{B}V\hat{C})^T & 0 \\ * & \Xi_{22} + J & 0 & 0 \\ * & * & -\mu\hat{B}^T\hat{B}U - \mu U^T(\hat{B}^T\hat{B})^T & (G\hat{B} - \hat{B}U)^T \\ * & * & * & -\frac{J}{\mu^2} \end{bmatrix} < 0, \tag{3.10}$$

then, the H_∞ performance γ is guaranteed, where $\Xi_{22} = -\eta G - \eta G^T + \eta^2 \begin{bmatrix} \hat{P} & 0 \\ * & I \end{bmatrix}$ and controller gain matrix $\hat{K} = U^{-1}V$

Proof. Define a Lyapunov function as

$$V(k) = \bar{x}(k)^T \hat{P} \bar{x}(k), \tag{3.11}$$

where $\hat{P}$ is a positive definite symmetric matrix. Correspondingly,

$$\begin{aligned} \Delta V &= v(k+1) - v(k) \\ &= \bar{x}(k+1)^T \hat{P} \bar{x}(k+1) - \bar{x}(k)^T \hat{P} \bar{x}(k) + y(k)^T y(k) - y(k)^T y(k) \\ &+ \gamma^2 w(k)^T w(k) - \gamma^2 w(k)^T w(k). \end{aligned} \tag{3.12}$$

Using(3.7), one can write (3.12) as:

$$\begin{aligned} \Delta V(k) &= \begin{bmatrix} \bar{x}(k)^T \\ w(k)^T \end{bmatrix}^T \left((\hat{A} + \hat{B}\hat{K}\hat{C})^T \begin{bmatrix} \hat{P} & 0 \\ 0 & I \end{bmatrix} (\hat{A} + \hat{B}\hat{K}\hat{C}) - \begin{bmatrix} -\hat{P} & 0 \\ * & -\gamma^2 I \end{bmatrix} \right) \begin{bmatrix} \bar{x}(k) \\ w(k) \end{bmatrix} \\ &- y(k)^T y(k) + \gamma^2 w(k)^T w(k). \end{aligned} \tag{3.13}$$

Let

$$\left((\hat{A}+\hat{B}\hat{K}\hat{C})^T\begin{bmatrix}\hat{P} & 0\\ 0 & I\end{bmatrix}(\hat{A}+\hat{B}\hat{K}\hat{C})-\begin{bmatrix}-\hat{P} & 0\\ * & -\gamma^2 I\end{bmatrix}\right)<0, \tag{3.14}$$

then from (3.13) one can write

$$\Delta V(k) < -y(k)^T y(k)+\gamma^2 w(k)^T w(k) \tag{3.15}$$

Following this, one can write

$$\sum_{k=0}^{+\infty}\Delta V(k) < \sum_{k=0}^{+\infty}(-y(k)^T y(k)+\gamma^2 w(k)^T w(k)) \tag{3.16}$$

This leads to

$$V(\infty)-V(0) < \sum_{k=0}^{+\infty}(-y(k)^T y(k)+\gamma^2 w(k)^T w(k)) \tag{3.17}$$

Considering zero initial condition, $V(0)=0$ and by definition of $\hat{P}$, $V(\infty)>0$. Therefore,

$$\sum_{k=0}^{+\infty}(-y(k)^T y(k)+\gamma^2 w(k)^T w(k)) > 0. \tag{3.18}$$

Then the system satisfies H_∞ performance of γ as per (3.9). Taking Schur complement of (3.14), we can write that, for the closed loop system (3.7) and $\gamma>0$, if there exist appropriate dimension matrix $\hat{P}$ and $\hat{K}$ such that

$$\begin{bmatrix}\Xi_{11} & (\hat{A}+\hat{B}\hat{K}\hat{C})^T\\ * & -\begin{bmatrix}\hat{P} & 0\\ 0 & I\end{bmatrix}^{-1}\end{bmatrix}<0, \Xi_{11}=\begin{bmatrix}-\hat{P} & 0\\ * & -\gamma^2 I\end{bmatrix}, \tag{3.19}$$

then the H_∞ performance γ is guaranteed. Pre- and post-multiplying (3.19) by $\begin{bmatrix}I & 0\\ * & G\end{bmatrix}$ and its transpose, respectively the inequality can be written as,

$$\begin{bmatrix}\Xi_{11} & (G\hat{A}+G\hat{B}\hat{K}\hat{C})^T\\ * & -G\begin{bmatrix}\hat{P} & 0\\ 0 & I\end{bmatrix}^{-1}G^T\end{bmatrix}<0 \tag{3.20}$$

Also for a scalar η, note that $-(V_1-\eta Q)Q_1^{-1}(V_1-\eta Q_1)^T\leq 0$ implies that $\eta V_1+\eta V_1^T-\eta^2 Q_1 \leq V_1 Q_1^{-1} V_1^T$, Thus from (3.20) one has,

$$\begin{bmatrix}\Xi_{11} & (G\hat{A}+G\hat{B}\hat{K}\hat{C})^T\\ * & \Xi_{22}\end{bmatrix}<0. \tag{3.21}$$

The above equation can also be written as:

$$\begin{bmatrix} \Xi_{11} & (G\hat{A}+\hat{B}V\hat{C}) \\ * & \Xi_{22} \end{bmatrix} + \begin{bmatrix} 0 & 0 \\ G\hat{B}\hat{K}\hat{C}-\hat{B}V\hat{C} & 0 \end{bmatrix} + \begin{bmatrix} 0 & (G\hat{B}\hat{K}\hat{C}-\hat{B}V\hat{C})^T \\ 0 & 0 \end{bmatrix} < 0. \quad (3.22)$$

Taking $\hat{K} = U^{-1}V$, from (3.22) one can obtain,

$$\begin{bmatrix} \Xi_{11} & * \\ G\hat{A}+\hat{B}V\hat{C} & \Xi_{22} \end{bmatrix} + \begin{bmatrix} 0 \\ I \end{bmatrix} (G\hat{B}-\hat{B}U)U^{-1}V\hat{C} \begin{bmatrix} I & 0 \end{bmatrix} + (U^{-1}V\hat{C} \begin{bmatrix} I & 0 \end{bmatrix})^T (G\hat{B}-\hat{B}U)^T \begin{bmatrix} 0 \\ I \end{bmatrix}^T < 0 \quad (3.23)$$

If there exist appropriate dimension matrices X, Y and $J > 0$, then

$$XY + Y^T X^T \leq XJX^T + Y^T J^{-1} Y \quad (3.24)$$

holds and we have

$$\begin{bmatrix} \Xi_{11} & * \\ G\hat{A}+\hat{B}V\hat{C} & \Xi_{22} \end{bmatrix} + \begin{bmatrix} 0 \\ I \end{bmatrix} J \begin{bmatrix} 0 \\ I \end{bmatrix}^T + (U^{-1}V\hat{C} \begin{bmatrix} I & 0 \end{bmatrix})^T (G\hat{B}-\hat{B}U)^T J^{-1} (G\hat{B}-\hat{B}U)U^{-1}V\hat{C} \begin{bmatrix} I & 0 \end{bmatrix} < 0. \quad (3.25)$$

The above equation can also be written as:

$$\begin{bmatrix} \Xi_{11} & * \\ G\hat{A}+\hat{B}V\hat{C} & \Xi_{22}+J \end{bmatrix} + (U^{-1}V\hat{C} \begin{bmatrix} I & 0 \end{bmatrix})^T (G\hat{B}-\hat{B}U)^T J^{-1} (G\hat{B}-\hat{B}U)U^{-1}V\hat{C} \begin{bmatrix} I & 0 \end{bmatrix} < 0 \quad (3.26)$$

If the following LMI

$$\begin{bmatrix} T_1 & (L_1 N_1)^T \\ * & -\mu L_1 - \mu {L_1}^T + \mu^2 P_1 \end{bmatrix} < 0, \quad (3.27)$$

where T_1, P_1, L_1 and N_1 are appropriate dimension matrices and μ is a scalar exist, then we have

$$T_1 + {N_1}^T P_1 N_1 < 0. \quad (3.28)$$

Hence, with $T_1 = \begin{bmatrix} \Xi_{11} & * \\ G\hat{A}+\hat{B}V\hat{C} & \Xi_{22}+J \end{bmatrix}$, $L_1 = \hat{B}^T\hat{B}U$, $N = U^{-1}V\hat{C} \begin{bmatrix} I & 0 \end{bmatrix}$ and $\hat{P} = (G\hat{B}-\hat{B}U)^T J^{-1}(G\hat{B}-\hat{B}U)$, one can write,

$$\begin{bmatrix} \begin{bmatrix} \Xi_{11} & * \\ G\hat{A}+\hat{B}V\hat{C} & \Xi_{22}+J \end{bmatrix} & * \\ \hat{B}^T\hat{B}V\hat{C} \begin{bmatrix} I & 0 \end{bmatrix} & \Lambda \end{bmatrix} < 0 \quad (3.29)$$

where $\Lambda = -\mu\hat{B}^T\hat{B}U - \mu U^T(\hat{B}^T\hat{B})^T + \mu^2(G\hat{B} - \hat{B}U)^T J^{-1}(G\hat{B} - \hat{B}U)$. The equation (3.29) is the Schur complement of the inequality (3.10). For feasible solution of this inequality, $\hat{P} > 0$, $J > 0$ and G and U are non-singular. □

Hence, after solving this LMI for matrix variables, gain values are given by

$$K_{d(k)} = U^{-1}V \tag{3.30}$$

These gain values are used for implementing the output-feedback controller and a particular gain value is selected based on the the delay information at that moment.

Let $\hat{d}(k)$ be the estimated delay at an instant. In the NCS configuration shown in Figure 3.1, a delay estimator is used to estimate $\hat{d}(k)$. This information on $\hat{d}(k)$ is used to choose the gain of the controller. Hence, the control signal can be modified as:

$$v(k) = K_{\hat{d}(k)}\bar{y}(k), \tag{3.31}$$

The gain values are chosen based on the values of $\hat{d}(k)$ and these delay values are estimated using algorithms presented in next section.

3.3 Delay Estimators

Once controller gain values are obtained, one may try to estimate the delay values online to make use of the variable controller gains. For a particular gain value a system can tolerate certain maximum amount of delay. In [43], a concept of jitter margin is introduced which is used to determine the maximum time-varying delay tolerance of the system. Also, [44] deals with stability and performance of such systems. This section describes two delay estimators used for the purpose and also computes the jitter margin for the specified controller gain. These are presented next.

3.3.1 Error-comparison method based delay estimator

To estimate $\hat{d}(k)$, an error-comparison method based estimator is designed. At a particular instant let the dynamics of the plant considered in (3.1), for $d(k)$ delay in the network be written as:

$$y(k - d(k)) = Cx(k - d(k)). \tag{3.32}$$

The output-estimator can be written for different values of $d(k)$, $0 \leq d(k) \leq N$ in the form of following equations:

$$\begin{aligned} \hat{y}(k) &= C\hat{x}(k), \\ \hat{y}(k-1) &= C\hat{x}(k-1), \\ &\vdots \\ \hat{y}(k-N) &= C\hat{x}(k-N). \end{aligned} \tag{3.33}$$

The delayed output of the plant (3.32) is directly compared with each value of estimated output (3.33). Hence, the estimated delay can be given by

$$\hat{d}(k) = i \quad for \min_{i \in [0 \ldots N]} ||y(k - d(k)) - \hat{y}(k-i)|| \tag{3.34}$$

This $\hat{d}(k)$ value is used for multiple gain-valued controller implementation that uses delay in the network at a specific instant. But, as the amount of delay increases, the design of this estimator gets complex. Next, we consider another estimator based on well known adaptation algorithm.

3.3.2 Gradient descent method based delay estimator

In this section, to estimate $\hat{d}(k)$, a Gradient Descent method based estimator is designed. To incorporate this method, regressor form of plant (3.1) is considered. The dynamics of the plant (3.1) can also be represented as:

$$\alpha(z^{-1})y(k) = z^{-d(k-1)}\beta(z^{-1})u(k) \tag{3.35}$$

where, $\alpha(z^{-1}) = 1 - a_1(k-1)z^{-1} - \ldots - a_n(k-1)z^{-n}$ $\beta(z^{-1}) = b_0(k-1) + b_1(k-1)z^{-1} + \ldots + b_m(k-1)z^{-n}$ where, a_i and b_j with $i = 1, \ldots, n$ and $j = 0, \ldots, m$ are time-varying parameters of the plant. Considering known plant parameters, the output of the estimator for the next instant can be estimated using last estimated delay value, and this output can be defined as:

$$\alpha(z^{-1})\hat{y}(k) = z^{-\hat{d}(k-1)}\beta(z^{-1})u(k) \tag{3.36}$$

The error between the plant (3.35) and the estimated output (3.36) is

$$\begin{aligned} e(k) &= y(k) - \hat{y}(k) \\ &= u(k)[\frac{\beta(z^{-1})}{\alpha(z^{-1})}z^{-d(k-1)} - \frac{\beta(z^{-1})}{\alpha(z^{-1})}z^{-\hat{d}(k-1)}] \end{aligned} \tag{3.37}$$

Now, the cost function is defined as

$$J_d = \frac{1}{2}\sum_{i=1}^{k} e^T(i)e(i) \tag{3.38}$$

To estimate the delay values, one may invoke gradient descent method [29] as follows:

$$\hat{d}(k) = \hat{d}(k-1) - \lambda \frac{\partial J_d(k)}{\partial \hat{d}(k-1)}, \tag{3.39}$$

where $\lambda \in [0, 1]$ is the learning rate. Using second order approximation as $\ln(z) \approx -1.5 + 2z^{-1} - 0.5z^{-2}$, one can write from (3.37) and (3.38):

$$\begin{aligned} \frac{\partial J_d(k)}{\partial \hat{d}(k-1)} &= -e(k)^T \Big(\frac{\beta(z^{-1})}{\alpha(z^{-1})} z^{-\hat{d}(k-1)} \\ &\quad (-1.5 + 2z^{-1} - 0.5z^{-2})u(k)\Big) \\ &= -e(k)^T \hat{y}(k)(-1.5 + 2z^{-1} - 0.5z^{-2}) \\ &= -e(k)^T \Delta\hat{y}(k), \end{aligned} \tag{3.40}$$

where $\Delta\hat{y}(k) = [-1.5\hat{y}(k) + 2\hat{y}(k-1) - 0.5\hat{y}(k-2)]$. Then from (3.39), one can write:

$$\hat{d}(k) = \hat{d}(k-1) + \lambda e(k)^T \Delta\hat{y}(k) \tag{3.41}$$

Note that, $\hat{d}(k)$ should take integer values for discrete-time implementation. However, the second term in (3.41) may yield decimal values, which requires further approximation. We use rounding off this term as:

$$\hat{d}(k) = \hat{d}(k-1) + \lfloor \lambda e(k)^T \Delta\hat{y}(k) \rceil. \tag{3.42}$$

Next, since the network induced delays are time-varying and non-zero in nature, the above estimator may diverge on a long run. A modification to ensure that $\hat{d}(k)$ remains bounded could be by considering a decaying term in the estimator. With this modification, (3.42) can be written as:

$$\hat{d}(k) = \hat{d}(k-1) - \epsilon_d + \lfloor \lambda e(k)^T \Delta\hat{y}(k) \rceil, \tag{3.43}$$

where $\epsilon_d \geq 1$ is an integer. This estimator is used in this work with the choice $\epsilon_d = 1$. Note that, since the round-off error is always less than one the choice of $\epsilon_d = 1$ is sufficient to ensure the bounding effect provided the third term in the RHS of (3.43) is bounded. Since the Round of Error (RE) satisfies $-1 \leq RE \leq 1$, (3.43) can also be written as:

$$\hat{d}(k) = \hat{d}(k-1) - \bar{\epsilon_d} + \lambda(k) e(k)^T \Delta\hat{y}(k), \tag{3.44}$$

Therefore, $\hat{d}(k)$ remains bounded, if $e(k)$ and $\Delta\hat{y}(k)$ are bounded.

3.3.3 Jitter margin calculation

Jitter margin is defined as the maximum variable delay a system can tolerate before it gets unstable. For the discrete-time plant transfer function (2.8) and the PI controller

$$C(z) = \frac{K_o}{1 - z^{-1}} \left[(1 - z^1) + \frac{T}{2T_i}(1 + z^{-1}) \right], \tag{3.45}$$

the jitter margin N_{max} as described in [44], is given by

$$\left| \frac{G(z)C(z)}{1+G(z)C(z)} \right| < \frac{1}{N_{max}|z-1|}, \tag{3.46}$$

For calculating the jitter margin, the frequency plot of L.H.S of (3.46) is drawn. Also frequency plot of R.H.S for different values of N_{max} is drawn and checked for the condition in (3.46). The maximum value of N_{max} satisfying (3.46), gives the jitter margin. Thus, using the above equation jitter margin is calculated and the results are presented in the next section.

3.4 Simulation and Experimental Results

For simulation and experimental results, the same temperature control plant as described in chapter 2 is used for study. At first, the performance of output-feedback controller is studied with error-comparison method based estimator and then with gradient descent method based estimator.

3.4.1 For sampling time of 1 second

Plant model

The discrete-time model used in this case (2.9) for both experimental and simulation studies is as described:

$$x(k+1) = Ax(k) + Bu(k), \qquad y(k) = Cx(k), \tag{3.47}$$

where $A = \begin{bmatrix} 0 & 0 & 0 \\ 1 & 0 & 0 \\ 0 & 1 & 0.9965 \end{bmatrix}$, $B = \begin{bmatrix} 0.5739 \\ 0 \\ 0 \end{bmatrix}$, $C = \begin{bmatrix} 0 & 0 & 1 \end{bmatrix}$.

Control gains

Considering sampling time as 1 second, the gain values for $N = 7$, $\eta = -4$, $\mu = -1$ and $\gamma = 1e6$ are obtained solving the LMI (3.10) as:
$K_i = \begin{bmatrix} -0.1478 & 0.1459 \end{bmatrix}, \begin{bmatrix} -0.1251 & 0.1232 \end{bmatrix},$
$\begin{bmatrix} -0.1121 & 0.1102 \end{bmatrix}, \begin{bmatrix} -0.1008 & 0.0990 \end{bmatrix},$
$\begin{bmatrix} -0.0937 & 0.0921 \end{bmatrix}, \begin{bmatrix} -0.0872 & 0.0857 \end{bmatrix},$
$\begin{bmatrix} -0.0831 & 0.0817 \end{bmatrix}, \begin{bmatrix} -0.0776 & 0.0763 \end{bmatrix}$ for $i = 0, \ldots, 7$ respectively.

Simulation result

Performance of Error-comparison method based delay estimator: When the sampling time of 1 second and the corresponding gain values are taken into account, the response of the plant settles at 350 seconds as shown in Figure 3.2. The response has an initial negative course. Due to the delay in the network, the initial conditions are sent as feedback. These initial conditions are less than the reference input, which makes the error signal negative and gives the output a negative course.

The control input is shown in Figure 3.3. Due to the negative error values, the initial control signal is also too small. Figure 3.4 shows the estimated delay values. The maximum delay estimated is of 7 seconds and the delay values are estimated during both transient and steady state.

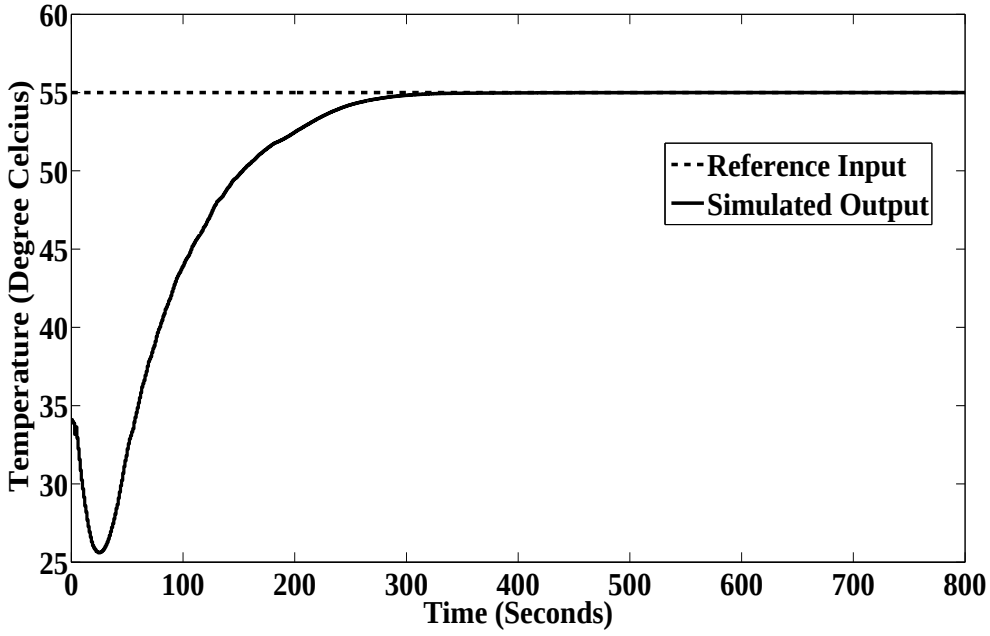

Figure 3.2: Simulation response of the closed loop system

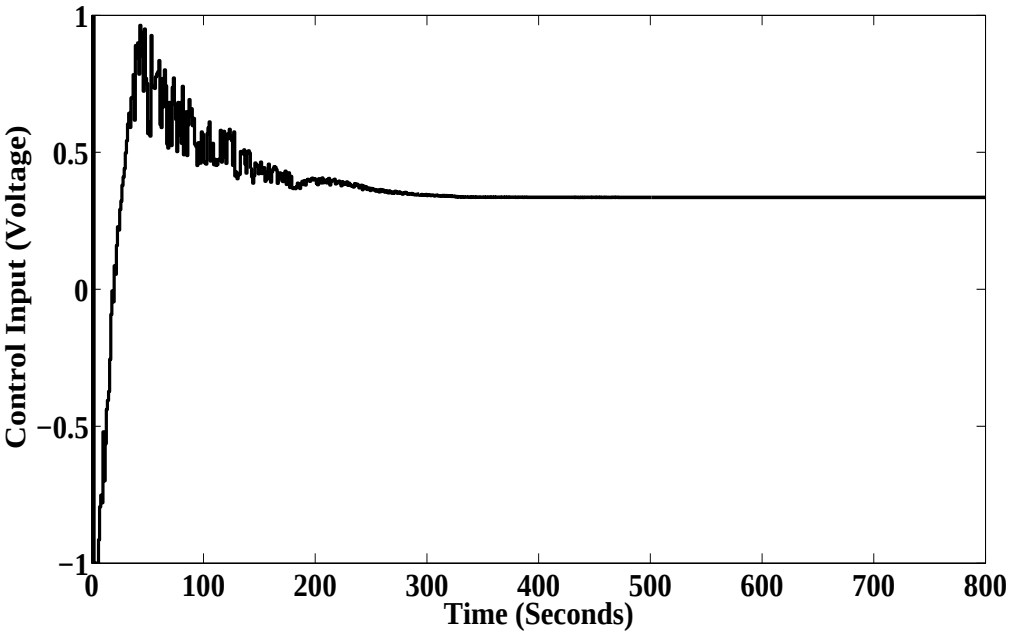

Figure 3.3: Control input for the system during simulation

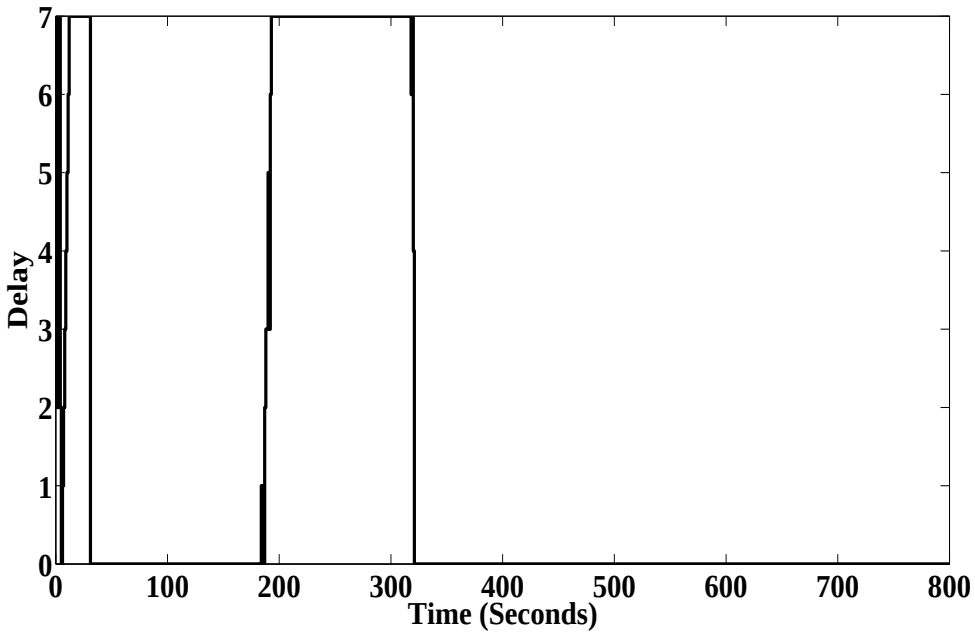

Figure 3.4: Delay estimated by the estimator during simulation

Performance of Gradient descent method based delay estimator: Using gradient descent estimator, when the sampling time of 1 second and the corresponding gain values are

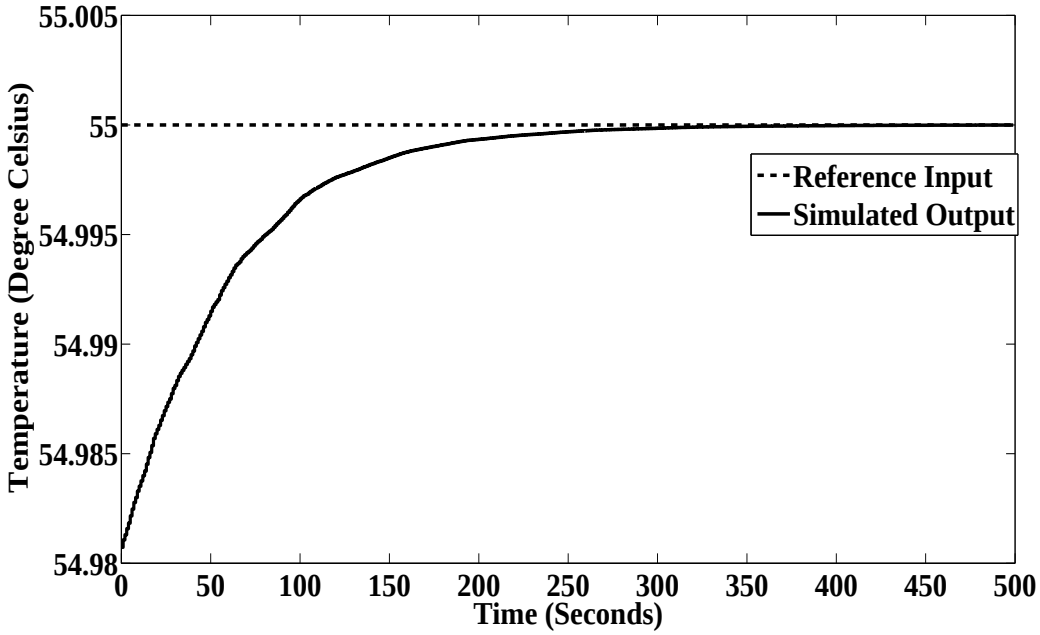

Figure 3.5: Simulation response of the closed loop system

taken into account, the response of the plant settles at 315 seconds as shown in Figure 3.5. The control input is shown in Figure 3.6 and Figure 3.7 shows the estimated delay values.

The delay values are estimated during transient response as the error between actual and estimated output goes to zero during steady state. The maximum delay estimated using gradient descent method based estimator is of 3 seconds.

Jitter Margin: The jitter margin is calculated using relation (3.46). The solid graph gives the frequency plot of L.H.S. whereas, the dotted one gives the frequency plot of R.H.S of (3.46) respectively. For $N_{max} = 25$, the condition (3.46) is satisfied. If the value of N_{max} is increased further, the condition is no longer satisfied. Note that, this value is quite large than the network delay of 7.

Experimental result

Performance of Error-comparison method based delay estimator: The experimental response of the plant has a settling time around 300 seconds as shown in Figure 3.9. The control input for the same is shown in Figure 3.10 and Figure 3.11 shows the estimated delay values.

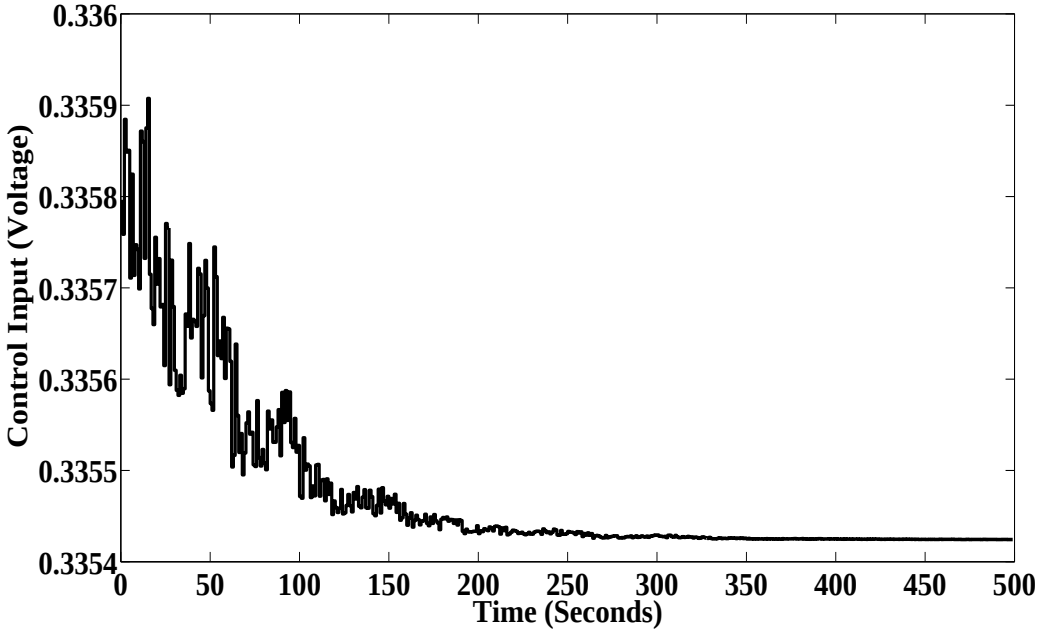

Figure 3.6: Control input for the system during simulation

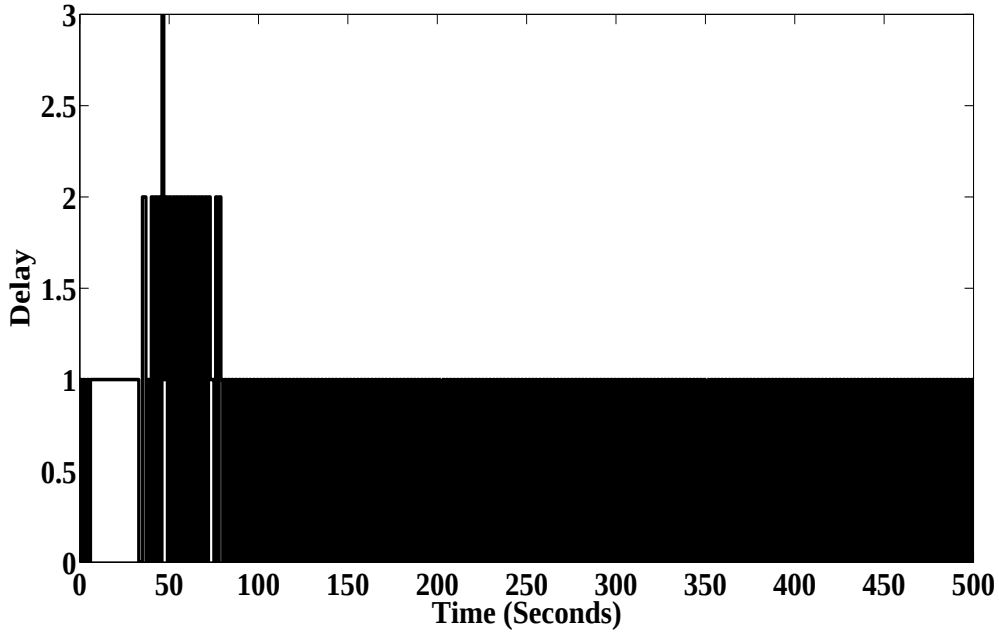

Figure 3.7: Delay estimated by the estimator during simulation

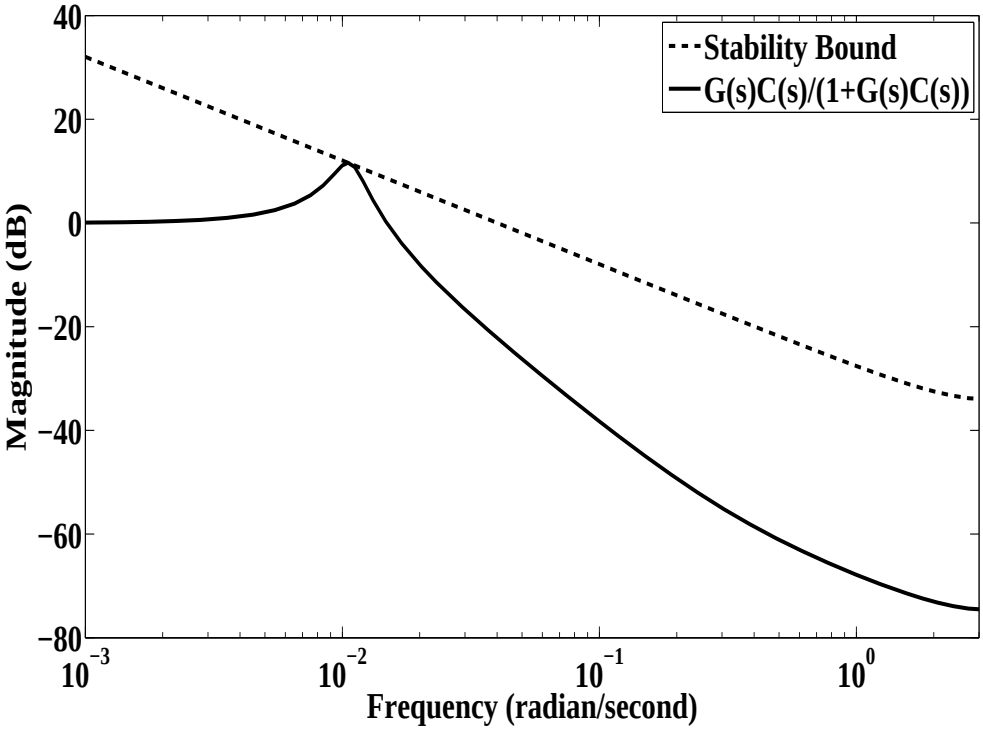

Figure 3.8: Frequency plot showing stability bound with maximum delay

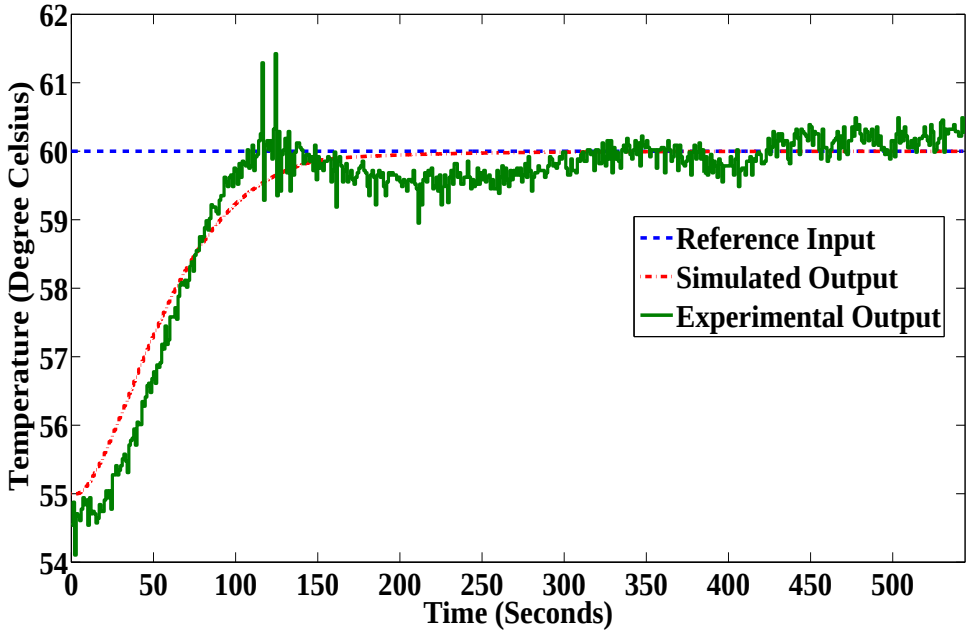

Figure 3.9: Experimental response of the closed loop system

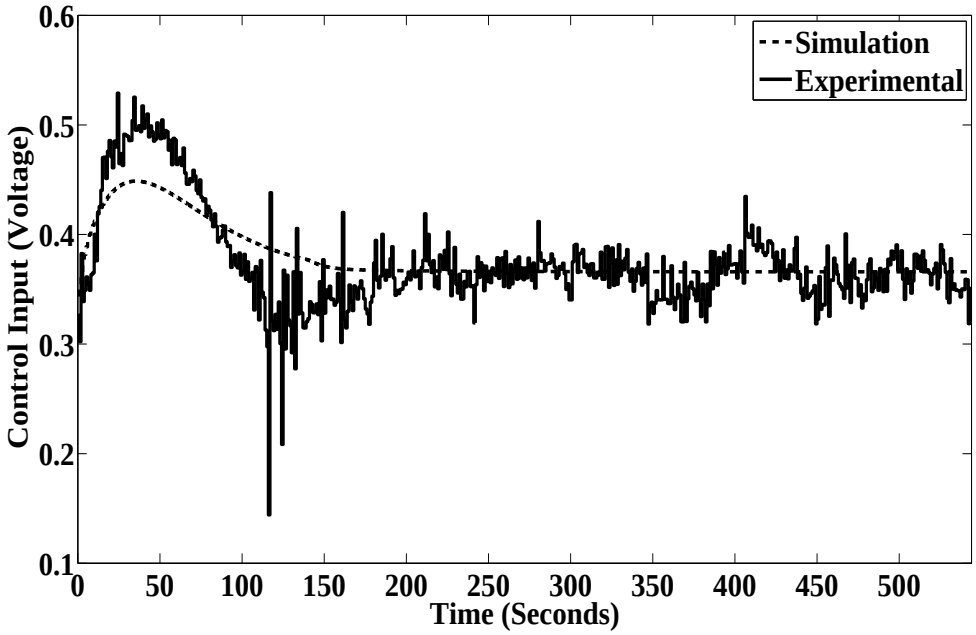

Figure 3.10: Control input of the plant during experiment

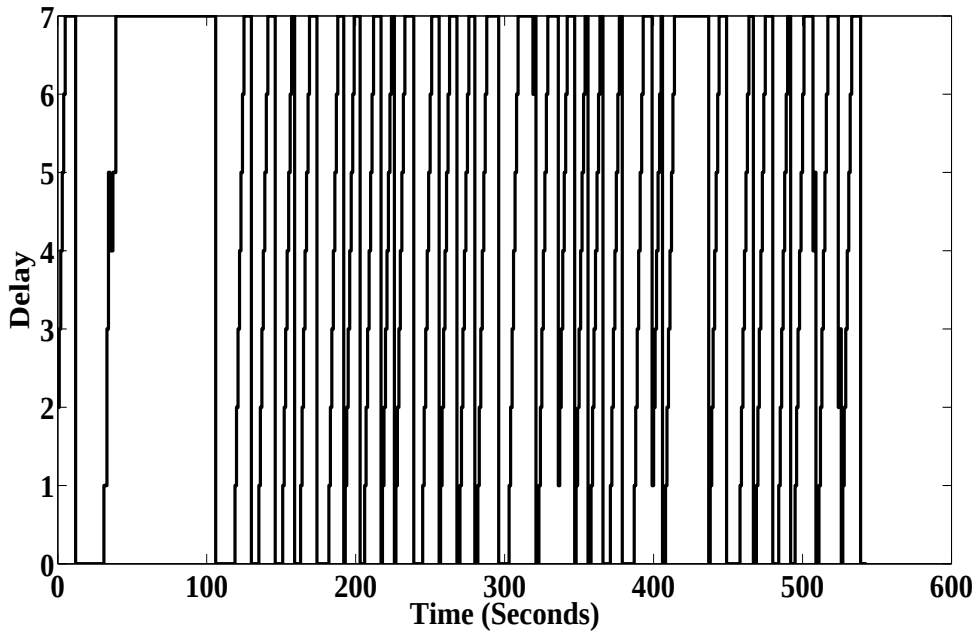

Figure 3.11: Delay estimated by the estimator during experiment

Performance of Gradient descent method based delay estimator: The experimental response of the plant for $\lambda = 0.01$, settles around 220 seconds as shown in Figure 3.12. The control input for the same is shown in Figure 3.13 and Figure 3.14 shows the estimated delay

values. The response of the plant during experiment closely matches the simulation one. The initial response has abrupt changes due to the change in control input. This high control input is due to the larger initial delay.

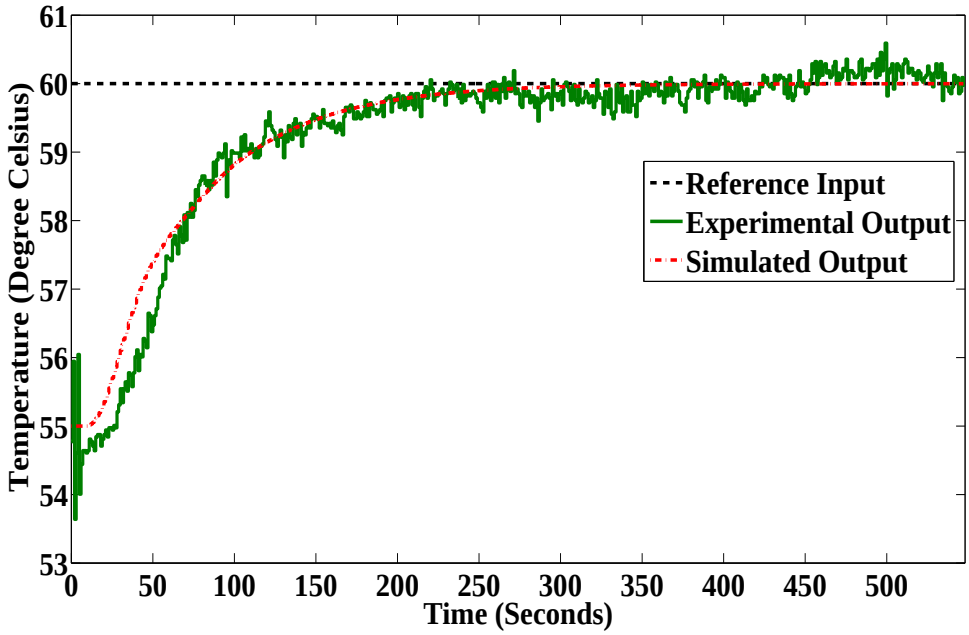

Figure 3.12: Experimental response of the closed loop system

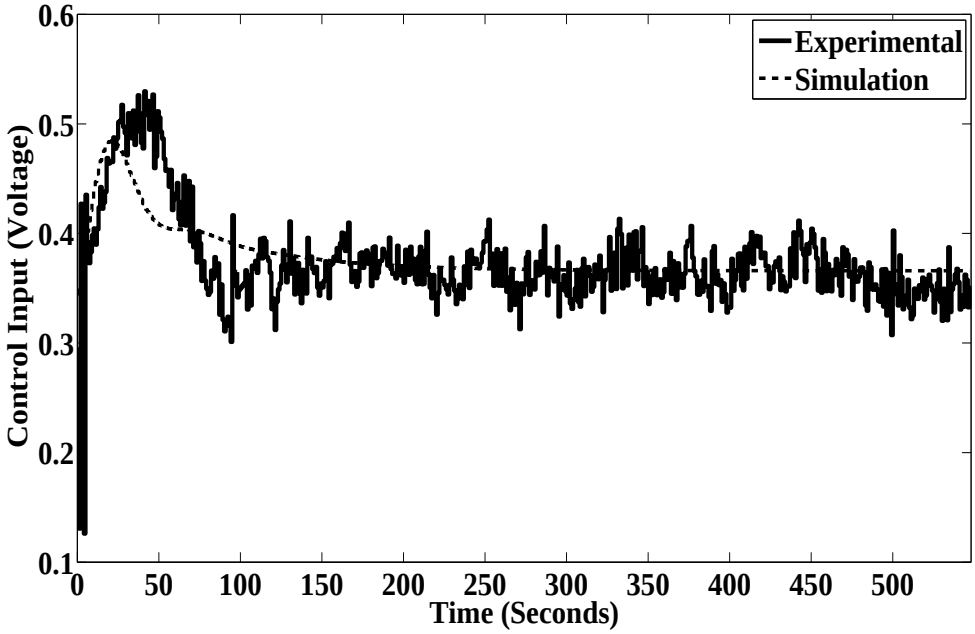

Figure 3.13: Control input of the plant during experiment

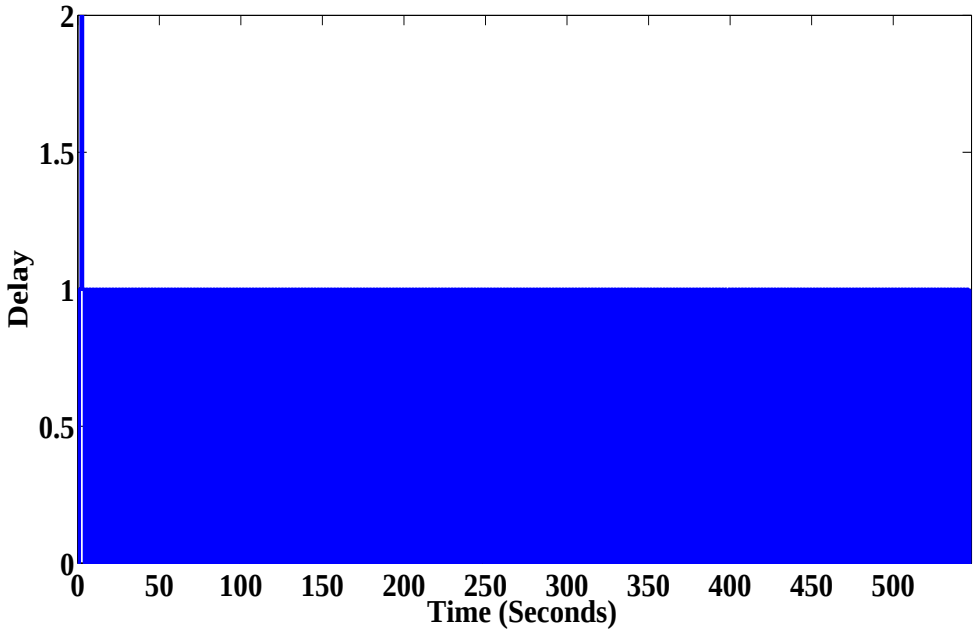

Figure 3.14: Delay estimated by the estimator during experiment

3.4.2 For sampling time of 2 second

Plant Model

The discrete-time model for a sampling time of 2 seconds (2.11) is obtained as:

$$x(k+1) = Ax(k) + Bu(k), \qquad y(k) = Cx(k), \tag{3.48}$$

where $A = \begin{bmatrix} 0 & 0 \\ 1 & 0.9930 \end{bmatrix}$, $B = \begin{bmatrix} 1.1458 \\ 0 \end{bmatrix}$, $C = \begin{bmatrix} 0 & 1 \end{bmatrix}$.

Control gains

The variable output feedback gains corresponding to different delays i.e. $N = 7$ and sampling time= 2 seconds are obtained solving the LMI (3.10) for $\eta = -4$, $\mu = -1$ and $\gamma = 1e6$:
$K_i = \begin{bmatrix} -0.1318 & 0.1297 \end{bmatrix}, \begin{bmatrix} -0.1083 & 0.1065 \end{bmatrix},$
$\begin{bmatrix} -0.0918 & 0.0901 \end{bmatrix}, \begin{bmatrix} -0.0817 & 0.0800 \end{bmatrix},$
$\begin{bmatrix} -0.0727 & 0.0714 \end{bmatrix}, \begin{bmatrix} -0.0680 & 0.0666 \end{bmatrix},$
$\begin{bmatrix} -0.0587 & 0.0578 \end{bmatrix}, \begin{bmatrix} -0.0555 & 0.0544 \end{bmatrix}$ for $i = 0, \ldots, 7$ respectively.

Gains for another set of data values i.e. $\eta = -2$, $\mu = -10$, $\gamma = 1e6$ and sampling time=2 seconds are also calculated so as to study their effects with respect to output

response.
$K_i = \begin{bmatrix} -0.1526 & 0.1437 \end{bmatrix}, \begin{bmatrix} -0.0855 & 0.0803 \end{bmatrix},$
$\begin{bmatrix} -0.0555 & 0.0527 \end{bmatrix}, \begin{bmatrix} -0.0390 & 0.0371 \end{bmatrix},$
$\begin{bmatrix} -0.0273 & 0.0261 \end{bmatrix}, \begin{bmatrix} -0.0271 & 0.0250 \end{bmatrix},$
$\begin{bmatrix} -0.0160 & 0.0152 \end{bmatrix}, \begin{bmatrix} -0.0136 & 0.0129 \end{bmatrix}$ for $i = 0, \ldots, 7$ respectively.

Simulation result

Performance of controller with known delay values: Figure 3.15, shows the system response to a reference input of 70 degree Celsius. The simulation response of plant when controller chooses gain values according to the actual delay values settles around 786 seconds. The gain values considered here are corresponding to $\eta = -4$, $\mu = -1$.

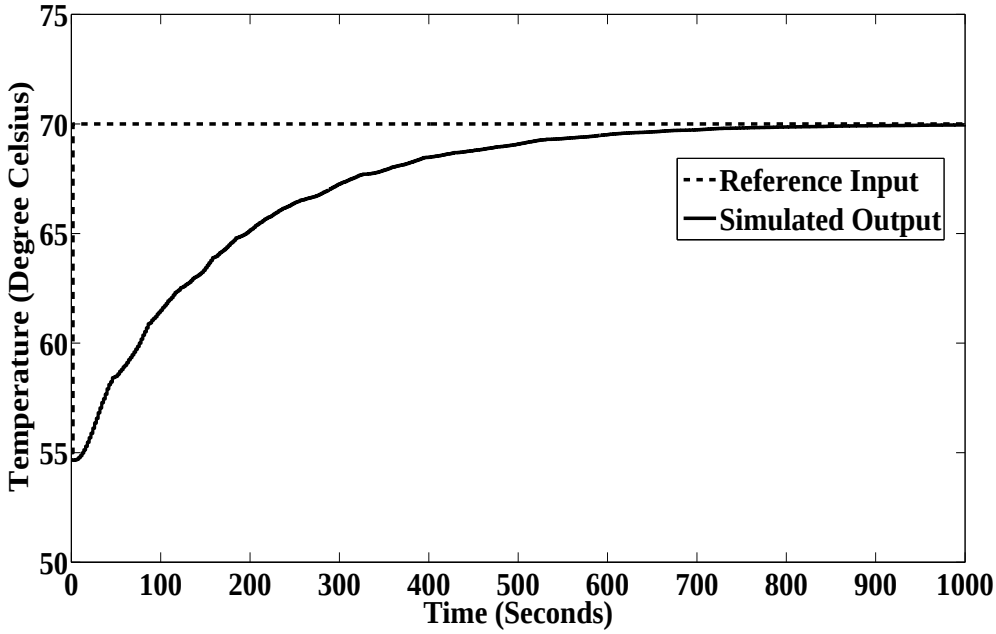

Figure 3.15: Simulation response with known delay values

Performance of Error-comparison method based delay estimator: The gain values for 2 seconds sampling time, $\eta = -4$, $\mu = -1$, are used to study the performance of the plant as well as estimator during simulation as well as experiment. Figure 3.16 shows the response of the plant during simulation. The response has a settling time of 610 seconds.

The control input of the plant during simulation is shown in Figure 3.17 and the estimated delay values using Error-Comparison Method based approach is shown in Figure 3.18. The response has an initial undershoot due to larger initial delay. Moreover, to

prevent any damage the limit of control input for the temperature control plant is kept between ±1V.

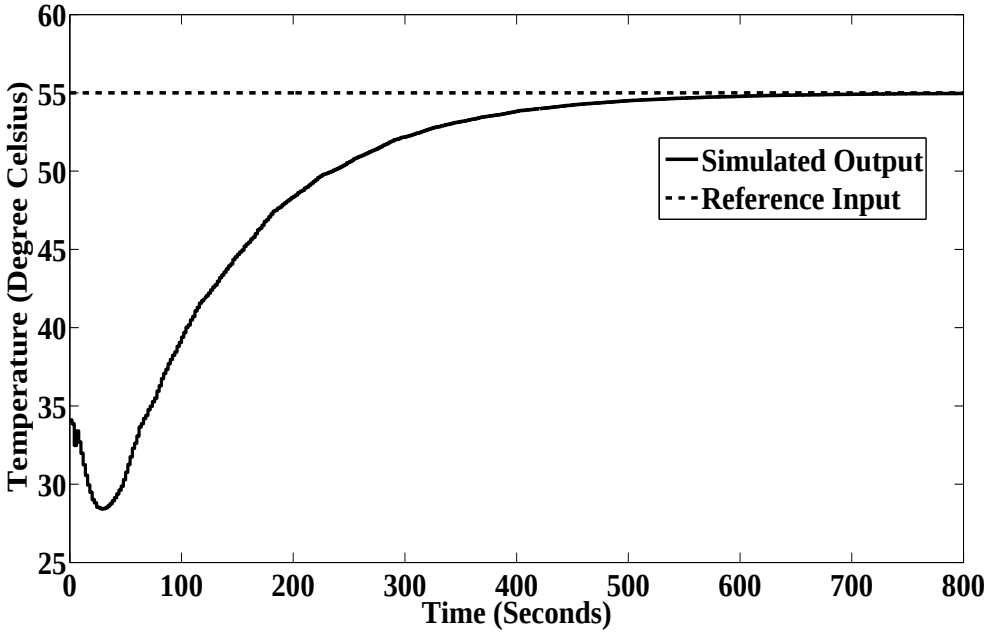

Figure 3.16: Simulation response of the closed loop system

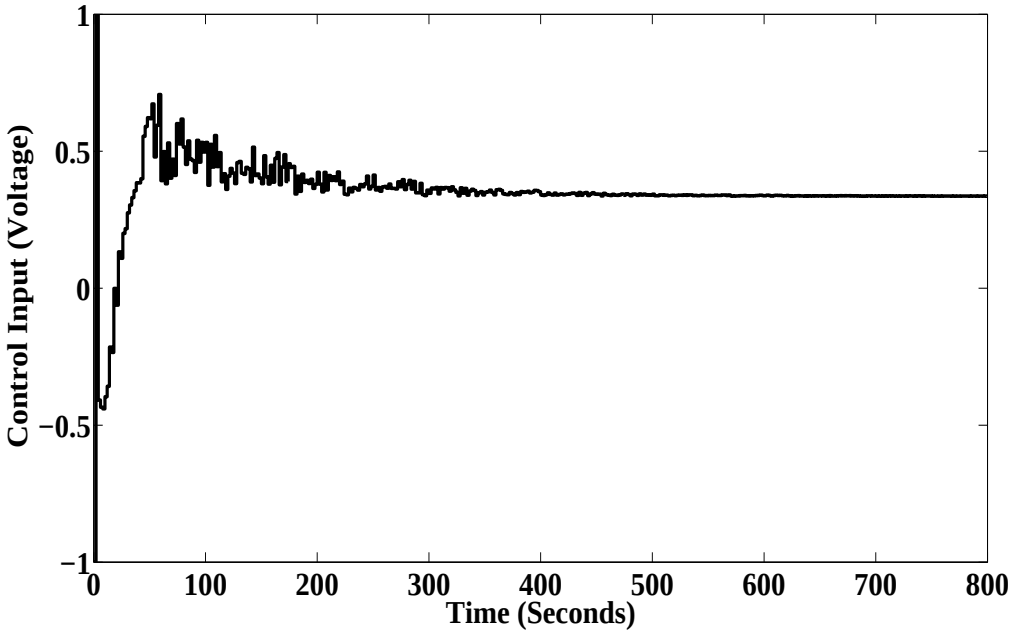

Figure 3.17: Control input for the system during simulation

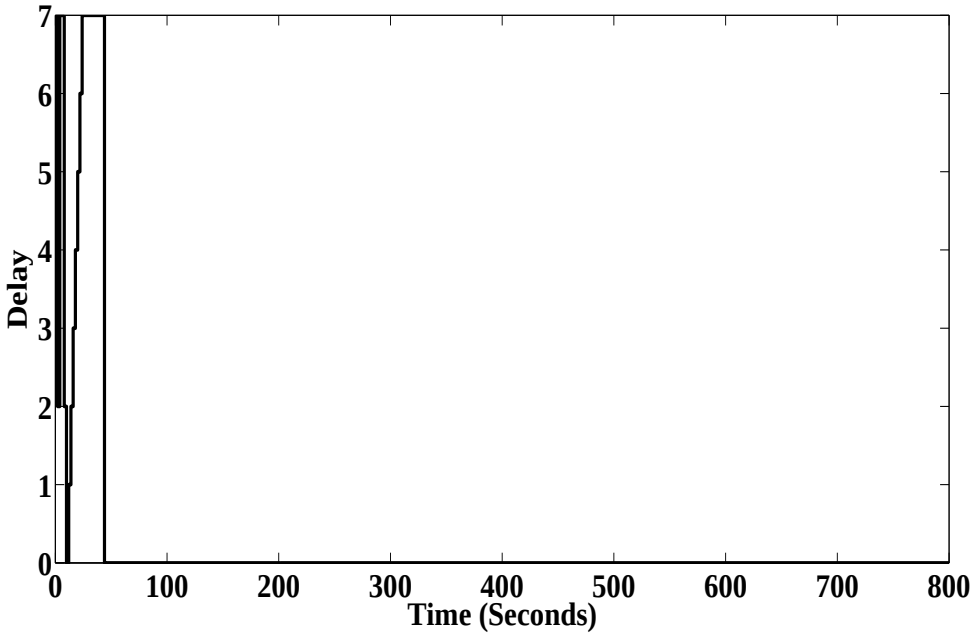

Figure 3.18: Delay estimated by the estimator during simulation

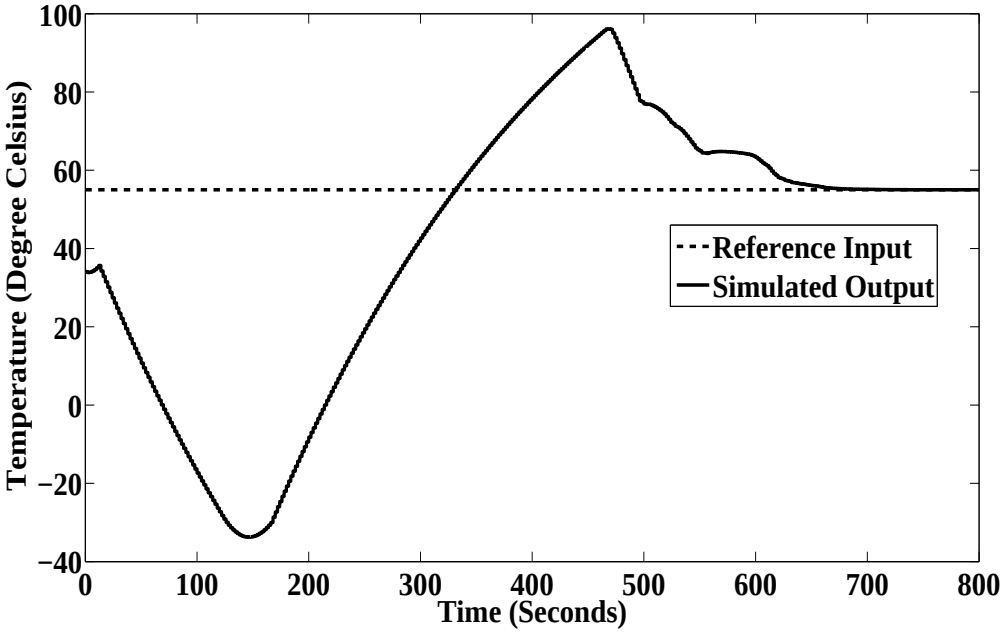

Figure 3.19: Simulation response of system for $\eta = -2$, $\mu = -10$

When the gains corresponding to second set of data values i.e. $\eta = -2$, $\mu = -10$, $\gamma = 1e6$ and sampling time=2 seconds are taken into account the output response is as shown in Figure 3.19. The response settles around 696 seconds, which is a larger selling

time as compared to settling time of above response for $\eta = -4$, $\mu = -1$. Also it has a peak overshoot of 41.1 degrees. Hence, for further analysis the gains corresponding to $\eta = -4$, $\mu = -1$ are considered as using them gives a response that settles fast and has no overshoot.

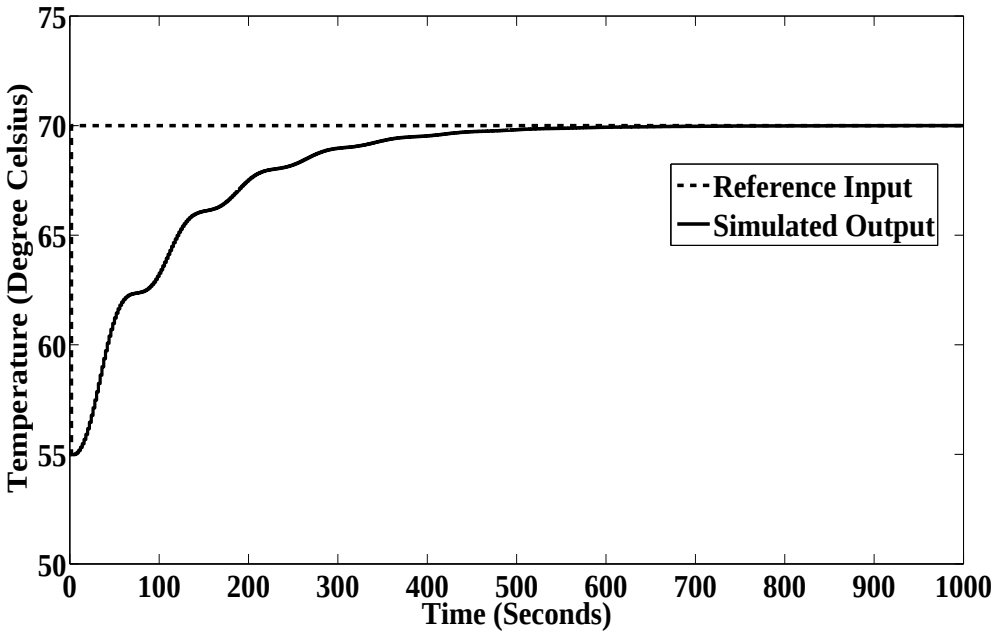

Figure 3.20: Simulation response of the closed loop system

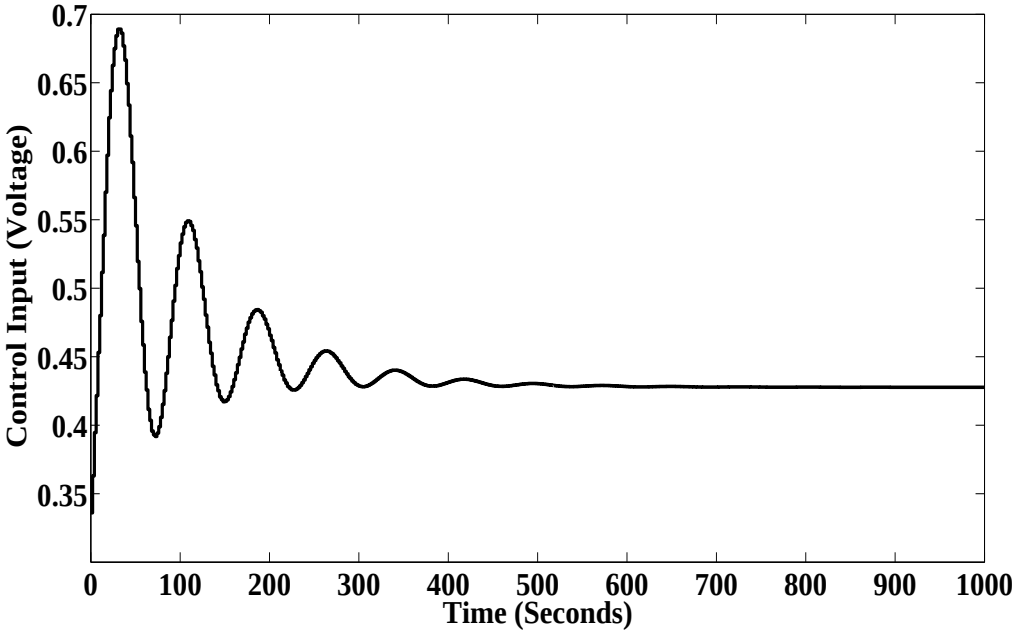

Figure 3.21: Control input for the system during simulation

Performance of Gradient descent method based delay estimator: The control gain values for sampling time of 2 seconds are used to study the performance of the plant as well as estimator during simulation as well as experiment. Figure 3.20 shows the response of the plant during simulation. The response has a settling time of 535 seconds. The control input of the plant during simulation is shown in Figure 3.21 and the estimated delay values using Gradient Descent Method based approach is shown in Figure 3.22. The maximum delay estimated in this case is of 1 second. Also, to prevent any damage to temperature control plant, control input is kept within the range of ±1V.

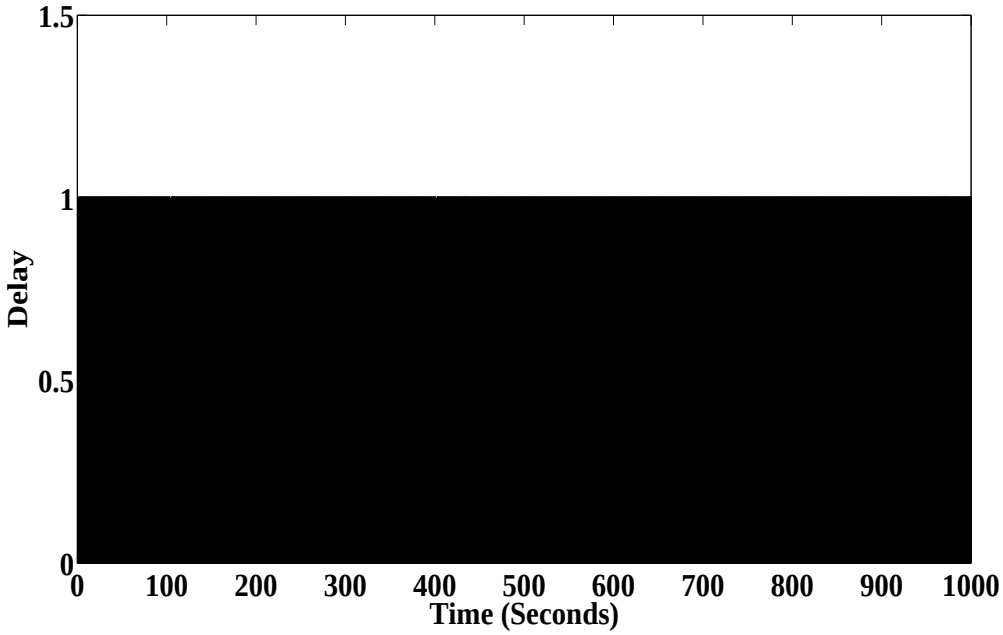

Figure 3.22: Delay estimated by the estimator during simulation

Experimental result

Performance of Error-comparison method based delay estimator: The response of the plant during experiment with 2 seconds sampling time, has a settling time of 488 seconds which is shown in Figure 3.23. Figure 3.24 shows the corresponding control input and Figure 3.25 shows the estimated delay during experiment. the simulated and experimental response closely match each other. The effect of delay can be seen on the initial response as it rises after few seconds.

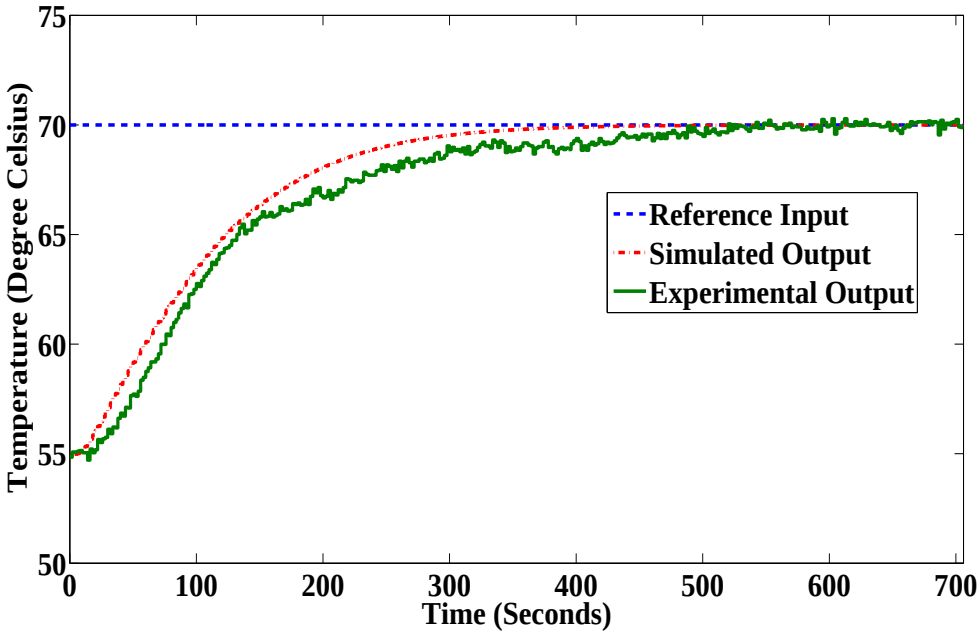

Figure 3.23: Experimental response of the closed loop system

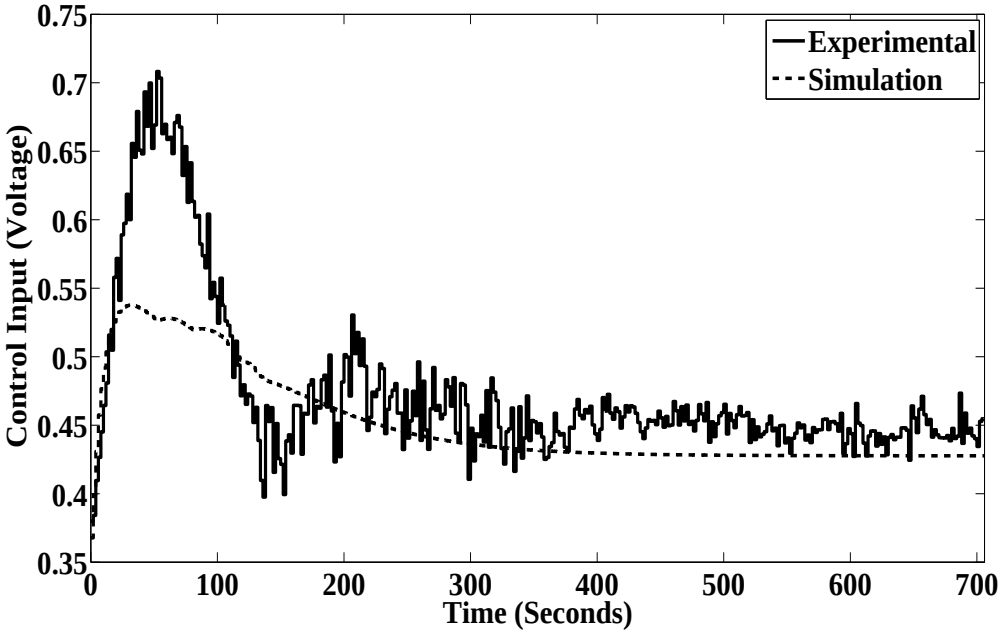

Figure 3.24: Control input of the plant during experiment

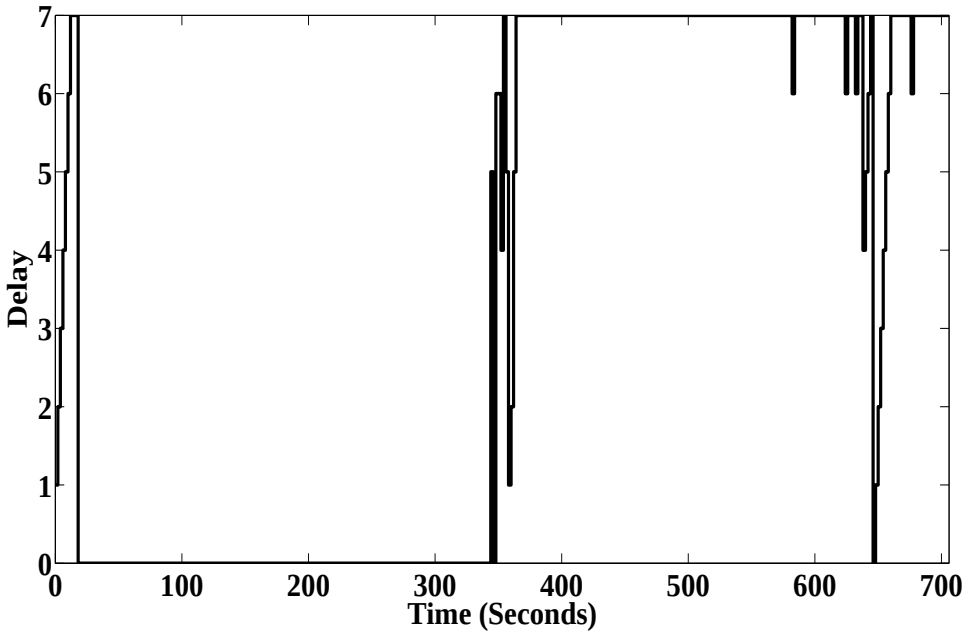

Figure 3.25: Delay estimated by the estimator during experiment

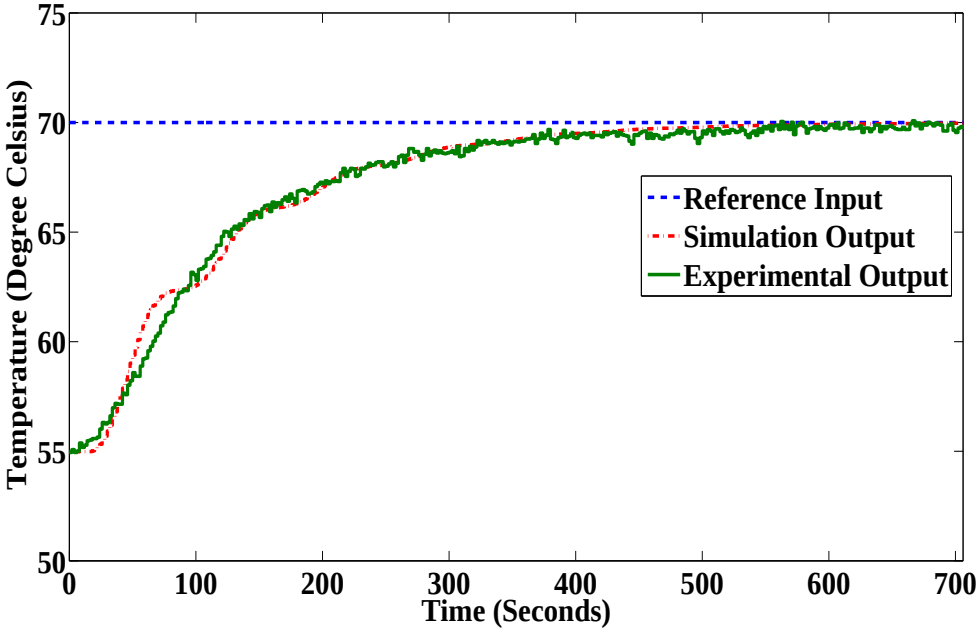

Figure 3.26: Experimental response of the closed loop system

Performance of Gradient descent method based delay estimator: The response of the plant during experiment with 2 seconds sampling time, $\lambda = 0.05$ and using gradient descent method based estimator, has a settling time of 558 seconds which is shown in Figure 3.26.

The response during simulation and experiment match each other closely. Here also, the effect of delay can be seen on the initial response. Figure 3.27 shows the corresponding control input and Figure 3.28 shows the estimated delay during experiment. For experimental results also, the delay values are estimated only during the transient response.

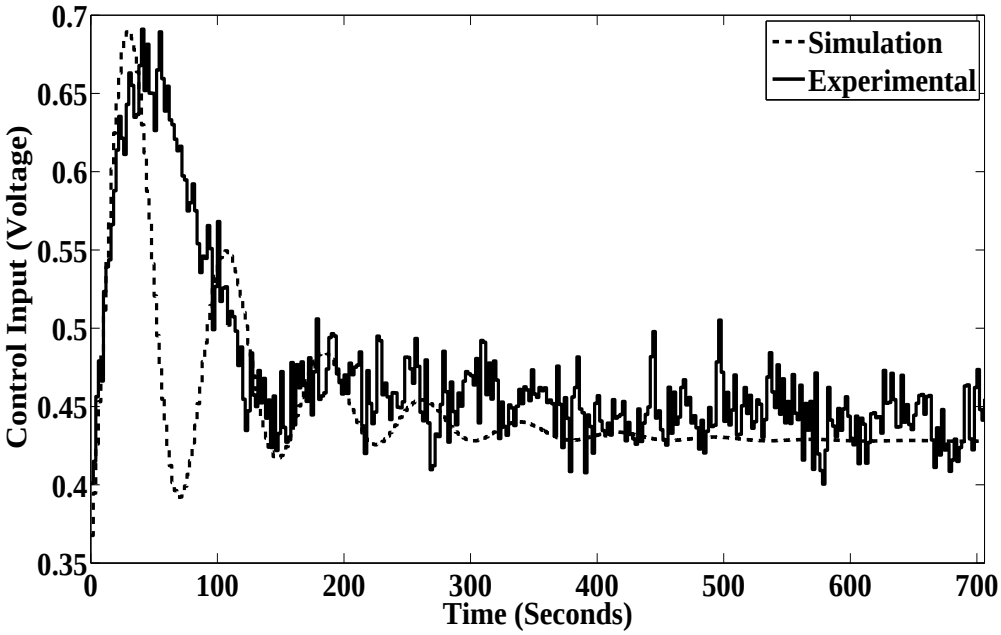

Figure 3.27: Control input of the plant during experiment

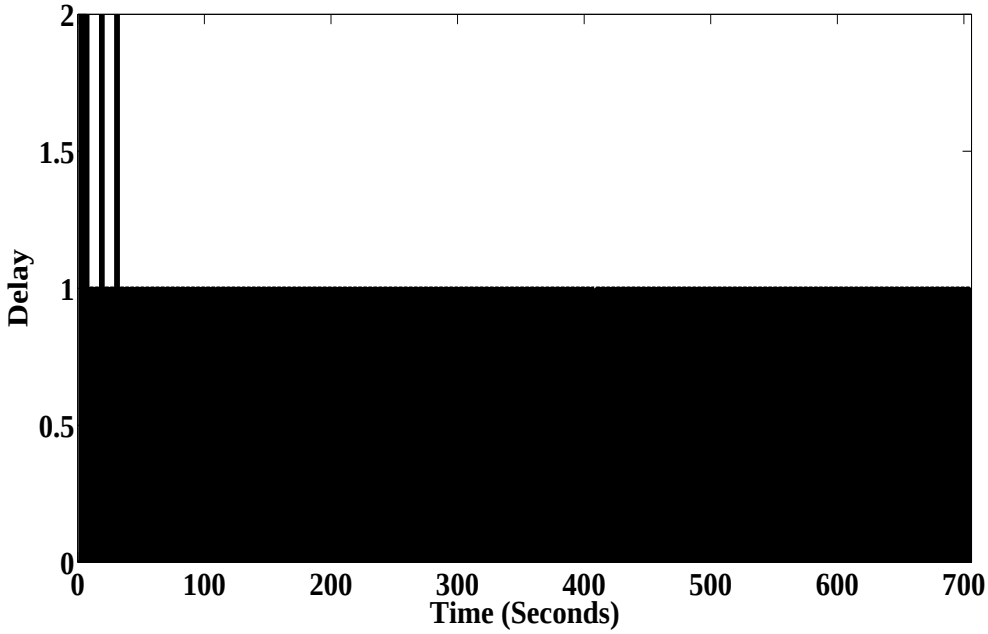

Figure 3.28: Delay estimated by the estimator during experiment

3.4.3 Comparison between the proposed estimators

The plant output response taking into account 1 second sampling time and the gradient descent method based estimator settles around 300 seconds whereas that of error-comparison method based estimator settles around 220 seconds. For a sampling time of 2 seconds the settling time is 488 seconds and 558 seconds respectively. This difference may be attributed to the different sampling-time for both the cases. With smaller sampling time the response improves, as the control input gets updated more frequently. Also from the estimated delay values it is evident that the gradient descent method based estimator though guarantees the non-divergence of delays, estimates delay only for the transient period. Since, during steady state the error between the actual and estimated output reduces to zero. But the error-comparison method based estimator estimates delay for both transient and steady-state though its complexity increases with increasing delay values.

3.5 Chapter Summary

A detailed description of output feedback closed loop controller design is presented. For implementing the controller, delay information is required. Hence, an error-comparison and gradient descent method based delay estimators are designed. Simulation and experimental studies are carried out to demonstrate the validity of the designed estimator. From the simulation and experimental results, it is evident that the error-comparison estimator estimates delay values for both transient and steady-state response. Since, during steady state the error between the plant and the estimated output goes to zero, the gradient descent estimator though guarantees the non-divergence, estimates delay values only for transient response. The maximum tolerable delay or the jitter margin is of 25 seconds. The response of the output feedback controller in terms of settling time though large, is improved as the sampling time is reduced because the controller gets updated more often.

Chapter 4

Observer Based Output-Feedback Controller with Delay Estimator

4.1 Introduction

Designing of a closed loop control for the plant (2.11), may require different feedback control like direct output-feedback, observer based output-feedback, state-feedback etc.. As per the available literature, [45] has used a state feedback control approach to deal with long delays which are basically stochastic delay being transformed into deterministic delay by using proper quantities of buffer. In [46], the stabilization problem of NCS has been investigated using the same state feedback approach. Authors of [47] and [48] used the same approach with an observer to deal with bounded delays but the former extended it for packet losses also. In [49], an observer based H_∞ controller has been designed to deal with network induced uncertain time-delays and packet losses. In all these works, the stability of the systems is discussed. Similar to the above works, design of a closed-loop control for the plant (2.11) using observer based output-feedback approach is discussed in this chapter. The controller is modified to be a predictive controller. Moreover, while dealing with time-varying delays of the network, fixed as well as an adaptive gain strategy is employed. In case of adaptive gain, the gain varies in accordance with the delay occurring at that very instant. To obtain these delay values both error-comparison [28] and gradient descent method [29] based estimators are used. Also observer based output-feedback controller with estimators is employed to evaluate performance of the plant.

The chapter deals with designing of a fixed as well as variable gain observer based output-feedback controller for dealing with uncertain delays introduced by the network. Also performance of error-comparison and gradient descent method based estimator with

observer based output-feedback controller is evaluated. The simulations are done using MATLAB/SIMULINK and the real time experimentation results are obtained using LabVIEW.

4.2 Observer based Output-Feedback Controller Design

4.2.1 Problem definition

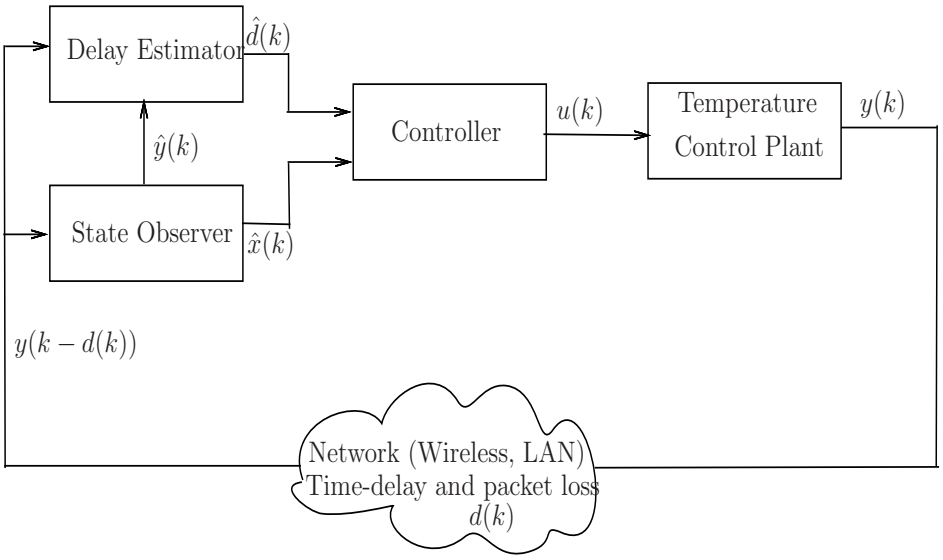

Figure 4.1: Schematic diagram of NCS for observer based output feedback control

The NCS with the controller configuration is considered in Figure 4.1. In this figure the delayed output of the plant due to network is used by the delay estimator to estimate the delay values. The same output is used by the observer to estimate the states of the plant. The delay value and the state information is used by the controller to calculate the control input. Time-driven control is used for the analysis. A discrete-time plant for this NCS configuration is considered as:

$$x(k+1) = Ax(k) + Bu(k), \qquad y(k) = Cx(k), \tag{4.1}$$

where $x(k) \in R^n$ is the state vector; $u(k) \in R^m$ is the control input to the plant; $y(k) \in R^p$ is the plant output; A, B and C are constant matrices of suitable dimensions. $d(k)$, $0 \leq d(k) \leq N$ is the random time-delays induced by the network in the feedback channel, which possibly includes the packet losses. For NCS configuration as shown in Figure 4.1, predictive control is used to predict the states of the plant for the current instant using the delayed output. A predictive controller for an NCS configuration has been considered in

[14] for network in feedback channel, whereas the same but for network in both feedback and forward channel in [15] and [19]. In [16], the technique is used to deal with time-delays and packet losses simultaneously. In such schemes, an observer is used to estimate the states from the delayed plant output, having its configuration as:

$$\hat{x}(k+1) = A\hat{x}(k) + Bu(k) + L(y(k-d(k)) - C\hat{x}(k)),$$
$$\hat{y}(k) = C\hat{x}(k), d(k) = 0, 1, ..., N, \quad (4.2)$$

where $\hat{x}(k) \in R^n$ is the model state vector; $u(k) \in R^m$ is the control input; and L be the observer gain.

In a variable gain observer based output-feedback controller, the gain varies in accordance with the time-delays. Thus, such a controller is found to be more effective as compared to its fixed gain counterpart. Further, variable gain can be chosen using the information on $d(k)$. Hence, the controller is considered:

$$u(k) = K_{d(k)}\hat{x}(k), \quad (4.3)$$

where, $K_{d(k)} \in R^{m\times n}$ is the controller gain which varies according to delay values $d(k)$. The fixed gain observer based output-feedback controller is a special case of (4.3), i.e.,

$$u(k) = K\hat{x}(k), \quad (4.4)$$

Therefore, the observer (4.2) and the plant dynamics (4.1) can be written as:

$$\hat{x}(k+1) = (A + BK_{d(k)} - LC)\hat{x}(k) + LCx(k-d(k)), \quad (4.5)$$

$$x(k+1) = Ax(k) + BK_{d(k)}\hat{x}(k), \quad (4.6)$$

respectively. The overall system can be written using (4.5) and (4.6) as:

$$\bar{x}(k+1) = \Lambda_{d(k)}\bar{x}(k), \qquad d(k) = 0, 1, ..., N, \quad (4.7)$$

where

$$\bar{x}(k) = [x(k)^T, x(k-1)^T \quad \dots \quad x(k-d(k))^T$$
$$x(k-d(k)-1)^T \quad \dots \quad x(k-N)^T \quad \hat{x}(k)^T]^T$$

and

$$\Lambda_{d(k)} = \tilde{A} + B_1K_{d(k)}\tilde{I} - \tilde{I}'LC\tilde{I} + \tilde{I}'LCI_{d(k)}$$

where, $\tilde{A} = \begin{bmatrix} A & 0_{n\times(N+1)n} \\ I_{Nn} & 0_{Nn\times 2n} \\ 0_{n\times(N+1)n} & A \end{bmatrix}$; $B_1 = \begin{bmatrix} B \\ 0_{Nn\times m} \\ B \end{bmatrix}$;

$\tilde{I} = \begin{bmatrix} 0_{n\times(N+1)n} & I_n \end{bmatrix}$

$I_{d(k)} = \begin{bmatrix} 0_{n\times(d(k))n} & I_n & 0_{n\times(N+1-d(k))n} \end{bmatrix}$. Here, the matrix $I_{d(k)}$ depends on the delay in the network. Let $\hat{d}(k)$ be the estimated delay at an instant. In the NCS configuration shown in Figure 4.1, a delay estimator is used to estimate $\hat{d}(k)$. And this information on $\hat{d}(k)$ is used to choose the gain of the controller. Accordingly, the control signal (4.4) can be modified as:

$$u(k) = K_{\hat{d}(k)}\hat{x}(k). \tag{4.8}$$

The system description (4.5) and (4.6) can be modified accordingly.

The objective is to design the controller gain $K_{d(k)}$ using an observer based output feedback approach. This gain value is chosen in accordance with the delay values $d(k)$, which is estimated using the proposed estimator.

4.2.2 Controller design

The result below may be used for obtaining $K_{d(k)}$ that satisfies guaranteed cost performance of the NCS as in [19].

Lemma 1. [19] *For system* (4.7)*, if there exist an appropriate dimension matrix* P *satisfying*

$$\Lambda_{d(k)}^T P \Lambda_{d(k)} - P + \bar{Q} + \bar{R} < 0 \tag{4.9}$$

then the performance index

$$J_c = \sum_{k=0}^{+\infty} (x(k)^T Q x(k) + u(k)^T R u(k)) \tag{4.10}$$

satisfies

$$J_c < \bar{x}(0)^T P \bar{x}(0), \tag{4.11}$$

where, Q *and* R *are chosen positive definite weighted matrices and* $\bar{Q} = \begin{bmatrix} Q & 0_{n\times(N+1)n} \\ 0_{n\times(N+2)n} & \end{bmatrix}$.

Proof. To guarantee the cost of the plant, we define a Lyapunov function as:

$$V(k) = \bar{x}(k)^T P \bar{x}(k), \tag{4.12}$$

where P is a positive definite symmetric matrix. Hence, the energy change of the system using (4.12) is:

$$\Delta V = \bar{x}(k)^T (\Lambda_{d(k)}^T P \Lambda_{d(k)} - P + \bar{Q} + \bar{R}) \bar{x}(k) - \bar{x}(k)^T (\bar{Q} + \bar{R}) \bar{x}(k) \tag{4.13}$$

Satisfying (4.9), from (4.13) one obtains:

$$\Delta V < -\bar{x}(k)^T(\bar{Q} + \bar{R})\bar{x}(k) \tag{4.14}$$

Moreover, from (4.14),

$$V(\infty) - V(0) < -J_c$$

As $V(\infty) \to 0$:

$$J_c < \bar{x}(0)^T P \bar{x}(0)$$

□

One may now solve (4.9) for obtaining the controller gain(s) for different delay values. In this regard, note that, (4.9) is not an LMI since multiplication of P and controller gains $K_{d(k)}$ are involved in it. We follow the iterative algorithm of [19] for solving (4.9) as described next. By choosing $\bar{R} = \tilde{I}^T K_{d(k)}^T R K_{d(k)} \tilde{I}$, the inequalities in (4.9) are converted into matrix inequalities which can be written as:

$$\begin{bmatrix} -P + \bar{Q} & \Lambda_{d(k)}^T & \tilde{I}^T {K_{d(k)}}^T \\ * & -P^{-1} & 0 \\ * & * & -R^{-1} \end{bmatrix} < 0 \tag{4.15}$$

Putting the value of $\Lambda_{d(k)}$, (4.15) becomes:

$$\begin{bmatrix} -P + \bar{Q} & (\tilde{A} + B_1 K_{d(k)} \tilde{I} - \tilde{I}' L C \tilde{I} + \tilde{I}' L C I_{d(k)})^T & \tilde{I}^T {K_{d(k)}}^T \\ * & -P^{-1} & 0 \\ * & * & -R^{-1} \end{bmatrix} < 0 \tag{4.16}$$

Due the presence of P^{-1}, (4.16) is a non-linear problem. Substituting P^{-1} by W, (4.16) can be written in the form of a Linear Matrix Inequality (LMI):

$$\begin{bmatrix} -P + \bar{Q} & (\tilde{A} + B_1 K_{d(k)} \tilde{I} - \tilde{I}' L C \tilde{I} + \tilde{I}' L C I_{d(k)})^T & \tilde{I}^T {K_{d(k)}}^T \\ * & -W & 0 \\ * & * & -R^{-1} \end{bmatrix} < 0 \tag{4.17}$$

The cone complementary linearization algorithm [50] is used to convert the non-convex optimization problem to LMI based minimization problem. The obtained trace minimization subjected to (4.18), will drive the inequality to its boundary condition i.e. $P = W^{-1}$. The algorithm for solving the values of $K_{d(k)}$, L and P for a particular value of γ is presented as follows:

Algorithm 1 Controller Design Algorithm

$$\text{minimize trace}(PW);$$
$$\text{subject to satisfying (4.17)},$$

$$\begin{bmatrix} P & I \\ I & W \end{bmatrix} \geq 0, \tag{4.18}$$

$$\begin{bmatrix} -\gamma & \bar{x}(0)^T \\ \bar{x}(0) & -W \end{bmatrix} < 0 \tag{4.19}$$

The optimal values of $K_{d(k)}$ and L can be obtained by iteratively reducing the value of γ using the following steps:

Algorithm 2 Optimal Controller Design Algorithm

Step-1 Large initial value of γ is taken and for that value a feasible solution for the (1) is obtained.

Step-2 If feasible solution occurs, for $l = 0$, the following LMI problem is solved:

minimize

$$trace(P_l W + P W_l) \tag{4.20}$$

subject to (4.17)-(4.19) LMIs, for a defined number of iterations. The above trace minimization including previous and present values of P and W, will drive the inequality (4.18) to the boundary condition $P = W^{-1}$.

Step-3 If (4.16) is satisfied, after decreasing γ goto Step-2. If LMI conditions (4.17)-(4.19) are not fulfilled then exit, else put $l = l + 1$, $P_{l+1} = P$, $W_{l+1} = W$ and again solve the LMI problem (4.20).

The values of gain $K_{d(k)}$ is chosen based on the value of estimated delay $\hat{d}(k)$. For estimating these delay values, the proposed delay estimators in chapter 3 are used.

4.3 Results and Discussion

In this section, the performance of the plant as well as of the proposed estimators is evaluated by simulation as well as experimental results taking into account the observer based output-feedback controller for the temperature control plant described in Chapter 2. To achieve guaranteed cost control, the value of weight matrices of cost function is chosen as $Q = 0.1I$, $R = 0.1I$.

4.3.1 For sampling time of 1 second

Plant model

The discrete-time model used in this case (2.9) for both experimental and simulation studies is as described:

$$x(k+1) = Ax(k) + Bu(k), \qquad y(k) = Cx(k), \tag{4.21}$$

where $A = \begin{bmatrix} 0 & 0 & 0 \\ 1 & 0 & 0 \\ 0 & 1 & 0.9965 \end{bmatrix}$, $B = \begin{bmatrix} 0.5739 \\ 0 \\ 0 \end{bmatrix}$, $C = \begin{bmatrix} 0 & 0 & 1 \end{bmatrix}$.

Control gains

The variable gains values for N=7 and sampling time of 1 second, are
$K_i = \begin{bmatrix} -0.2096 & -0.1528 & -0.1271 \end{bmatrix}, \begin{bmatrix} -0.2114 & -0.1533 & -0.1255 \end{bmatrix},$
$\begin{bmatrix} -0.2085 & -0.1521 & -0.1232 \end{bmatrix}, \begin{bmatrix} -0.2051 & -0.1493 & -0.1205 \end{bmatrix},$
$\begin{bmatrix} -0.2010 & -0.1451 & -0.1173 \end{bmatrix}, \begin{bmatrix} -0.1963 & -0.1392 & -0.1134 \end{bmatrix},$
$\begin{bmatrix} -0.1933 & -0.1346 & -0.1095 \end{bmatrix}, \begin{bmatrix} -0.1938 & -0.1369 & -0.1067 \end{bmatrix}$ for $i = 0, \ldots, 7$ respectively and the observer gain is obtained as: $L = \begin{bmatrix} -0.0157 & -0.0430 & 0.4678 \end{bmatrix}^T$.
By choosing a constant gain K in (4.4) instead of the variable $K_{d(k)}$, in the Control Design Algorithm in Section IV, the value of fixed gain is obtained as: $K = \begin{bmatrix} -0.2229 & -0.1551 & -0.1098 \end{bmatrix}$ and the corresponding observer gain is $L_s = \begin{bmatrix} -0.0101 & -0.03405 & 0.4057 \end{bmatrix}^T$. Next, the above gain values are used to study performance of the plant by simulation. We use random function in MATLAB to generate random delay situation.

Simulation results

Performance of Error-comparison method based delay estimator: The simulated response of the plant for fixed and variable gain settles around 88 and 58 seconds respectively as shown in Figure 4.2. The actual and estimated delay values are shown in Figure 4.3.

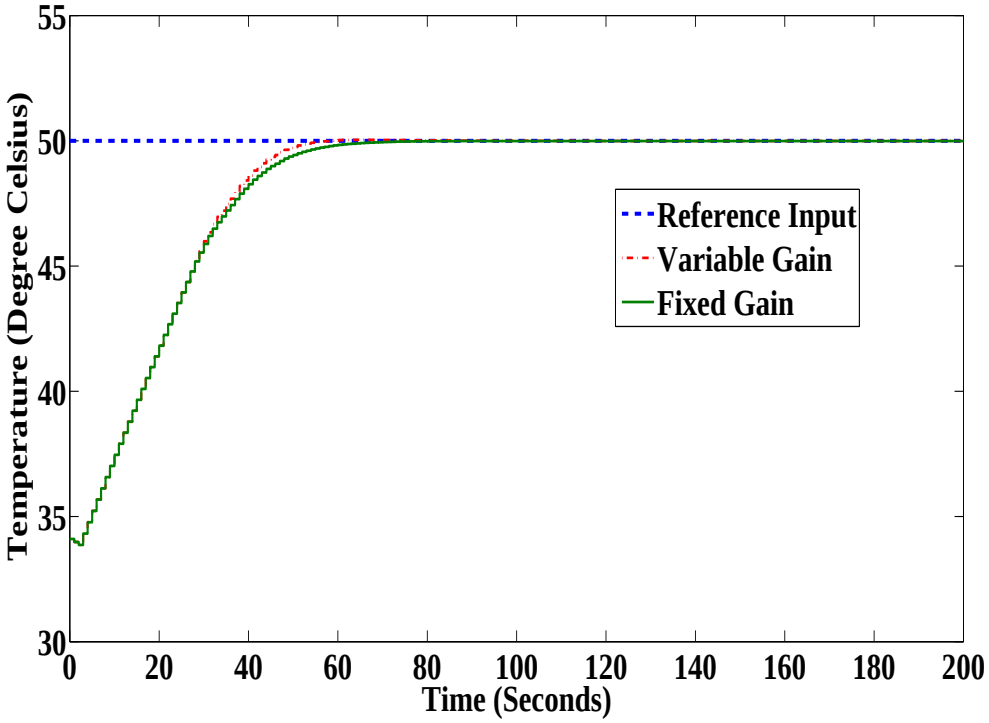

Figure 4.2: Simulation response of temperature control plant

The response with variable gain controller settles faster because the gains adapt according to the delay values.

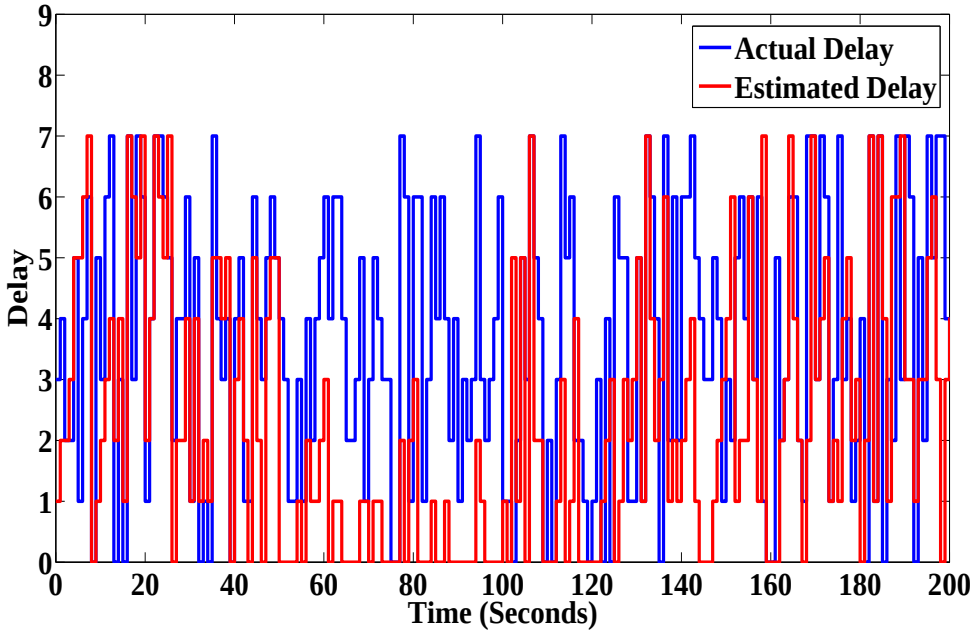

Figure 4.3: Actual and estimated delay values

Performance of gradient descent method based delay estimator: When using gradient descent method for delay estimation, the plant response for fixed and variable gain settles around 95 and 85 seconds respectively as shown in Figure 4.4.

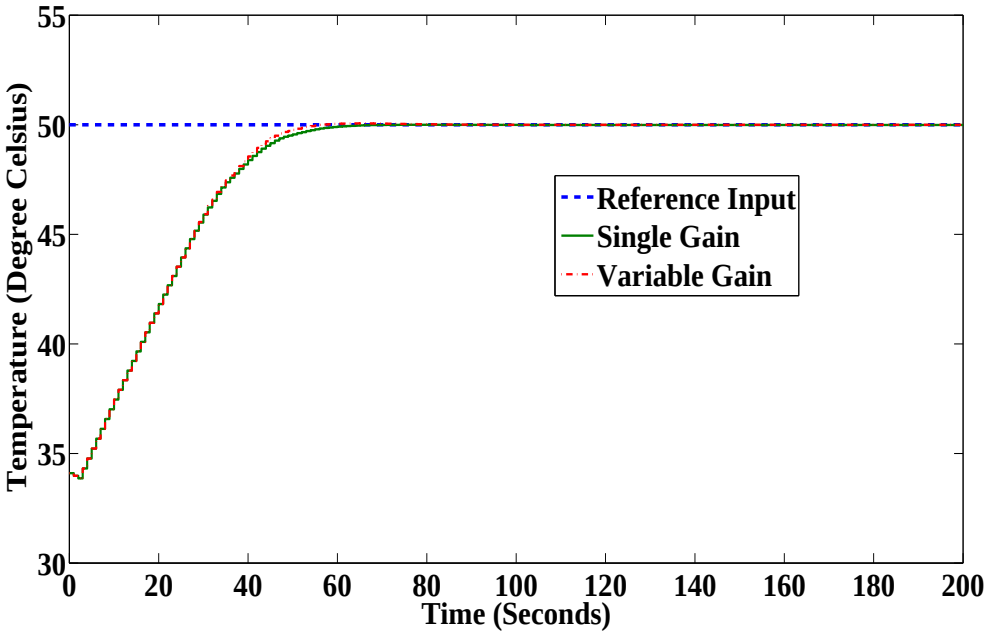

Figure 4.4: Simulation response of the closed loop system

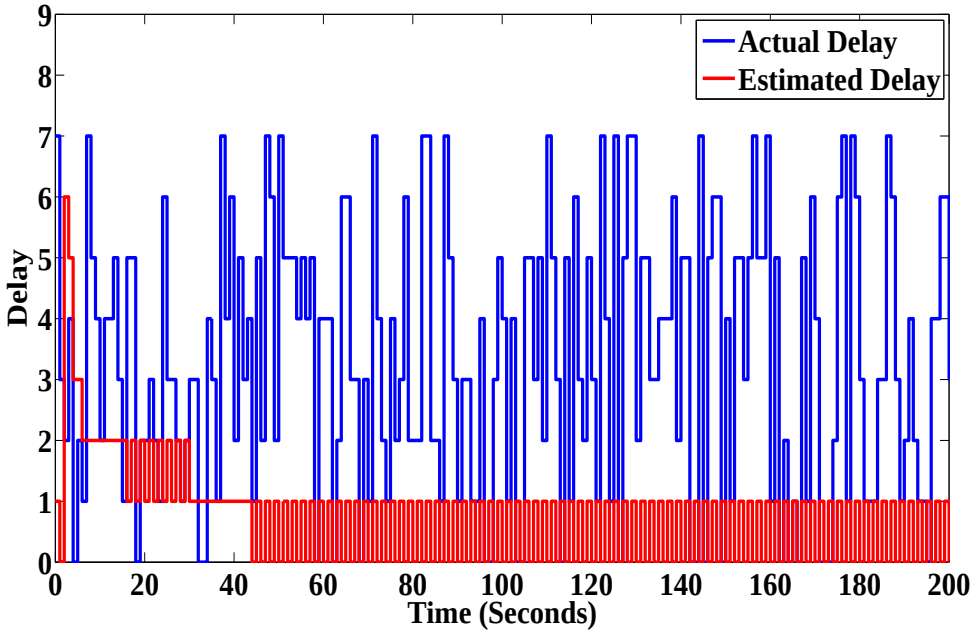

Figure 4.5: Actual and estimated delay values for simulation case

The actual and estimated delay values are shown in Figure 4.5. The response for variable gain controller here also settles faster due to the change in gains in accordance with the delay values.

Experimental results

Performance of Error-comparison method based delay estimator: The temperature control plant is designed for heating of the oven. For 1 second sampling time, the response of plant using corresponding fixed gain has a settling time of 132 seconds and peak overshoot of 0.6 degrees as shown in Figure 4.6.

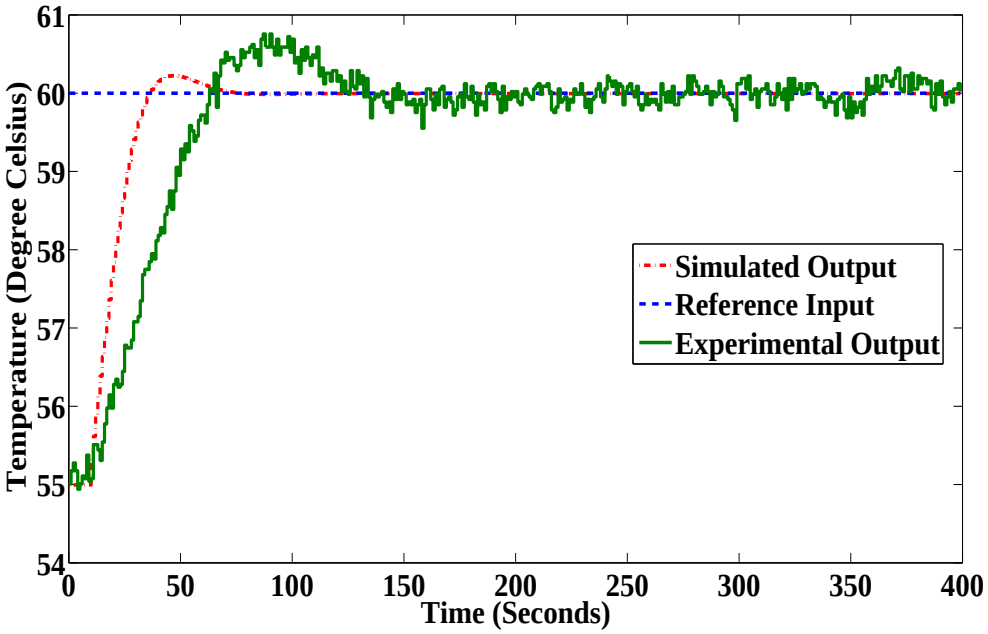

Figure 4.6: Experimental and simulation response for fixed gain

The response of the plant for variable gain, has a settling time of 114 seconds and peak overshoot of 0.6 degrees as shown in Figure 4.7. The corresponding control input is shown in Figure 4.8 and Figure 4.9 shows the estimated delay values.

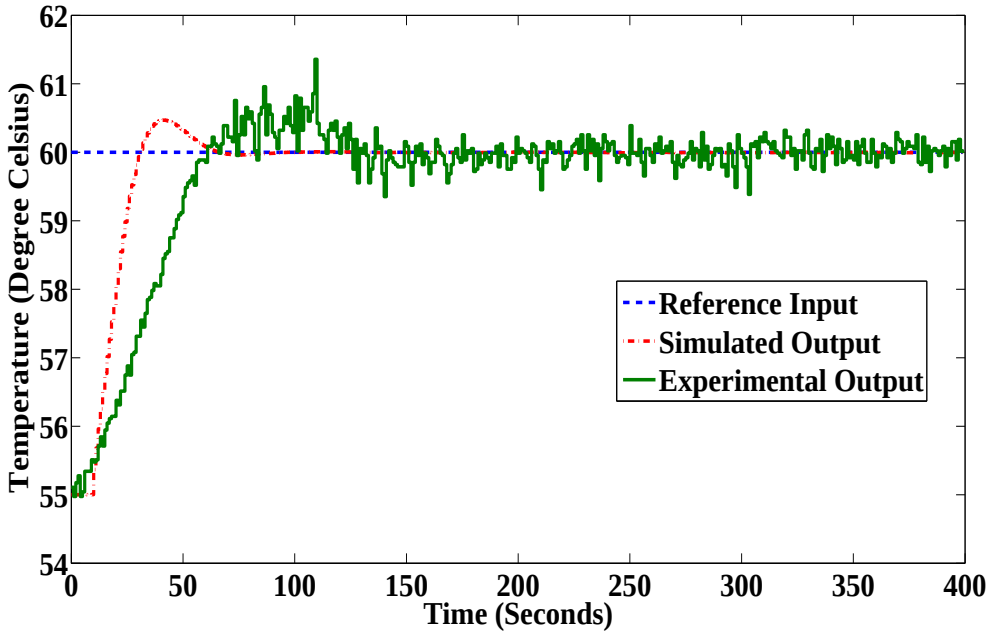

Figure 4.7: Experimental and simulation response for variable gain

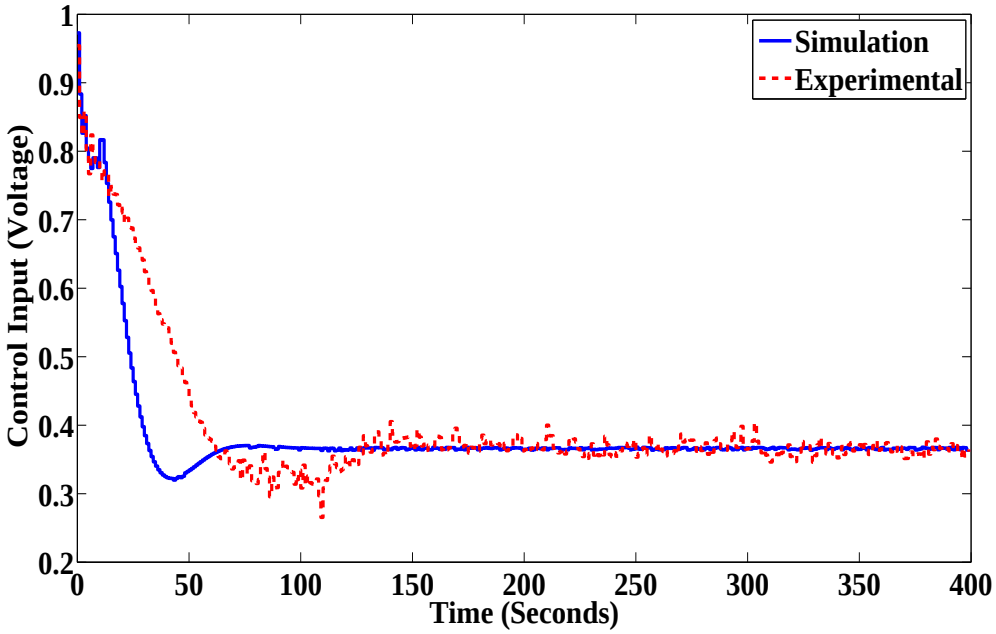

Figure 4.8: Experimental control input for fixed and variable gain

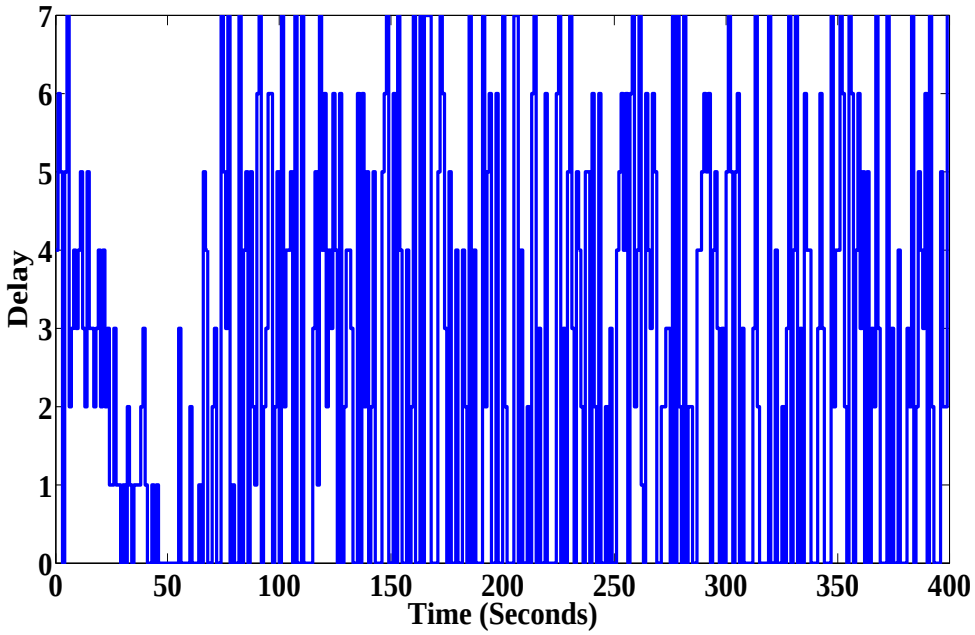

Figure 4.9: Delay estimated by the estimator during experiment

Performance of gradient descent method based delay estimator: The response of the plant for variable gain with $\lambda = 0.9$, using gradient descent method based estimator, has a settling time of 120 seconds and peak overshoot of 1 degree as shown in Figure 4.10.

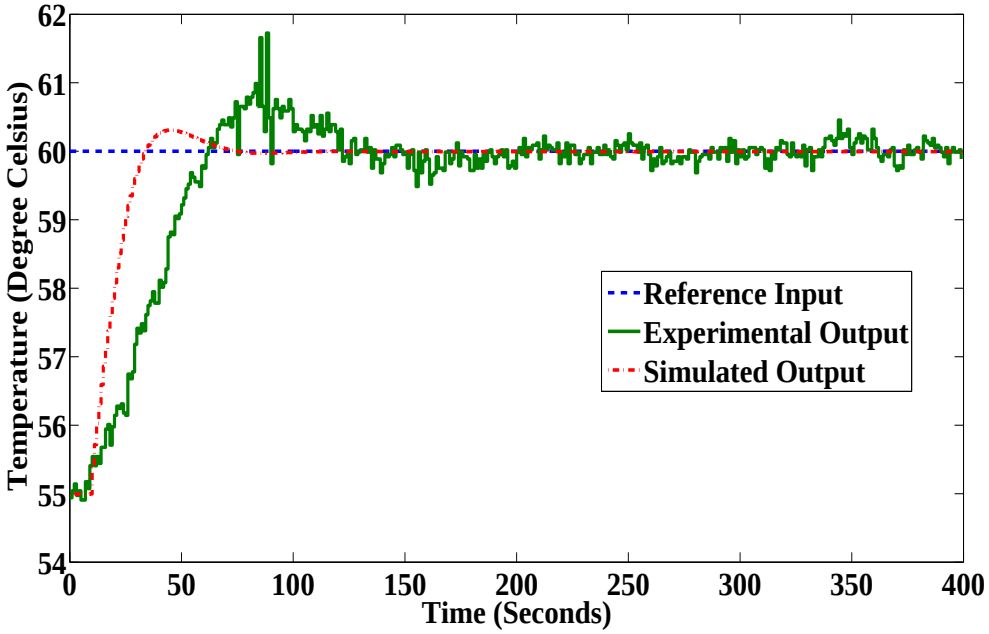

Figure 4.10: Experimental and simulation response for variable gain

The corresponding control input is shown in Figure 4.11 and Figure 4.12 shows the estimated delay values.

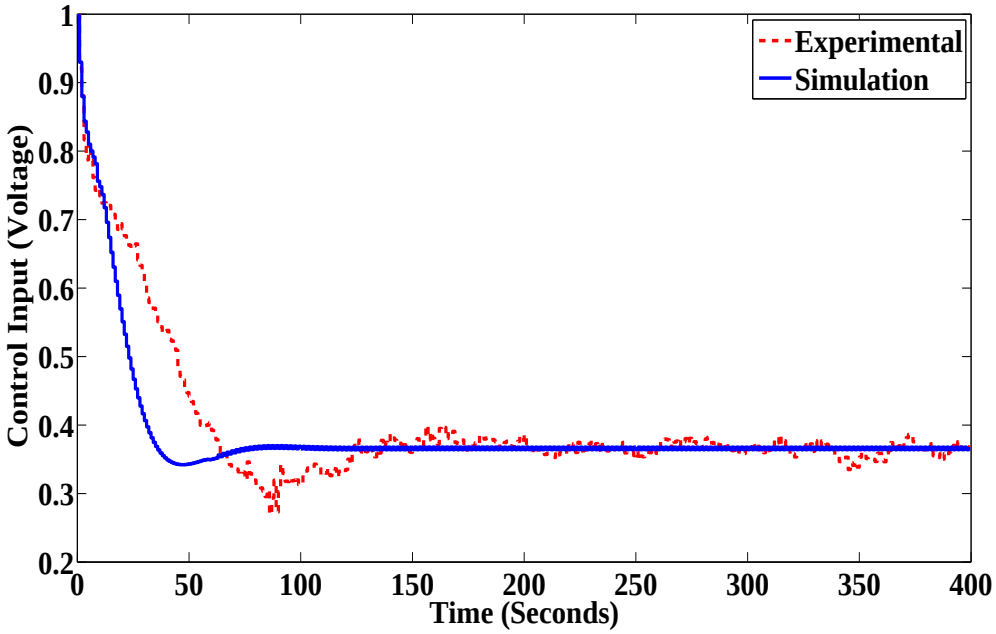

Figure 4.11: Experimental control input for fixed and variable gain

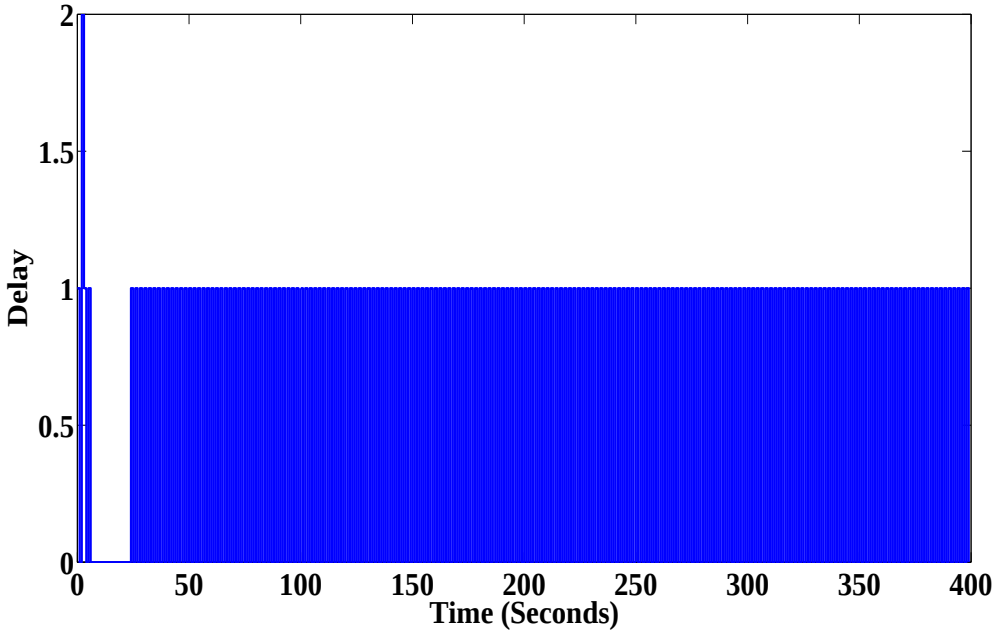

Figure 4.12: Delay estimated by the estimator during experiment

4.3.2 For sampling time of 2 seconds

Plant model

The discrete-time model in this case (2.11) is obtained as:

$$x(k+1) = Ax(k) + Bu(k), \qquad y(k) = Cx(k), \tag{4.22}$$

where $A = \begin{bmatrix} 0 & 0 \\ 1 & 0.9930 \end{bmatrix}$, $B = \begin{bmatrix} 1.1458 \\ 0 \end{bmatrix}$, $C = \begin{bmatrix} 0 & 1 \end{bmatrix}$.

Control gains

The variable gains corresponding to chosen Q, R, Sampling time=2seconds and for N=7 are obtained using the algorithm in section 3.2:
$K_i = \begin{bmatrix} -0.1105 & -0.0726 \end{bmatrix}, \begin{bmatrix} -0.1092 & -0.0714 \end{bmatrix},$
$\begin{bmatrix} -0.1066 & -0.0699 \end{bmatrix}, \begin{bmatrix} -0.1040 & -0.0680 \end{bmatrix},$
$\begin{bmatrix} -0.1010 & -0.0656 \end{bmatrix}, \begin{bmatrix} -0.0974 & -0.0623 \end{bmatrix},$
$\begin{bmatrix} -0.0937 & -0.0581 \end{bmatrix}, \begin{bmatrix} -0.0922 & -0.0549 \end{bmatrix}$ for $i = 0, \ldots, 7$ respectively and the observer gain is obtained as: $L = \begin{bmatrix} -0.0036 & 0.3332 \end{bmatrix}^T$.
The value of fixed gain using the same Q and R is obtained as: $K = \begin{bmatrix} -0.09434 & -0.0534 \end{bmatrix}$ and the corresponding observer gain is $L_s = \begin{bmatrix} 0.0011 & 0.3414 \end{bmatrix}^T$.

Simulation results

Performance of fixed and variable gain controller with known delay values: Figure 4.13 shows the simulation response of plant with 2 seconds sampling time, when variable gain controller chooses gain values according to the actual delay occurring in the network. This response settles at 92 and 144 seconds for variable and fixed gain respectively.

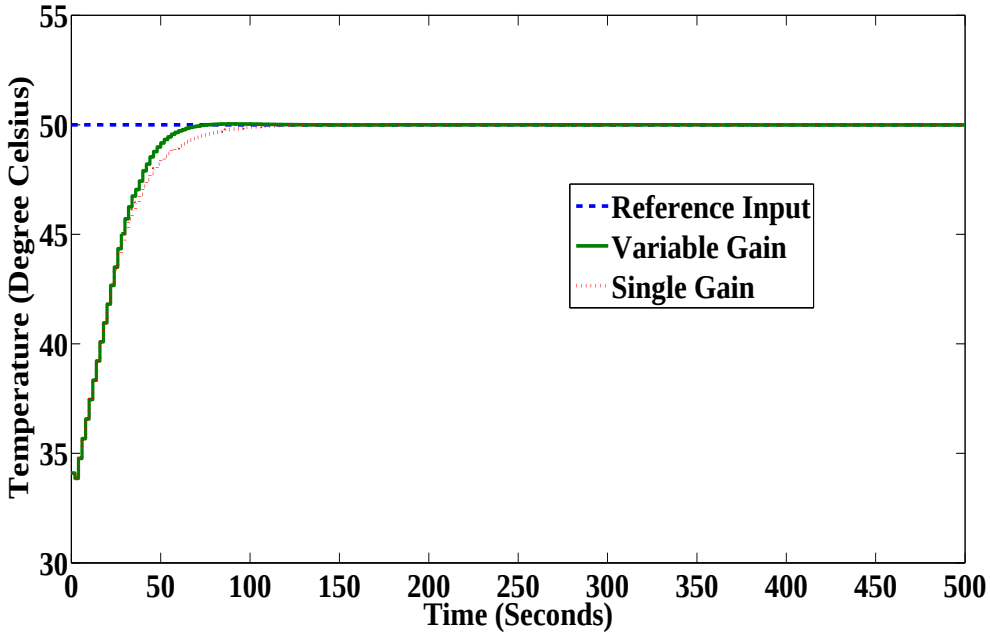

Figure 4.13: Simulation response with known delay values

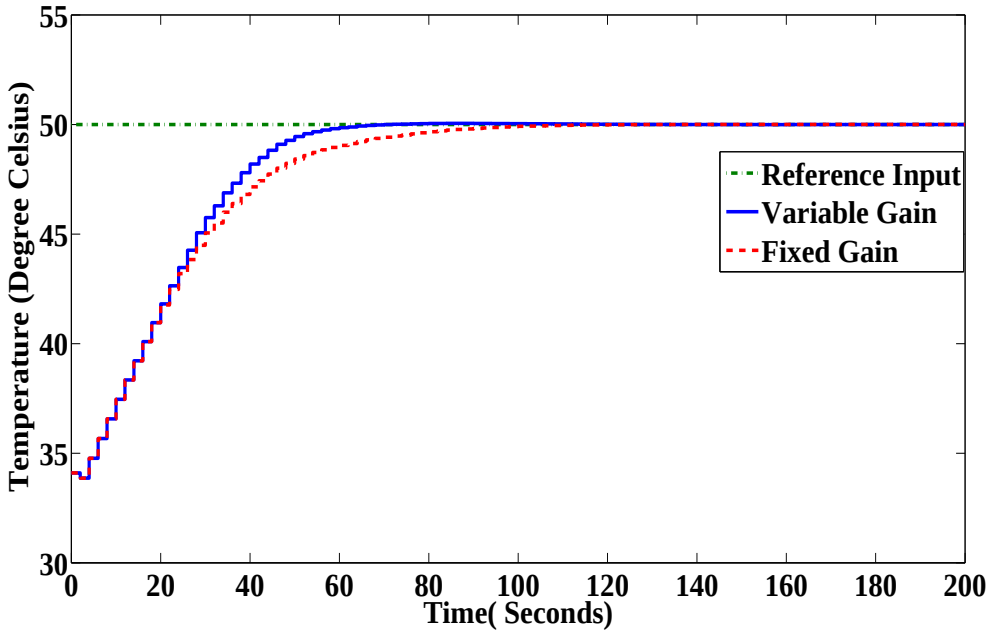

Figure 4.14: Simulation response of temperature control plant

Performance of error-comparison method based delay estimator: The simulation result for response of the plant for fixed gain and variable gain observer based output-feedback controller with the delay estimator is shown in Figure 4.14. The response of the plant

settles around 60 seconds for variable gain controller whereas around 100 seconds for fixed gain controller. Thus, the response for variable gain controller with estimator settles 40 seconds faster as compared to the fixed gain one. The response as shown in Figure 4.14 does not have any overshoot but as the delay value increases, the system suffers slight overshoot of 0.2 degrees. The estimated and actual values of delay for $d(k)$, $0 \leq d(k) \leq 7$ is shown in Figure 4.15. The correlation coefficient, to know the similarity between actual and estimated values of delay signals is calculated to be 0.2041. The value of the coefficients being positive demonstrates similarity between the signals to some extent. The performance measure as per equation (4.10) for fixed and variable gain is shown in Table 4.1.

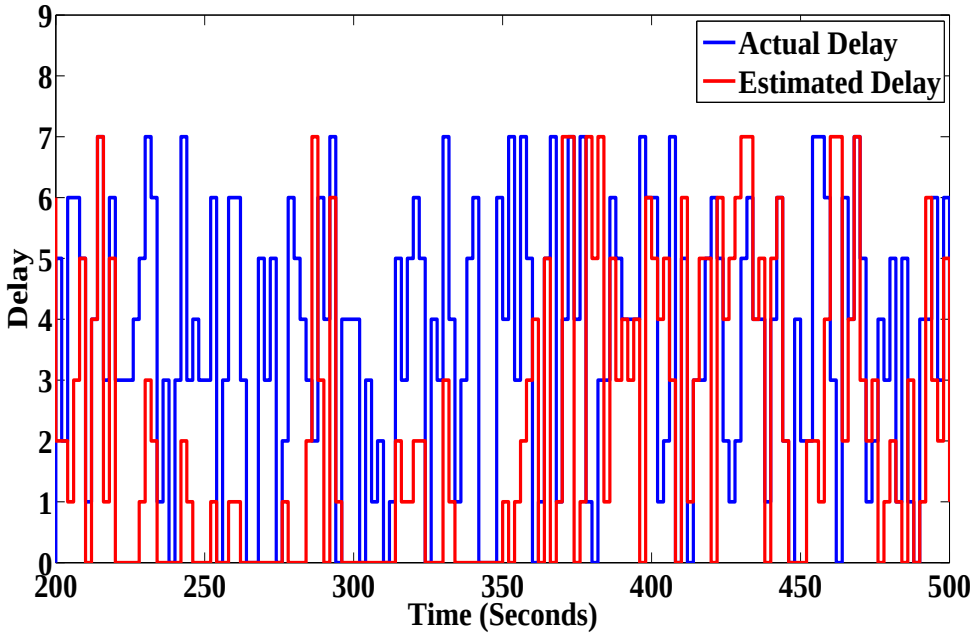

Figure 4.15: Actual and estimated delay values

Performance of gradient descent method based delay estimator: Considering 2 second sampling time, the simulation response of the plant for variable as well as for fixed gain controller, with the delay estimator used in variable gain case, is shown in Figure 4.16. The response of plant with variable gain and fixed gain controller settles around 72 and 108 seconds respectively. The actual and estimated values of delay for $d(k)$, $0 \leq d(k) \leq 7$ is shown in Figure 4.17. The performance index as per (4.10) for fixed and variable gain with different values of $\lambda = 0.7, 0.8, 0.9$ is shown in Table 4.2. From the cost function values it is evident that increase in λ values show slight improvement in cost function. Whereas, this improvement is considerable when cost function values of fixed gain and variable gain are compared.

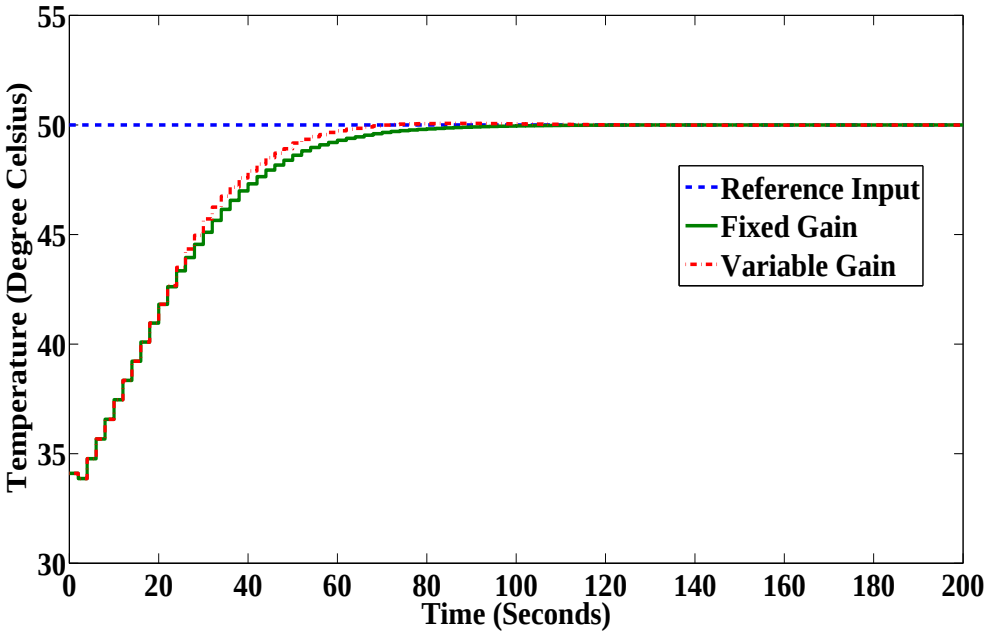

Figure 4.16: Simulation response of the closed loop system

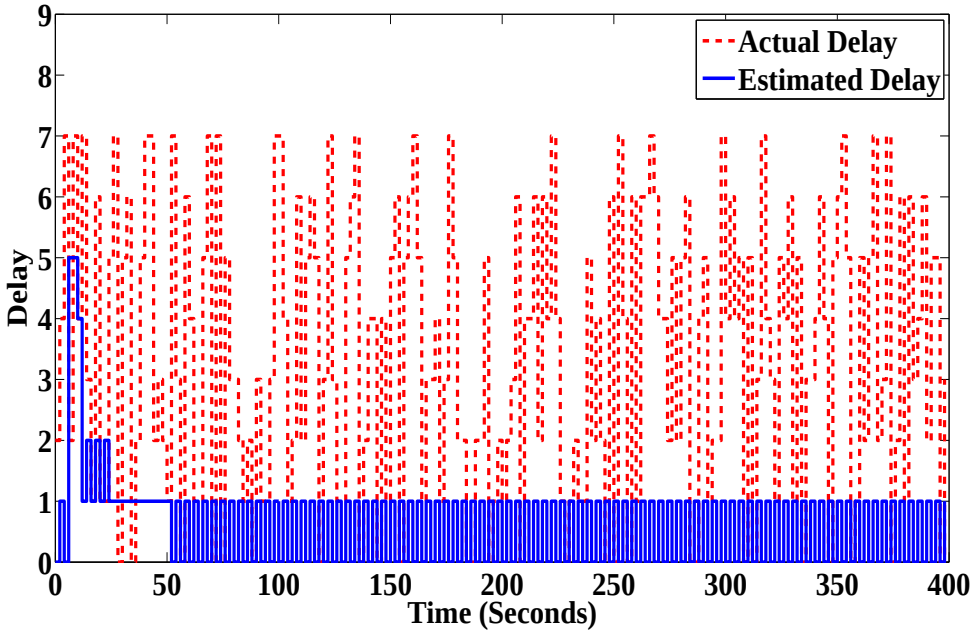

Figure 4.17: Actual and estimated delay values for simulation case

Experimental results

Performance of error-comparison method based delay estimator: The simulation and experimental result for response of temperature control plant for fixed gain controller is shown

in Figure 4.18 and for variable gain controller is shown in Figure 4.19.

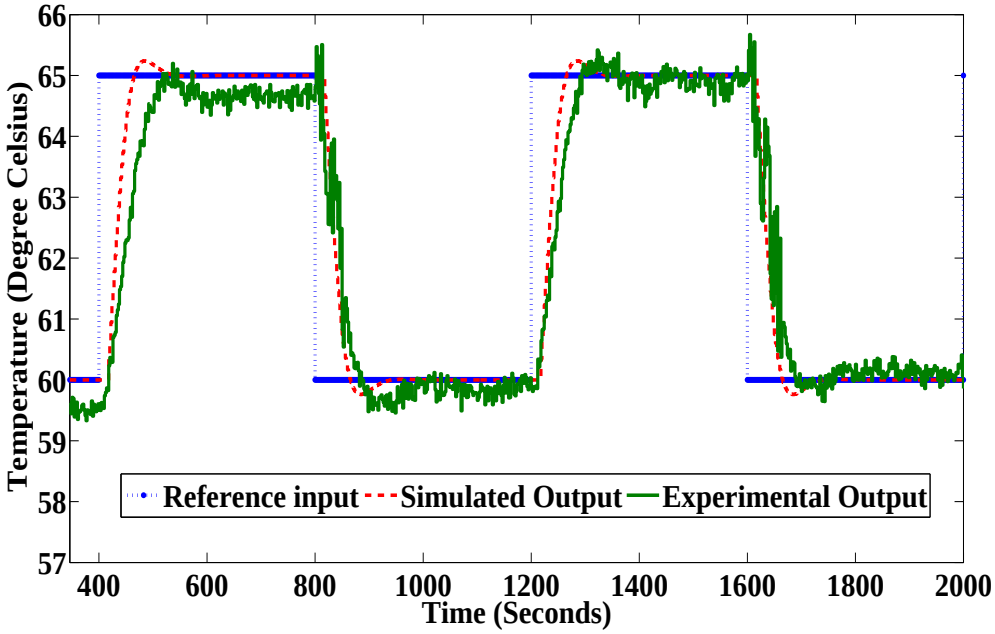

Figure 4.18: Experimental and simulation response for fixed gain

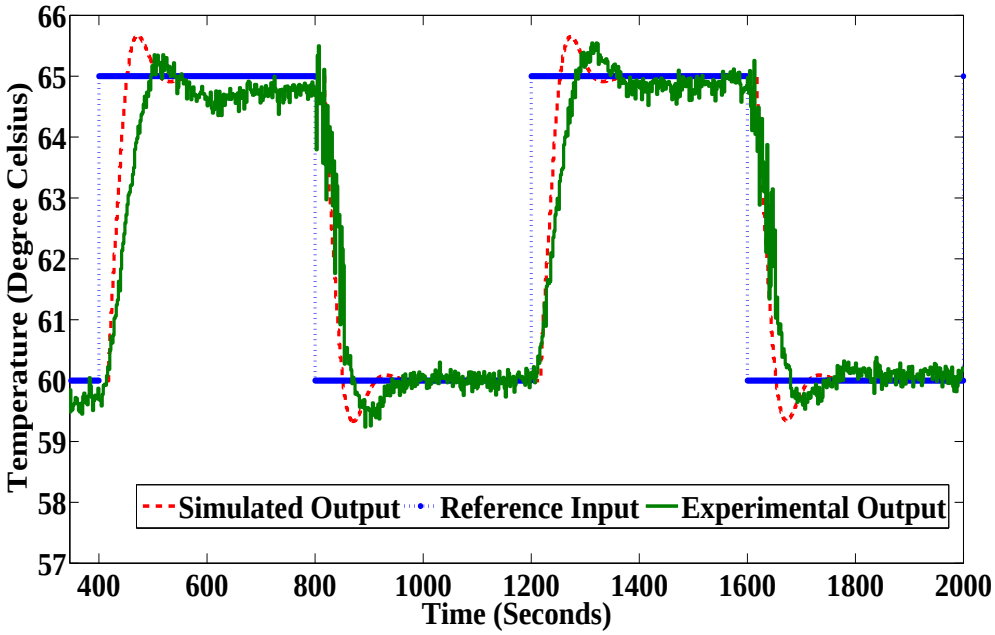

Figure 4.19: Experimental and simulation response for variable gain

A peak-overshoot of 0.1 degree and 0.2 degree respectively for fixed and variable gain is observed. The response for fixed gain settles in 230 seconds whereas for variable gain

in 170 seconds after some cycles. The control input of fixed and variable gain controller is shown in Figure 4.20. The values of delay estimated during the experiment are shown in Figure 4.21. The cost function values are presented in Table 4.1.

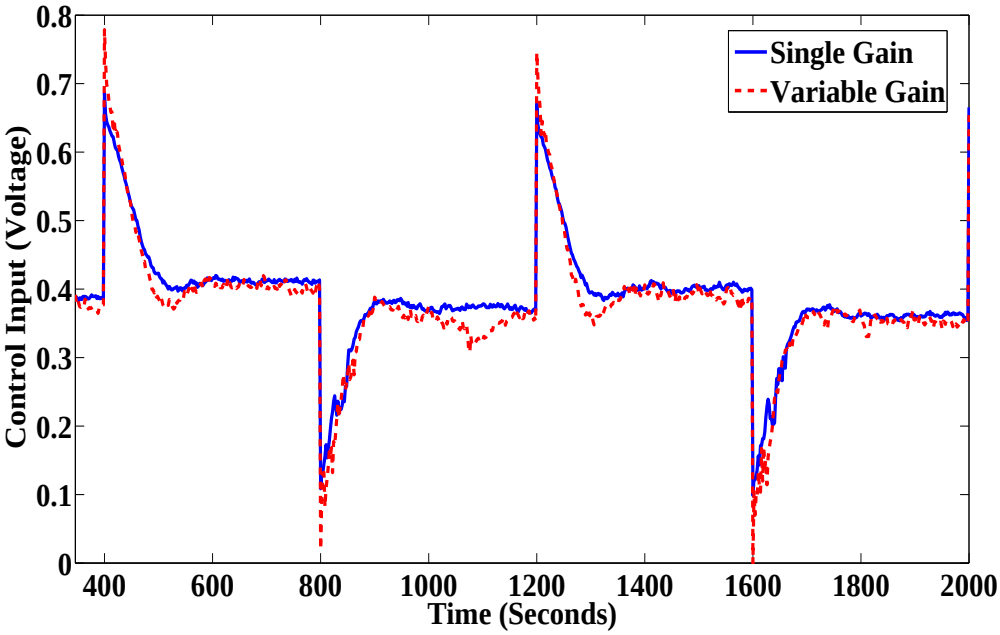

Figure 4.20: Experimental control input for fixed and variable gain

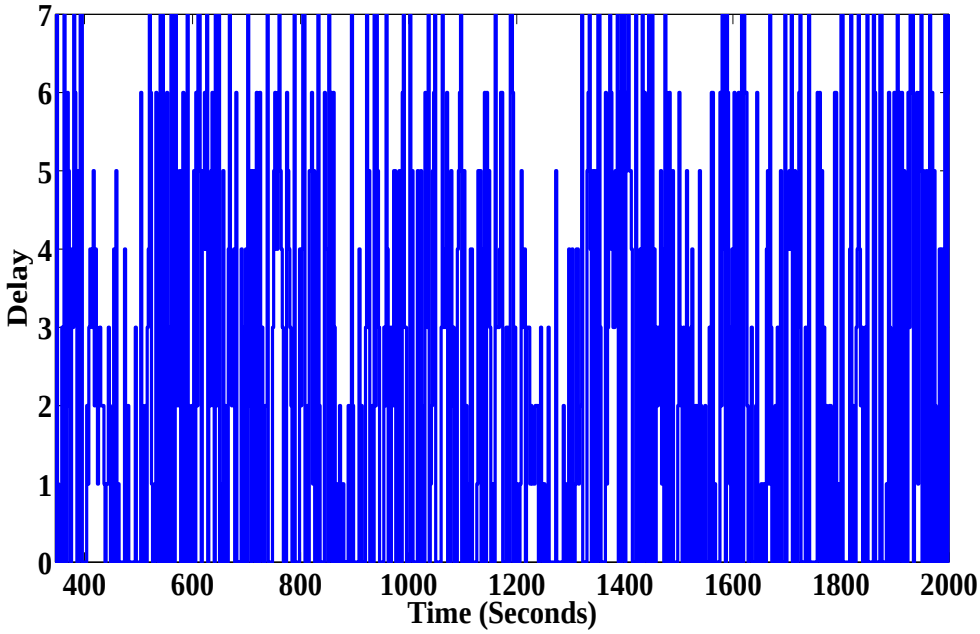

Figure 4.21: Delay estimated by the estimator during experiment

COST FUNCTION	Simulation result	Experimental Result
Fixed Gain	1412	1432
Variable Gain	810	1230

Table 4.1: Cost Functions for error-comparison estimator

Performance of gradient descent method based delay estimator: The experimental with simulation response of temperature control plant for fixed gain controller is displayed in Figure 4.22. In Figure 4.23, the response for variable gain controller with estimator considering different values of $\lambda = 0.7, 0.9$ is shown. The response of the system with fixed gain controller settles at 170 seconds whereas for variable gain controller settles at 150 seconds. The estimated delay values for different λ during the experiment are shown in Figure 4.25. For $\lambda = 0.9$, the maximum delay estimated is of 2 seconds, whereas, for $\lambda = 0.7$, the maximum estimated delay value is of 1 second. The delay values are estimated only during transient response, because the error between actual and estimated output goes to zero. Figure 4.24 shows the control input of fixed and variable gain controller.

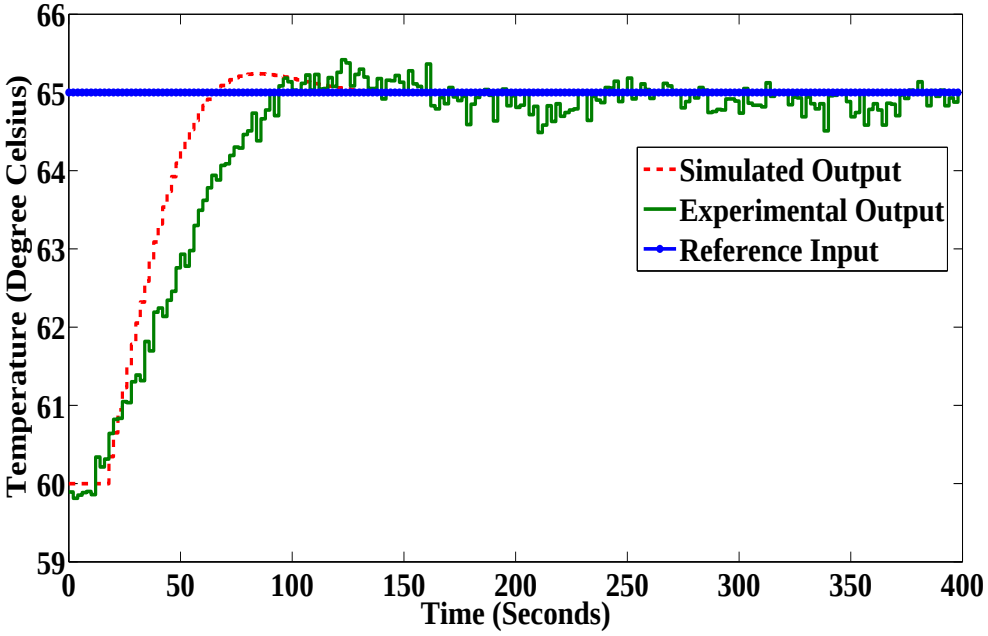

Figure 4.22: Experimental and simulation response for fixed gain case

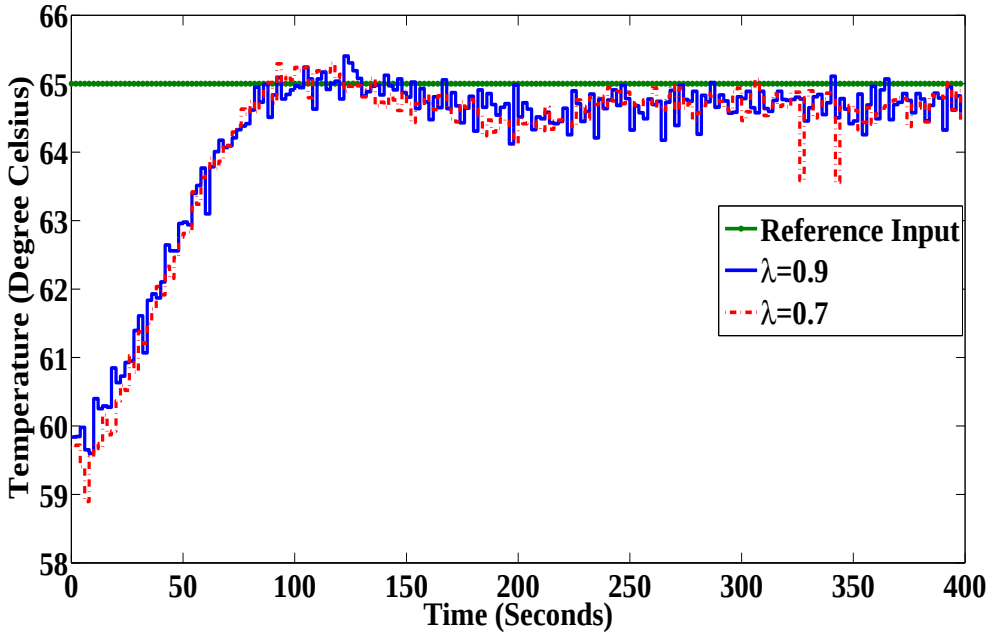

Figure 4.23: Experimental response for variable gain case with different λ values

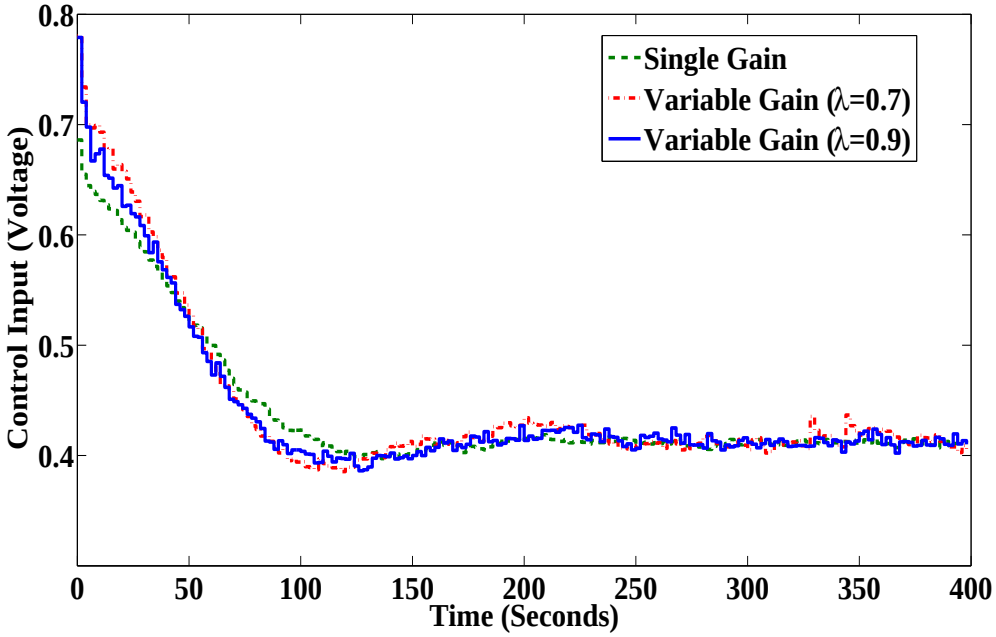

Figure 4.24: Experimental control input for the system with fixed and variable gains

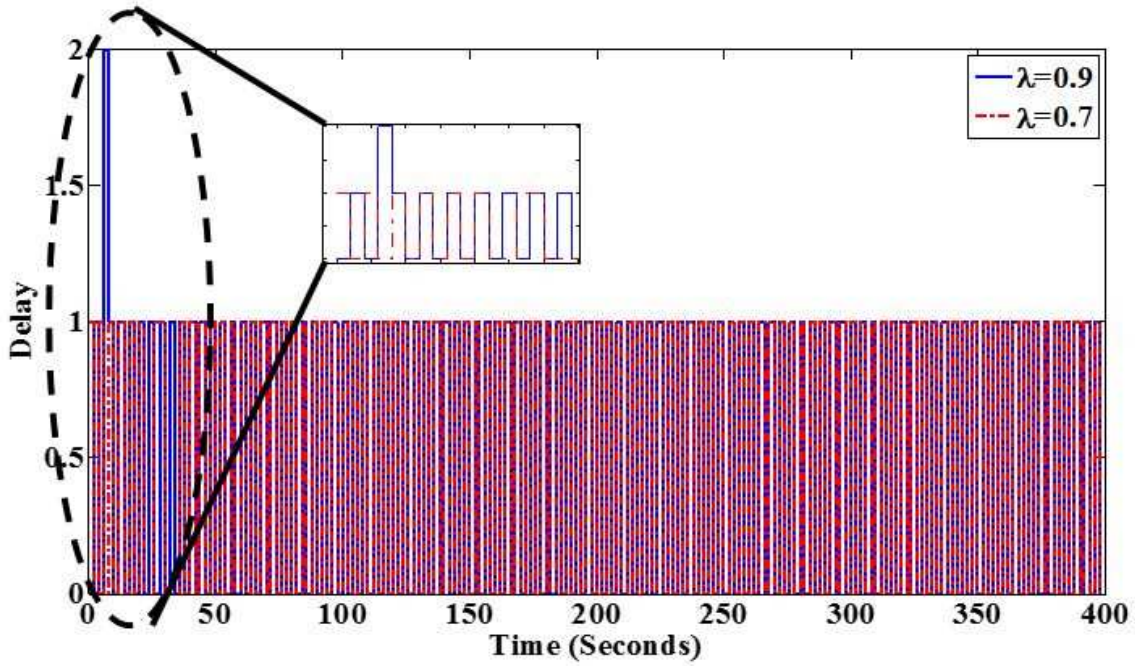

Figure 4.25: Delay estimated by the estimator during experiment

COST FUNCTION	Simulation result		Experimental Result	
Fixed Gain	34.3		70.63	
Variable Gain	$\lambda = 0.8$	23.15	$\lambda = 0.7$	50.5
			$\lambda = 0.8$	50
			$\lambda = 0.9$	45

Table 4.2: Cost Functions for gradient descent estimator

4.3.3 Comparison between the proposed estimators

From the simulation and experimental results we deduce that the error-comparison method based estimator estimates delay for both transient and steady state response but gets complex as the delay value increases. Gradient descent method based estimator estimates delay during transient response since the error between the actual and estimated output reduces to zero but, it guarantees the non-divergence of delays. From the plant output response for both 1 second and 2 seconds sampling time, it is evident that the response of variable gain controller together with the delay estimator settles faster as compared to the fixed gain controller response. The plant response using variable gain controller for 1 second sampling time for error based and gradient descent estimators settles around 114 seconds and 120 seconds respectively. For 2 seconds sampling time, the settling time is

170 seconds and 150 seconds respectively. Due to faster controller updation, with reduced sampling time, an improved response is obtained in case of 1 second sampling time.

4.4 Chapter Summary

In this chapter, the performance of plant with fixed and variable observer based output-feedback controller together with estimators is presented. An Error-Comparison method and Gradient Descent method based delay estimators are used for estimating delay values. Also, Simulation and experimental studies are carried out to demonstrate the validity of designed estimators for different sampling times of 1 and 2 seconds. From the simulation and experimental results it is evident that the variable gain controller using estimated delay values shows improved response in comparison to the fixed gain controller. Also gradient descent method based estimator guarantees non-divergence of delays. Moreover, in Gradient Descent approach, for larger values of λ, the cost function slightly improves. Also for both simulation and experimental results the cost function of the plant shows considerable improvement for variable gain controller as compared to fixed gain controller.

Chapter 5

Conclusions, Contributions and Future Work

5.1 Conclusions

The thesis considers network issues like packet loss and time-delays for the network present in the feedback loop. Here, the effect of these impediments is studied when the plant output gets delayed while it is communicated to the controller. This delayed output is used by the delay estimator to estimate the delay occurring at that sampling interval. The estimated delay value is used by the controller for selecting the controller gain. The delayed output is also used by the controller either directly or in the form of states estimated by the observer to form the control input for the plant.

This NCS configuration is implemented by considering a widely used control system of any process industry i.e. a temperature control plant. A laboratory setup for the same is considered for simulation and experimental studies. The Wireless Sensor Network (WSN) modules comprising of WSN node 3202 nad WSN gateway 9791 forms the wireless network of the feedback loop. LabVIEW is used as a platform for controller design.

Two types of controllers are designed namely direct output feedback controller and observer based output feedback controller. For both of these controllers a variable gain approach is used i.e. the gain varies according to the estimated delay values. For estimating these delay values an error-comparison and a gradient descent method is used. Both these methods estimates delay on an online basis.

The conclusions drawn from the simulation and experimental results are the proposed error-comparison method based estimator provides estimated delay values for both transient and steady state. But the gradient descent method based estimator provides estimated delay values only during the transient response. This is because the error between

the plant and estimated output is reduced to zero during steady state and the latter approach is based on error adaptation mechanism. But it guarantees non-divergence of delay values. Design of output-feedback controller is less computationally involved as compared to observer based output-feedback controller since observer design is not required. But the settling time for output feedback controller is high. The response of observer based output-feedback controller has lesser settling time as compared to output-feedback controller. Moreover, variable gain observer based output-feedback controller with estimated value of delay information gives better response as compared to the fixed gain controller. The response of the plant settles faster as the sampling time is reduced. For larger values of λ, the cost function slightly improves when using gradient descent method based estimator. Also for both simulation and experimental results the cost function of the plant shows considerable improvement for variable gain observer based output-feedback controller as compared to fixed gain controller.

5.2 Contributions

The thesis has the following contributions:

- An experimental setup of networked temperature control system is developed: A closed loop system of temperature control plant with network in the feedback loop is developed. The maximum round-trip delay is measured. This setup is used to study the effects of network.

- Two types of estimators are designed:

  - Error-comparison method: In this method actual and estimated output of the plant is compared to estimate delay values.

  - Gradient-Descent method: This method estimates delay values and guarantees their non-divergence.

- The performance of output-feedback controller is studied for both simulation and experimental case.

- The performance of observer based output-feedback controller is studied for both simulation and experimental case: The direct and observer based output-feedback controller with both the estimators is developed to deal with network issues.

5.3 Suggestions for Future Work

- The future work may include development of more accurate estimators based on other methods of estimation like maximum likelihood estimation, adaptive least mean square filter (LMS) etc.
- This thesis takes into account the delay effects of network present only in the feedback channel. This can be extended to study the effects of delay in both forward and feedback channels.
- Since, the network delay in the cases studied was quite high i.e. 14 seconds. Hence, a slow plant involving transportation lag was taken for experimental and simulation study. Thus for future work, the performance of the controllers and the estimators can be studied for plants not involving the transportation lag terms i.e. plants that respond fast to the applied input like critical chemical plants, unmanned aerial vehicle etc.. Since, these plants are more likely to destabilize in the presence of delays.
- Also the decaying factor is arbitrarily chosen while designing gradient descent method based estimator. Algorithms can be developed to update this factor adaptively.
- For the experiments carried out, it is observed that there is no saturation in the actuator or in the control data communication section. However, in situation, this issue may arise. Study of the effect of wind-up or limiting value of actuator output during experiments may be carried out in future.

Thesis Dissemination

- C. Suryendu, S. Ghosh and B. Subudhi,"Online Delay Estimation and Guaranteed Cost Control of Temperature Control System with Network in Feedback Loop", *International Conference on Signal Processing, Informatics, Communication and Energy Systems (IEEE SPICES, 2015)*, NIT Calicut, 19-21 Feb. 2015.
- C. Suryendu, S. Ghosh, B. Subudhi,"Delay Estimation for Variable Gain Control of Networked Control System: An Experimental Result for a Temperature Control System with Network",*ISA Transactions, Elsevier* (Submitted in Jan. 2015).

References

[1] G. C. Walsh and H. Ye, "Scheduling of networked control systems," *IEEE Control Syst. Mag.*, vol. 21, no. 1, pp. 57–65, January 2001.

[2] W. Zhang, M. Branicky, and S. M. Philipsm, "Stability of networked control systems," *IEEE Control Syst. Mag.*, vol. 21, no. 1, pp. 84–99, January 2001.

[3] T. C. Yang, "Networked control systems: A brief survey," *IEE Proc.-Control Theory Appl.*, vol. 153, no. 4, pp. 403–412, 2006.

[4] Y. Tipsuwan and M. Chow, "Control methodologies in networked control systems," *Control Engineering Practice*, pp. 1099–1111, February 2003.

[5] J. P. Hespanha, P. Naghshtabrizi, and Y. Xu, "A survey of recent results in networked control systems," *Proceedings of the IEEE*, vol. 95, no. 1, 2007.

[6] X. H. Chang and G. Yang, "New results on output feedback H_∞ control for linear discrete-time systems," *IEEE Transactions on Automatic Control*, vol. 52, no. 10, pp. 1930–1936, 2014.

[7] L. Zhang, Y. Shi, T. Chen, and B. Huang, "A new method for stabilization of networked control systems with random delays," *IEEE Transactions on Automatic Control*, pp. 633–637, 2005.

[8] H. Yu and P. J. Antsaklis, "Event-triggered output feedback control for networked control systems using passivity: time-varying network induced delays," in *IEEE Conference on Decision and Control and European Control Conference*, Orlando, 2011, pp. 205–210.

[9] Y. Shi and B. Yu, "Output feedback stabilization of networked control systems with random delays modeled by markov chains," *IEEE Transactions on Automatic Control*, vol. 54, no. 7, pp. 1668–1674, 2009.

[10] W. A. Zhang and L. Yu, "Output feedback stabilization of networked control systems with packet dropouts," *IEEE Transactions on Automatic Control*, vol. 52, no. 9, pp. 1705–1710, 2007.

[11] I. Pan, S. Das, and A. Gupta, "Tuning of an optimal fuzzy PID controller with stochastic algorithms for networked control systems with random time delay," *ISA Transacions*, vol. 50, p. 28–36, 2011.

[12] N. Tan, "Computation of stabilizing PI and PID controllers for processes with time delay," *ISA Transacions*, vol. 44, pp. 213–223, 2005.

[13] C. W. Alexander and R. E. Trahan, "A comparison of traditional and adaptive control strategies for systems with time delay," *ISA Transacions*, vol. 40, p. 353–368, 2001.

[14] G. P. Liu, Y. Xia, D. Rees, and W. Hu, "Design and stability criteria of networked predictive control systems with random network delay in the feedback channel," *IEEE Transactions on Systems, Man, and Cybernetics, Part C: Applications and Reviews*, vol. 37, no. 2, pp. 173–184, 2007.

[15] G. P. Liu, Y. Xia, J. Chen, D. Rees, and W. Hu, "Networked predictive control of systems with random network delays in both forward and feedback channels," *IEEE Transactions on Industrial Electronics*, vol. 54, no. 3, pp. 1282–1297, 2007.

[16] G. S. Tian, F. Xia, and Y. C. Tian, "Predictive compensation for variable network delays and packet losses in networked control systems," *Computer and Chemical Engineering*, vol. 39, pp. 152–162, 2012.

[17] X. M. Tang and B. Ding, "Design of networked control systems with bounded arbitrary time delays," *International Journal of Automation and Computing*, vol. 9, no. 2, pp. 182–190, 2012.

[18] D. E. Quevedo and D. Nesic, "Input-to-state stability of packetized predictive control over unreliable networks affected by packet-dropouts," *IEEE Transactions on Automatic Control*, vol. 56, no. 2, pp. 370–375, 2011.

[19] R. Wang, G. Liu, W. Wang, D. Rees, and Y. B. Zhao, "Guaranteed cost control for networked control systems based on an improved predictive control method," *IEEE Transactions on Control Systems Technology*, vol. 18, no. 5, pp. 1226–1232, 2010.

[20] D. Wang, J. Wang, and W. Wang, "H_∞ controller design of networked control systems with markov packet dropouts," *IEEE Transactions on Systems, Man, and Cybernectics*, vol. 43, no. 3, pp. 689–697, 2013.

[21] I. Pan, S. Das, S. Ghosh, and A. Gupta, "Stabilizing gain selection of networked variable gain controller to maximize robustness using particle swarm optimization," in *IEEE Conference on Process Automation, Control and Computing (PACC)*, 2011, pp. 1–6.

[22] A. T. Bahill, "A simple adaptive smith-predictor for controlling time-delay systems: A tutorial," *IEEE Control Systems Magazine*, vol. 3, no. 2, pp. 16–22, 1983.

[23] M. Behan, M. Cahill, M. Carry, G. Clausen, V. Dooley, N. English, W. Grainger, D. O'Connor, A. O'Dwyer, and J. V. Ringwood, "Closed loop time domain gradient methods for parameter and time delay estimation," in *Irish Signals and Systems Conference*, University of Ulster, Magee College, Derry, Ireland, June 1997, pp. 217–224.

[24] J. P. Georges, T. Divoux, and E. Rondeau, "Confronting the performances of a switched ethernet network with industrial constraints by using the network calculus," *International Journal of Communication Systems*, vol. 18, no. 9, pp. 877–903, November 2005.

[25] N. Vatanski, J. P. Georges, C. Aubrun, E. Rondeau, and S. L. J. Jounela, "Networked control with delay measurement and estimation," *Control Engineering Practice*, vol. 17, no. 2, pp. 231–244, February 2009.

[26] N. Vatanski, J. P. Georges, C. Aubrun, E. Rondeau, and S. Jounela, "Control compensation based on upper bound delay in networked control systems," in *17th International Symposium on Mathematical Theory of Networks and Systems (MTNS)*, Kyoto, Japan, July 2006.

[27] R. L. Cruz, "A calculus for network delay. I. network elements in isolation," *IEEE Transactions on Information Theory*, vol. 37, no. 1, pp. 114–131, 1991.

[28] Y. Gu and R. Ding, "A least squares identification algorithm for state space model with multi-state delays," *Applied Mathematics Letters*, vol. 26, no. 7, pp. 748–753, 2013.

[29] L. Chunmao and X. Jian, "Adaptive delay estimation and control of networked control systems," in *International Symposium on Communications and Information Technologies*. Bangkok: IEEE, 2006, pp. 707–710.

[30] L. Yuegang, Y. Zhiyuan, L. Huining, and T. Minghui, "Parameter identification and self tuning control for time varying stochastic system," *Journal of North China Institute of Electric Power*, no. 1, pp. 48–54, 1994.

[31] *Temperature Control System Manual*, Techno Instruments, Roorkee.

[32] *System Identification Toolbox user guide*, MathWorks.

[33] *NI PCI-6221 User guide and specifications*, National Instruments Corporation.

[34] *NI WSN-9791 User guide and specifications*, National Instruments Corporation.

[35] *NI WSN-3202 User guide and specifications*, National Instruments Corporation.

[36] *LabVIEW User manual*, April 2003 ed., National Instruments.

[37] J. Xu, C. E. de Souza, and L. Xie, "A scaling LMI approach to output feedback control of discrete-time LTI systems," in *International Symposium on Communications and Information Technologies*. Guangzhou: IEEE, 2007, pp. 42–46.

[38] J. Dong and G. Yang, "Static output feedback control synthesis for linear systems with time-invariant parametric uncertainties," *IEEE Transactions on Automatic Control*, vol. 52, no. 10, pp. 1930–1936, 2007.

[39] S. Jiang and H. Fang, "H_∞ static output feedback control for nonlinear networked control systems with time delays and packet dropouts," *ISA Transacions*, vol. 52, pp. 215–222, 2013.

[40] J. Yu, J. Tan, H. Jiang, and H. Liu, "Dynamic output feedback control for markovian jump systems with time-varying delays," *IET Control Theory and Applications*, vol. 6, no. 6, pp. 803–812, 2012.

[41] R. Yang, G. P. Liu, P. Shi, C. Thomas, and M. V. Basin, "Predictive output feedback control for networked control systems," *IEEE Transactions on Industrial Electronics*, vol. 61, no. 1, pp. 512–520, 2014.

[42] M. Gopal, *Digital control and state variable methods: conventional and intelligent control*, 4th ed. Tata McGraw-Hill Education Pvt. Ltd, 2012.

[43] A. Cervin, B. Lincoln, J. Eker, K. E. Årzén, and G. Buttazzo, "The jitter margin and its application in the design of real-time control systems," in *10th International Conference on Real-Time and Embedded Computing Systems and Applications (RTCSA), Sweden*, 2004, pp. 1–6.

[44] B. Lincoln, *Dynamic programming and time-varying delay systems*. Department of Automatic Control, Lund Institute of Technology, Box 118, SE-221 00 Lund, 2003.

[45] Y. Zhang, V. Sircoulomb, and N. Langlois, "Stable observer-based control for long network-induced delays," in *Chinese Control and Decision Conference*. Taiyuan: IEEE, 2012, pp. 2966–2971.

[46] I. Dilaneh and L. Laval, "Stabilization of networked control systems with uncertain time-varying delays," in *17th Mediterranean Conference on Control and Automation*. Thessaloniki: IEEE, 2009, pp. 610–615.

[47] D. L. Wen, Y. Li, and S. Deng, "Controllers design of networked control systems with arbitrary bounded step delays and packet dropouts," in *Chinese Control and Decision Conference*. Yantai, Shandong: IEEE, 2008, pp. 419–422.

[48] W. Y. Feng, J. Y. Wei, and Y. B. Qi, "State feedback control for networked control systems based on state observer," in *Chinese Control and Decision Conference*. Mianyang: IEEE, 2011, pp. 310–313.

[49] L. Yanhui and Z. Xiujie, "Observer-based state feedback H-infinity control for networked control systems," *Indonesian Journal of Electrical Engineering*, vol. 12, no. 8, pp. 6144–6152, 2014.

[50] L. E. Ghaoui, F. Oustry, and M. A. Rami, "A cone complementarity linearization algorithm for static output-feedback and related problems," *IEEE Transactions on Automatic Control*, vol. 42, no. 8, p. 1171–1176, 1997.